Non-linear dynamics of a flexible aircraft under non-stationary random track induced excitation

By

Abhiram R Devesh

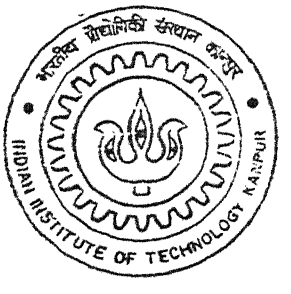

DEPARTMENT OF AEROSPACE ENGINEERING

Indian Institute of Technology Kanpur

APRIL, 2005

Non-linear dynamics of a flexible aircraft under non-stationary random track induced excitation

A Thesis submitted
in partial fulfillment of the requirements
for the degree of
Master of Technology

by

Abhiram R Devesh

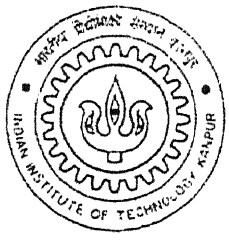

Department of Aerospace Engineering
Indian Institute of Technology, Kanpur
India

April 2005.

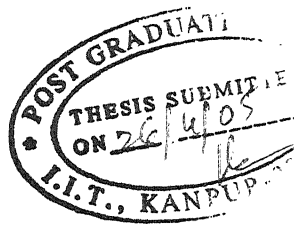

CERTIFICATE

It is certified that the work contained in this thesis entitled **NON-LINEAR DYNAMICS OF A FLEXIBLE AIRCRAFT UNDER NON-STATIONARY RANDOM TRACK INDUCED EXCITATION** by Abhiram R Devesh, has been carried out under my supervision and that this work has not been submitted elsewhere for a degree.

D. Yadav
Professor
Department of Aerospace engineering
I. I. T Kanpur.

26th April 2005.

Dedicated to
my Parents
and
my brother Eashwar.

CONTENTS

Acknowledgements

"All's Well That Ends Well" and at this juncture of the end of my Masters Program in this Institute, I wish to express my wholehearted gratitude with utmost reverence to the Almighty. I ventured into this explorative sojourn with an able support, constant guidance of none other than Prof. D. Yadav, the think tank of this work. Forever I remain bound to him for he has carved a niche in my memory.

Before entering into the field, one definitely requires conditioning and preparation and the field of research is no exception. I respectfully pay my gratitude to all my course instructors especially Prof. C. S. Upadhyay and Prof. A. K. Mallik for having made me equip with all that was needed for this work.

Even though the thesis bears on my name, the proper ambience and an amicable platform for its present manifestation was created by Mohite, Laxman, Amit and Atul, my illustrious lab-mates and Anil. I am indeed proud to associate myself with Structures Group comprising of Haldar, Utsa, Nilesh, Md. Sunny, Koushik and Prashant with a special word of thanks to Bhavani Prasad and my batch mates Raja Rao and Harigopal. With utmost joy I recollect the timely and knowledgeable interaction that I have had with Ramanathan, which helped me gain insight of very many things both academic and non-academic. Whatever I am is a combination of various attributes and among them my good old friends are an integral and a memorable part. I proudly recall my aeons of companionship with Ashvanth and Venkat, friends from distant galore.

Every good thing has a beginning and I made my beginning into this world by the caring and magical touch of my parents, in front of whom I utterly fall short of words to express my gratitude and a mere verbal gratitude would definitely not suffice. I consider my self highly fortunate to have a brother who is indeed a source of inspiration and encouragement.

Every student of this country hides somewhere deep in his heart the ever yearning wish to be in the intellectual paradise, The Indian Institute of Technology Kanpur, and with all my pride as well as humility I express my overwhelming joy as this paradise is anchored to my name for the days to come hereafter. No amount of words of gratitude would express in toto the contribution of Indian Institute of Technology Kanpur in various walks of my overall development, which has in effect made me today what I am.

Abhiram R Devesh

List of Figures

List of symbols used:

$\bar{x}, \bar{r}$	-	Any variable of interest, spatial variable
$f(\cdot), g(\cdot)$	-	Functions of the variables specified inside the braces.
ε	-	Small parameter / Tolerance
α	-	Constants / function of ε.
t	-	Temporal Variable.
Ω, ω	-	Frequency of oscillation / Angular frequency.
ψ	-	Total phase as a function of time.
a	-	Amplitude of oscillation
θ	-	Phase angle
u_i	-	Perturbation solutions / solutions of higher order deformation equations.
A_i, B_i	-	functions of a.
σ	-	Detuning parameter.
$N[\ ]$	-	Non-linear differential operator
$L[\ ]$	-	Linear differential operator
u_0	-	Initial guess of the solution
ϕ	-	Solution of the map / Homotopy
H	-	Map / Homotopy
p	-	Embedding parameter.
$\hbar$	-	Auxiliary Parameter.
$[M]$	-	Mass matrix.
$[K]$	-	Stiffness matrix.
$[C]$	-	Damping matrix.
$\{\dot{x}\}$	-	System velocity response vector.
$\{\ddot{x}\}$	-	System acceleration response vector.

$\{\mu_x\}$ - System mean displacement response vector.

$\{\dot{\mu}_x\}$ - System mean velocity response vector.

$\{\ddot{\mu}_x\}$ - System mean acceleration response vector.

$\{\phi_{xx}\}$ - System correlation of displacement response matrix.

$\{\dot{\phi}_{xx}\}$ - System correlation of velocity response matrix.

$\{\ddot{\phi}_{xx}\}$ - System correlation of acceleration response matrix.

$\{\phi_{fx}\}$ - Cross correlation between the displacement and force vectors.

$\{\dot{\phi}_{fx}\}$ - Cross correlation between the velocity and force vectors.

$\{\ddot{\phi}_{fx}\}$ - Cross correlation between the acceleration and force vectors.

$\{\kappa_{xx}\}$ - System covariance of displacement response matrix.

$\{\dot{\kappa}_{xx}\}$ - System covariance of velocity response matrix.

$\{\ddot{\kappa}_{xx}\}$ - System covariance of acceleration response matrix.

$\{\kappa_{fx}\}$ - Cross covariance between the displacement and force vectors.

$\{\dot{\kappa}_{fx}\}$ - Cross covariance between the velocity and force vectors.

$\{\ddot{\kappa}_{fx}\}$ - Cross covariance between the acceleration and force vectors.

$y_m(\xi)$ - Deterministic function describing the track mean profile from the datum.

$y_r(\xi)$ - Zero-mean random process.

ξ - Distance from the origin.

$R(y_1, y_2)$ - Correlation function.

v_i - Constants to represent vehicle's ground motion.

k_1, k_2 - Linear and non-linear spring constants.

c_1, c_2 - Linear and nonlinear damping constants.

T - Kinetic Energy.

W - Work done.

V - Potential energy. / Volume of the material.

δW_c	-	Virtual work done by the conservative forces.
δW_{nc}	-	Virtual work done by the non – conservative forces.
L	-	'Lagrangian' of the system.
R	-	Raleigh's dissipative function.
m_{us}	-	Mass of the Un-sprung mass.
m_s	-	Mass of the Sprung mass.
s_i	-	Distance from the root of the wing.
$\rho(s_i)$	-	Density of the wing's material as a function of s_i
$A(s_i)$	-	Area of cross-section of the wing - function of s_i
l_w	-	Length of the wing.
k_{us1}, k_{us2}	-	coefficients of the un-sprung mass's nonlinear spring.
c_{us1}, c_{us2}	-	coefficients of the un-sprung mass's nonlinear damper
k_{s1}, k_{s2}	-	coefficients of the sprung mass's nonlinear spring.
c_{s1}, c_{s2}	-	coefficients of the sprung mass's nonlinear damper.
σ_{ij}	-	Stresses induced in the body
ε_{ij}	-	Strain induced in the members.
ρ_a	-	Density of air,
C_L	-	Lift coefficient,
S_w	-	Wing surface area
w	-	Transverse displacement of the wing.
η	-	Natural coordinates
${}^t\{u\}$	-	Displacement response vector at time t.
${}^t\{\dot{u}\}$	-	Velocity response vector at time t.
${}^t\{\ddot{u}\}$	-	Acceleration response vector at time t.
${}^{(t+\Delta t)}\{\hat{R}\}$	-	Equivalent force vector at time $t+\Delta t$.
${}^{(t+\Delta t)}\{R\}$	-	Force vector at time $t+\Delta t$.
${}^{(t+\Delta t)}[\hat{K}]$	-	Equivalent stiffness matrix at time $t+\Delta t$.
${}^{(t+\Delta t)}[K]$	-	Equivalent stiffness matrix at $t+\Delta t$

$^{(t+\Delta t)}[M]$	-	Equivalent mass matrix at $t+\Delta t$
$^{(t+\Delta t)}[C]$	-	Equivalent damping matrix at $t+\Delta t$

Subscripts and Superscripts

i	-	1, 2, 3, ... / left or right wing
l	-	Left wing
r	-	right wing
m	-	Mean
r	-	Random
1, 2	-	Un-sprung mass and sprung mass.

Synopsis

Unevenness in the track induces vibrations in moving vehicles including aircrafts. This may cause excessive level of vibration in the airframe. This also causes discomfort among passengers, produces undesirable movement of the cargo, and may lead to uncontrollability of the vehicle while executing ground maneuvers. The dynamics may lead to fatigue and failure of the structural components of the vehicle. Hence the analysis of the dynamics response of the structure and its components has assumed greater importance for assessing ride quality, design of vehicle structures, control of vibration and optimization of the suspension system and tires.

In the present study, a combination of Finite element and Finite difference methods is used for obtaining the response of the vehicle under the random dynamic excitation. The vehicle is modeled as a single point contact, two degree of freedom heave model. This model also incorporates the cantilever wings as two one dimensional continuous structures attached to the sprung mass of the aircraft. The discrete elements are nonlinearly modeled and the continuous elements are modeled linearly. The rigid track's roughness is assumed to be homogenous in nature and is described by its correlation function. The vehicle's forward velocity is assumed uniform for taxi run, constant acceleration during take-off run and constant deceleration for the landing run. An iterative procedure is used to obtain the stochastic response of the vehicle. Results with three forward motion patterns have been obtained for each of the taxi run, take-off run and landing run of the aircraft. The effect of system parameter variation has been studied by considering three different non-linear stiffness coefficients for the aircraft ground runs. The effect of variation of the damping coefficients has also been studied by using three different damping coefficients with the extreme forward motion pattern in the three runs of the vehicle.

Chapter 1

Introduction

1.1 Overview

All vehicle structures are subjected to dynamic excitation from the surface over which they move because of the unevenness or roughness of the track. This unevenness or roughness is because of the variations in the longitudinal cross section profile of the track. It is induced by unequal settlements, fabrication defects, wear and tear in use and repair patches. Be it a railway track for locomotives or roadways for road bound vehicles or runway and taxiway for aircrafts, the unevenness is inherent and cannot be avoided. The effect of the track induced dynamic excitation is unfavorable vibration of the body/frame of the vehicle leading to structural stress-strain and fatigue, resulting ultimately in the failure of the vehicle structure. It also causes passenger discomfort, cargo damage and degraded controllability of the vehicle.

For the study of the effect of the track induced excitations on the vehicle, the vehicle structure with its suspension systems and tires can be modeled with different degrees of sophistications. As the complexity of these models increase, the response of the structure under these excitation loads can be predicted with higher precision. However with increase in complexity of the model, the computational requirement and analytical complexity also increases, so as to have an analytic solution. In engineering applications, the initial study is with a simple model and detailed model is used only in the secondary stage.

In general the track roughness is random in nature and the induced dynamic excitations to the vehicle do not possess a certain and defined form of variation; that is, they cannot be represented as a deterministic function. Hence they are modeled as random excitations. This would enable us to represent the excitation process more realistically and hence more

accurately. Further, most systems in the real world are predominantly nonlinear. During modeling we frequently consider them as linear ones. This would give us the advantage of generating the solution in closed form. An accurate nonlinear model results in an evolved nonlinear system equation that may not possess a closed form solution and would require numerical approach. With the advent of inexpensive high speed computational machines this disadvantage has been alleviated to a large extent and it is now possible to study the nonlinear models which depict the original system or process more realistically.

Vehicles are complex elastic structure which rests on a suspension system, in turn supported on wheels and tires. The excitation induced by the track unevenness is transmitted through the tires, to the substructure, then to the suspension system and finally to the superstructure of the vehicle. This unevenness causes variety of motions and deformations in the vehicle. They can be broadly classified into 2 categories, namely the "rigid body motion" and the "deformation of the structure". The rigid body motions are classified as heave, side-sway, forward sway or hunting, pitch, roll and yaw. The deformations are classified as bending, axial deformation and torsional deformations. The system may undergo deformations in one or more of the above modes and depending on the complexity of the model, we could quantitatively study the same. In general there are infinite degrees of freedom for a continuous system. For preliminary analysis, these continuous systems can be modeled as a system with finite degrees of freedom. Generally there would exist a coupling among the different types of possible body motions.

The mathematical models used to depict an aircraft can be from the simplest single degree of freedom rigid mass model to the most complex infinite degree of freedom continuous ones. Some of the typical models that can be used for analysis are a single point

input heave model, two point input heave-pitch model, and three point input heave-pitch-roll model. These models' degrees of freedom can be considered as rigid or elastic modes for analysis purposes.

Several analytical procedures have been put forward to solve systems with nonlinearities and/or random excitations. These procedures have their own merits and demerits. The Monte Carlo simulations can be used for any model with random excitations. These have the disadvantage that the solution is representative of the actual solution only after conducting a large number of simulations. As the system's complexity increase, the time taken for the results to converge increases drastically. So these simulations become computationally expensive.

1.2 Literature Survey

There has been a substantial rise in the volume and operating velocities of high speed transportation. The safety and comfort of the passengers has assumed significant importance. This has led to increased research activity in the field of vehicle dynamics, especially in the field of track induced vibration of these vehicles.

For the analysis of track induced vibrations of a vehicle with a nonlinear model, we need to know the characteristics of the equation to select an appropriate solution procedure. In other words *a priori* knowledge of the qualitative and quantitative aspects of the nonlinear vehicle's system equations is required. In our case of an aircraft, the parameters associated with the nonlinear terms in the system equations vary from medium to very large in comparison with that of the coefficients of the linear terms. This would prevent us from the "small parameter assumption". Hence the existing methods which depend on the small parameter assumptions fail severely.

Some of the methods that have been developed in the recent past have the advantage of not assuming small parameters associated with the nonlinear terms of the system equations. Some examples are the Kryloff-Bogolliuboff-Mitropolskii (KBM) method [1, 2, 3, 4], the Modified form of Multiple time scales method [5, 6] and the Homotopy analysis method (HAM) [7, 8, 9, 10, 11]. There are variants of this HAM like the Homotopy perturbation method, Ji-Huan He [12, 13]. The above mentioned methods give the solution in closed form or rather in a near closed form. These methods are predominantly used to solve deterministic systems.

When the input excitation is not only deterministic but is also superimposed by a random process the solution technique must incorporate to evaluate the statistical properties of the system. There are again several methods used to evaluate the probability statistics of a nonlinear system with random excitations. C. W. S. To [14, 15, 16] has developed a recursive expression to determine the probability characteristics of the response of the system using Stochastic Central Difference methods. There are methods developed which incorporate the modified form of the multiple time-scale method to determine the statistical characteristics of the response of the system. Zhu, Huang and Suzuki [20] who worked on a single degree of freedom, Duffing – van der Pol oscillator. They assumed that the strongly non-linear oscillator are with lightly linear and (or) lightly non-linear damping. Rong, Meng, Xu and Fang [21] studied the behavior of the steady state response of a single degree of freedom system under narrowband random excitations. Rong, Meng, Wang, Xu and Fang [22] have utilized the Modified multiple-scales method to determine the statistical characteristics of the response of the system. They studied the effect of weakly external and (or) parametric excitations of a single degree freedom system under wide band random excitations.

There are methods which do not take any assumption on the probability structure of the random processes. Yadav [17] obtained the vehicle response statistics to a

general non-stationary track excited ground vehicle. This approach was applied to a multi degree of freedom system and can be extended to incorporate a continuous system coupled with the discrete system and having stationary or non-stationary random excitation.

There were several studies carried out to evaluate the track induced vibrations on an aircraft. Most of these studies have considered simple lumped mass models of the aircraft. Tung et al. [23] used a heave-pitch model to obtain the response of aircraft to track roughness while including nonlinear shock absorber behavior. This study was done by numerical integration for deterministic input while statistical linearization and perturbation methods where used for stationary input.

Kirk and Perry [24] studied the taxiing induced vibrations in aircraft using the power spectral density function. The analysis of a constant velocity motion of a vehicle does not provide the response of the vehicle when accelerating or undergoing variable motion as in take-off and landing. Virchis and Robson [25] have obtained the response of a vehicle under acceleration when excited by random road undulations by analytically. They concluded that the non-stationary effects are not too large and can be neglected as a first approximation. A study of the non-stationary random vibration of a linear vehicle system traveling with variable velocity was done by Soboczyk and Macvean [26]. Both deterministic and random variations of the vehicle forward velocity were considered.

Aircraft landing responses with decelerating run on uneven runway impose some extreme loads on the landing gears and the airframe and has been studied with equal importance. Yadav and Ramamoorthy [27] have studied nonlinear landing gear behavior upon touch down. A heave pitch model of the aircraft with oleo-pneumatic shock strut in the articulated nose and telescopic main gear has been considered. The system equations have been numerically integrated to obtain the response in the duration of impact. Yadav and Singh [28] have studied the braked landing response of aircraft. Optimal landing run without any

skidding has been obtained with a one-step prediction of variable braking force with a linear two degrees of freedom aircraft model.

Flexible models of guided ground vehicles have been investigated for response by Wilson and Biggers [28]. In their analysis, the vehicle model was considered to be a slender beam of uniform mass and stiffness property. Interaction of the modes was also considered. The track irregularity was modeled as a stationary random process. Hac [29] considered a discrete - continuous vibratory system at constant forward speed. The system is modeled with active suspension. The road irregularity has been assumed to be a stationary Gaussian zero mean process. He studied the effect of body elasticity on the system response.

In the study of flexible vehicle, many authors have modeled the vehicle body as a uniform body as a uniform section beam for which modal parameters can be easily derived. However, in many practical applications the body has its system parameters varying along the length. The dynamic of non-uniform beam element is complex as governing differential equation contains space dependent coefficients. Analytical solutions of non-uniform bending vibrations haven been attempted by Conway and Dubil [30], Sanger [31], Gorman [32] and Talukdar [34].

A uniform section cantilever beam with tip mass has been analyzed for free and forced vibration by To [33]. Closed form solution for the response has obtained for deterministic base excitation.

Although technical literatures contain substantial amount of studies relating to various aspects of vehicle dynamics to track irregularities, the following observations can be made about the points that have not been adequately addressed.

1. Many of the models analyzed the vehicle as a discrete system only. Some literatures have analyzed the system as a combination of a linear discrete model with continuous attachments like in Talukdar [34] who studied the linear models of the aircraft. As stated

earlier, in reality all systems occur predominantly as nonlinear. Hence the assumption of linear vehicle does not suffice for the accurate prediction of the response of the vehicle.

2. Nonlinear suspension characteristics have been handled mostly by equivalent linearization, statistical linearization and perturbation methods. Statistical linearization may induce appreciable error in the response of the system if the probability density function is different from the form assumed, which may happen in most practical cases of non-stationary input. Perturbation methods have been used to obtain series solution for the response of the system. Nonlinear terms of the system equations are associated with small parameters. Though theoretically valid, this would bring in the restriction of the application to only weakly non-linear systems.

3. In most of the flexible systems the associated parameters do not remain uniform through out the structure. Hence the assumption of uniformly distributed continuous system does not suffice the accurate prediction of the vehicle structure.

1.1 Present Work

In the present work we study the track induced vibrations of a small aircraft. This model is represented as a combination of a two degree of freedom, single point input heave model with lumped sprung and the un-sprung masses along with two, one dimensional continuous attachments depicting the cantilever wings. The tire is modeled to have a single point ground contact with equivalent nonlinear spring and damper representing its behavior. The point contact would trace out the profile of the track. The un-sprung mass would include the mass of the substructure and the tires. The sprung and un-sprung masses are connected by another set of nonlinear spring and damper corresponding to the shock absorbers. The sprung mass would include the whole weight of the superstructure which includes the masses of the fuselage and the wings.

The model used here, though a primitive model is the starting point for future detailed analysis. The Nonlinear spring and damper are modeled as cubic restoring force and cubic damping with the coefficient of the quadratic term being zero.

The wing of the aircraft is modeled as a one dimensional continuous member which acts as a cantilever beam. It is modeled as a non uniform beam with variation in the cross sectional properties. The variation is considered as a power series. This representation is general and any type of variation can be accommodated with desired accuracy. The vibration of the cantilever beam with base excitation can be modeled as either linear or nonlinear oscillation.

The track is modeled as a rigid with homogenous random variations in the longitudinal cross sectional profile. The mean profile of the track is taken as a combination of a gradient slope superimposed with a harmonic function (single or multi harmonics).

In the present work for the solution of the system equation some of the most popular methods in the literature have been tried and due to the inadequateness of the methods to the present problem the solution technique has been resorted to a combination of Finite Element Method (FEM) (in space) and Finite Difference Method (FDM) (in time).

1.4 Layout of the Thesis report

The thesis report has been divided into 7 sections. The first chapter deals with the overview of the work, the literature survey and the concise description of the present problem. The second chapter deals with the solution techniques that have been tried to solve the present problem in hand. This chapter also deals with the advantages and disadvantages of the methods studied. Finally at the end of the chapter the methodology adopted is given.

The third chapter deals with the system modeling and the development of the corresponding non-linear system equations. The fourth chapter gives a detailed account on the

solution technique adopted to solve the non-linear system equation with random forcing function. The fifth chapter discusses the results obtained after solving the system equation. The discussion is divided into 2 parts. The first part deals with the parameter study by varying the non-linear stiffness coefficients and the latter part deals with the parameter study of the response when the damping coefficients are varied. The final chapter deals with the conclusions of the present work done and the possible variations in the model that can be incorporated.

Chapter 2

Solution Approaches

This chapter on solution approaches is divided into three major sections. The first part of this chapter presents solution approaches to solve nonlinear system equations for lumped and continuous systems and their relative merits. The second section deals with the methods available to solve for the response of a system when it is randomly excited. The final section gives the approach used in the present work for solving randomly excited nonlinear systems.

There are several methods available in the literature for solving nonlinear ordinary/partial differential equations analytically. Nayfeh [1, 2] has explained clearly and extensively about the methods of solving nonlinear differential equations using perturbation methods. This chapter discusses some of these popular methods along with their advantages and disadvantages. Predominantly most of these popular methods make use of the fact that there exists a small parameter associated with the nonlinear terms of the differential equation.

2.1 Solution Approaches for Non-Linear Equations

2.1.1 Krylov-Bogoliuboff-Mitroposlkii Method

The general form of any nonlinear differential equation can be given as follows

$$x^{(N)} + \alpha_1 x^{(N-1)} + \ldots + \alpha_{(N-1)} \dot{x} + \alpha_{(N)} x = \varepsilon f\left(x^{(N)}, \ldots, \dot{x}, x, \varepsilon, t\right) \qquad (2.01)$$

where,

$f(x^{(N)}, \ldots, \dot{x}, x, \varepsilon, t)$ - Known nonlinear function of the variables specified.

ε - Small parameter associated with the nonlinear function f

α_i - Real Constants.

$x^{(k)} = \frac{d^k x}{dt^k}$

Many problems in engineering and especially in vibrations lead to the equation form,

$$\frac{d^2x}{dt^2} + \omega^2 x = \varepsilon f\left(x, \frac{dx}{dt}, t\right) \tag{2.02}$$

where, ω is a constant.

For the sake of simplicity this nonlinear function $f\left(x, \frac{dx}{dt}, t\right)$ is replaced by an equivalent linear function. In many cases, this does not explain the phenomena occurring naturally.

If $\varepsilon = 0$ one has the harmonic oscillator or a homogenous ordinary second order differential equation.

$$\frac{d^2x}{dt^2} + \omega^2 x = 0 \tag{2.03}$$

whose general solution is given as

$$x = a\,Cos(\psi),\ \psi = \omega t + \theta \tag{2.04}$$

The amplitude a is a constant and the total phase ψ linearly increases with time. Hence

$$\frac{da}{dt} = 0 \tag{2.05a}$$

$$\frac{d\psi}{dt} = \omega \tag{2.05b}$$

The term $\varepsilon f\left(x, \frac{dx}{dt}, t\right)$ perturbs the simple solution procedure. The details of this method and its application have been described in detail by Mitropolskii and Van Dao [3]

and Kryloff and Bogoliuboff [4] in their books and their references. This nonlinear excitation leads to the dependence of the momentary frequency $\frac{d\psi}{dt}$ on the amplitude and may give rise to a systematic increase or decrease of the amplitude of oscillations, depending respectively on the generation or absorption of energy by the exciting forces. Hence the approximation for the solution of eq. 2.02 is given by the KBM method is as follows. It can be seen that this method comes under the category of perturbation methods.

$$x = a\,Cos(\psi) + \varepsilon u_1(a,\psi) + \varepsilon^2 u_2(a,\psi) + \ldots \tag{2.06}$$

To determine a and ψ we will use the following equations.

$$\begin{aligned} \frac{da}{dt} &= \varepsilon A_1(a) + \varepsilon^2 A_2(a) + \ldots \\ \frac{d\psi}{dt} &= \omega + \varepsilon B_1(a) + \varepsilon^2 B_2(a) + \ldots \end{aligned} \tag{2.07}$$

The problem transforms from determining a single solution *x(t)* to the determination of the functions $u_i(a,\psi), A_i(a), B_i(a); i = 1,2,3,\ldots$ such that their substitution into eq. 2.02 satisfies this equation with the prescribed accuracy. Thus instead of the single differential equation of second order in the unknown *x(t)* we have to solve a system of linear non homogenous differential equations to determine the unknown functions. If ε is small enough, only few terms of the series are sufficient.

The advantage of this KBM method is the simplicity, especially for computing higher approximation, and their applicability to a large class of problems. This large class of problems must be of the Quasi-linear form which is defined as a system with weak nonlinearity. That is, the ε in the equation must be a small parameter. This is the major disadvantage of this method. It cannot handle a strong nonlinear system.

2.1.2 Modified Multiple-scale Method

The common perturbation methods are applicable to weakly nonlinear problems. However, many engineering problems have strong nonlinearity. A solution approach must be such that it is able to solve a nonlinear system whose associated parameter is not a small number when compared to unity. So the current interest lies in the ability of the small parameter based perturbation methods can somehow be modified to solve one or more strongly nonlinear problems after some modifications. The modified form of multiple time-scale method helps us to solve strongly nonlinear systems.

This modification is employed on Multiple Time-Scale method (falls under the perturbation methods category). The modified method differs from the usual one as there is a new expansion parameter $\alpha = \alpha(\varepsilon)$ where, ε is the parameter associated with the nonlinear terms of the eq. 2.02. The detailed procedure for this method has been given in Burton and Hamadan [5]. In the case of a forced nonlinear system the frequency detuning parameter (σ) is introduced in the square of the forcing frequency Ω^2 rather than in Ω as the part of the solution procedure. After the modification the equation gets transformed into a form such that the parameter associated with the nonlinear part of the equation is a small parameter.

This method possesses a great advantage of solving a strongly nonlinear system. But in seeking to apply the present approach, difficulty arises when applied to the types of problems where coefficient of the higher harmonics may be nearly as large as the fundamental harmonics. So the qualitative picture of the problem must be known initially. More over there is no systematic procedure of selecting $\alpha = \alpha(\varepsilon)$ so as to achieve a significant improvement in the approximation. According to T. D. Burton [6] this method works well for the forced and free oscillation of un-damped nonlinear single degree freedom system. In reality all systems are damped.

2.1.3 Homotopy Analysis Method

This Homotopy analysis method (HAM) by Shijun Liao [7] is a relatively modern approach to solve nonlinear differential equations. This method uses the topological concept of deformation of a function. Homotopy is defined as the continuous transformation of one function to another function. A "Homotopy" between 2 functions *f(x)* and *g(x)* from space A and space B is a continuous map *G(x, p)* from A to B such that *G(x,0) = f(x)* and *G(x,1) = g(x)* as *p* varies from 0 to 1.

The system equations given in eq. 2.01 or eq. 2.02 are essentially nonlinear differential equations. These can be represented as,

$$N[u(\bar{r},t)]=0 \tag{2.08}$$

where, N is the nonlinear operator, $u(\bar{r},t)$ is an unknown function, and $\bar{r},t$ denote respectively spatial and temporal independent vector and variable.

Let $u_0(\bar{r},t)$ denote an initial guess of the exact solution $u(\bar{r},t)$. Using $p\in[0,1]$ as the embedding parameter we construct the map which deforms the initial guess of the solution of the system equation to the final solution.

$$H[\Phi(\bar{r},t;p);u_0(\bar{r},t),\hbar,p]=(1-p)\{L[\Phi(\bar{r},t;p)-u_0(\bar{r},t)]\}-p\hbar N[\Phi(\bar{r},t;p)] \tag{2.09}$$

Where, $\hbar$ is the auxiliary parameter and

$$\Phi(\bar{r},t;p)=u_0(\bar{r},t)+\sum_{m=1}^{+\infty}u_m(\bar{r},t)\,p^m \tag{2.10}$$

Eq. 2.10 is the series approximation for the solution of the map given by eq. 2.09. If we put $p = 0$ in eq. 2.10 we get the initial guess of the solution which is taken as the solution of the linear differential equation

$$L[\Phi(\bar{r},t;0)-u_0(\bar{r},t)]=0 \tag{2.11}$$

As p varies from 0 to 1 the solution $\Phi(\bar{r},t;p)$ deforms from the initial assumed solution to the solution of the equation

$$N\left[\Phi(\bar{r},t;1)\right]=0 \tag{2.12}$$

The form of the above equation (eq. 2.12) is same as the form of the eq. 2.08. Hence when $p=1$, $\Phi(\bar{r},t;1)=u(\bar{r},t)$ which is the solution of the eq. 2.08.

$$u(\bar{r},t)=u_0(r,t)+\sum_{i=1}^{+\infty}u_i(r,t) \tag{2.13}$$

The evaluation of these $u_i(r,t)$ is done by solving the so called the Higher order deformation equations. The details of this method have been addressed in detail by Liao [8, 9, 10, 11].

The homotopy analysis method provides us the great freedom of expressing the solutions of a given nonlinear problem by means of different base functions. Therefore we can approximate the solution more efficiently by choosing a proper set of base functions to approximate the solutions. Another great advantage of HAM is the control over the convergence region, the rate of convergence of the solution and the independence of the method over the presence of small/large parameters in the system equation.

However the homotopy analysis method has its own list of disadvantages. The method does not dictate the way in which we can properly choose the base functions, the initial guess of the solution and the form of the map or the form of the linear operator. This method also fails in solving damped nonlinear systems. The number of terms required for approximation of the solution of a forced system is very high and the handling of such high number of terms possess serious computational difficulties.

There is another variant of this method called as the "Homotopy Perturbation" technique by Ji Huan He [12, 13].

2.2 Solution Approaches for Randomly Excited systems

2.2.1 Monte-Carlo Simulation

Monte-Carlo simulation for a random variable or a random process is analogous to repeated numerical integration of ordinary or partial set of differential equations of a deterministic system. This method is based on the use of random numbers having the required probability characteristics to investigate the problems. The use of Monte-Carlo methods to model physical problems allows us to examine more complex systems that we otherwise can. Solving equations which describe a single degree of freedom vibrating system is fairly simple; solving for either a multi degree of freedom system or a continuous system is, although not impossible, is very tedious using Monte-Carlo methods. With this method, a large system can be sampled in a number of random configurations, and that data can be used to describe the system's response ensemble.

The major advantage of this simulation technique is that it can be used to simulate any system, simple or complex, linear or nonlinear and discrete or continuous. The time taken to obtain convergence on the probability structure of the response increases drastically with the complexity of the system. This increases the cost of computation for evaluating the probability structure of response of the system. This is a serious drawback of the Monte-Carlo simulations.

2.2.2 Using Analytical Solutions

This method uses the analytical solutions obtained by solving the system symbolically without assigning any numerical value to the parameters which are stochastic in nature. In order to determine the statistical characteristics (the mean, covariance, correlation and the higher order moments) of the stochastic response of the system we utilize the

analytical solution appropriately. In the case of a linear system the requirement on the number of moments on the response of the system calls for the availability of the same number of moments on the random parameter. But in the case of a nonlinear system, even for obtaining a good accuracy on the mean of the response, it requires a large number of higher order moments of the random parameter. In general this is not available which makes this method not suitable for the present work.

2.2.3 Stochastic Central Difference Method

This method comes under the category of various explicit and implicit schemes of direct integration for obtaining the response of single and multi degree of freedom or discretized continuous systems subjected to stationary or non-stationary random excitation. These algorithms enable one to compute covariance of response without using sophisticated mathematical concepts. C. W. S. To [14] has proposed an implicit direct integration scheme for the computation of response of multi-degree freedom system excited by stationary and non-stationary random disturbances. For the response of a continuous system, C. W. S. To [15] has shown that this method is equivalent to the deterministic central difference scheme employed for the direct integration of the equations of motion of discretized structures in structural dynamics. This method can also be used to evaluate the statistical response of nonlinear systems with random excitations. C. W. S. To [16] derived recursive expressions for the variance of response of general nonlinear system subjected to non-stationary random disturbances.

The major disadvantage of this stochastic central difference method is the requirement on correlation of the forcing function at t_l and the system response at t_l to be zero. This is applicable for white noise or modulated white noise excitations. In reality the input excitation may not always follow either white noise or modulated white noise. Hence

this method fails to provide response statistics of systems subjected to any general random excitations.

2.3 Solution Approach for the present work

As introduced earlier the system model adopted for the present study is a combination of a discrete system and continuous elements. The discrete elements nonlinearly modeled and the continuous elements are modeled linearly. To solve such a system with random excitation, a combination of FEM to discretize the continuous system and FDM to evaluate the system response in time is used.

Following this approach, the system equation is obtained in the matrix form. Their general form may be expressed as

$$[M]\{\ddot{x}\}+[C]\{\dot{x}\}+[K]\{x\}=\{f(t)\} \tag{2.14}$$

where,

[M] – System Mass Matrix.

[C] – System Damping Matrix.

[K] – System Stiffness Matrix.

$\{x\},\{\dot{x}\},\{\ddot{x}\}$ - System displacement, velocity and acceleration response.

Because of the presence of nonlinearity in the damper and the spring of the discrete system, the damping and the stiffness matrices are not constant and eq. 2.14 is valid from instant to instant with changed damping and stiffness matrices. We use an iterative procedure to evaluate these matrices. After the evaluation of these matrices we use FD scheme to solve the system at each time step to determine the displacements, velocity and the acceleration response of the system. This is used to determine the response of the system for a deterministic case.

When working on randomly excited systems, we need to find the response statistics. To calculate the same we us the procedure followed by Yadav [17]. A brief outline of the method is given. The evaluation of these parameters is done by solving their corresponding differential equations. Differential equations for response statistical characteristics are developed by utilizing the commutative property of the differentiation and expectation operators. Equation for the mean is obtained by taking term by tem expectation of eq. 2.14

$$[M]\ddot{\mu}_x + [C]\dot{\mu}_x + [K]\mu_x = E[f(t)] \tag{2.15}$$

In the evaluation of the covariance of the response we post multiply eq. (2.14) at t_1 by $x^T(t_2)$ and taking the expectation. The equation can be expressed as a differential equation in the response characteristics at time t_1 and t_2.

$$[M]\ddot{\phi}_{xx}(t_1,t_2) + [C]\dot{\phi}_{xx}(t_1,t_2) + [K]\phi_{xx}(t_1,t_2) = E[f(t_1)x^T(t_2)] \tag{2.16}$$

This would lead to the requirement on the cross-correlation between $x(t)$ and $f(t)$. To obtain this we develop the equation by taking expectation of eq. 2.14 at time t_2 after multiplying it with $f(t_1)$.

$$[M]\ddot{\phi}_{fx}(t_1,t_2) + [C]\dot{\phi}_{fx}(t_1,t_2) + [K]\phi_{fx}(t_1,t_2) = E[f(t_1)f^T(t_2)] \tag{2.17}$$

Solving eqs. 2.15, 2.16 and 2.17 would eventually lead to the solution of the response statistics of the system.

Chapter 3

System Description

The study of the effect of track induced excitation on the vehicle structure with its suspension systems and tires involves the development of a mathematical model. This mathematical model should depict the actual system with acceptable accuracy. As stated earlier the model adopted for the present study is a two degree of freedom single point heave model with two, one dimensional continuous structures to represent the cantilever wings. The development of the mathematical model of the system is divided into the development of a model for the track, model of the vehicle and its wings, its suspension systems and the tires and a model for the ground motion of the vehicle.

3.1 Track Roughness Model

The unevenness of the track is modeled as the superposition of a deterministic function for the mean profile and a zero mean random process for the track level fluctuation about the mean profile. This sum would represent the vertical height of the track along the longitudinal axis measured with respect to a flat datum at a distance ξ from the origin. The origin is taken as the point from which the aircraft starts its motion.

$$y(\xi) = y_m(\xi) + y_r(\xi) \tag{3.01}$$

where,

$y_m(\xi)$ - Deterministic function describing the track mean profile from the datum

$y_r(\xi)$ - Zero-mean random process.

The mean profile shape $y_m(\xi)$ can be represented with the following expressions.

1. Straight level track.

$$y_m(\xi) = 0 \tag{3.02a}$$

2. Straight track with a constant slope.

$$y_m(\xi) = a_1 \xi \tag{3.02b}$$

3. Harmonically curved road.

$$y_m(\xi) = \sum_{i=1}^{n} \left(a_i \, Sin(\Omega_i \xi) + a_i Cos(\Omega_i \xi) \right) \tag{3.02c}$$

The terms in the series can be adjusted to accommodate different spatial frequencies existing in the mean profile. Any general mean profile can be modeled by a combination of the three forms. The Random part of the track unevenness is assumed to be homogenous and is defined by its correlation function $R(y_1, y_2)$.

The correlation function must satisfy certain conditions so as to represent the randomness of the profile of the track. The description of the correlation function must admit differentiation i.e. $R'_{y_1 y_2}(\xi)$ and $R''_{y_1 y_2}(\xi)$ must be continuous at $\xi = 0$, where ξ is the difference between ξ_1 and ξ_2 that is $(\xi_1 - \xi_2)$.

3.2 Vehicle Ground Motion Model

The motion of a vehicle along the track can be characterized by the motion of the vehicle's center of gravity. The motion of an aircraft, which is predominantly a forward motion on a runway or taxiway can be divided to 3 distinct types they are the accelerating or take-off run, the constant velocity taxi run and the landing or decelerating run. These motions can be represented as a general algebraic function in time with v_i as constants.

$$\xi(t) = \sum_i v_i t^i \tag{3.03}$$

Here in the above expression various forms of motion can be represented depending upon what values the v_is take. If non-zero v_1 is alone the motion represents a constant velocity run. If v_2 takes a positive value and the other higher constant terms take zero

values, the vehicle has a uniform accelerating motion. If v_2 is negative the vehicle has a decelerating motion.

3.3 Vehicle Model

The aircraft is modeled with two lumped masses - single point ground contact - heave model (fig. 3.1). It has two degrees of freedom correspond to the sprung mass and the un-sprung mass of the aircraft. These masses are modeled as rigid masses. The sprung mass would include the mass of the fuselage, the cargo and the mass of other components of the aircraft's fuselage. This sprung mass is assumed not to include the mass of the wings, as they are modeled separately. The un-sprung mass will include equivalent part of the masses of the shock strut and the landing gear assembly and the mass of the wheel assembly with tires. The two wings are modeled as symmetrical continuous members attached to the sprung mass like cantilevers. The wings are assumed to have variable cross section, stiffness and damping along the length.

Fig(3.1) : Heave Model

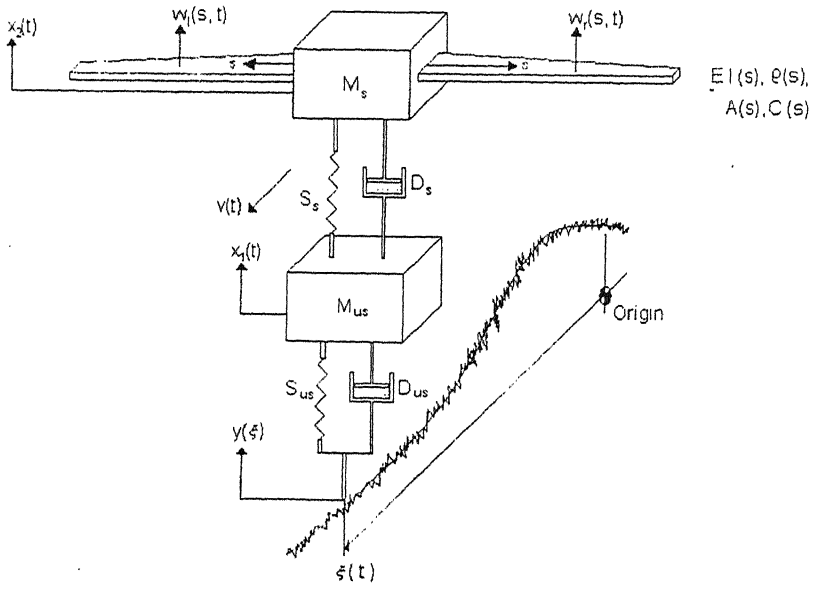

The vehicle position along the track is given by $\xi(t)$ from a fixed datum. The system is assumed to vibrate in the vertical plane only. The locations of the sprung and the un-sprung masses are $x_1(t)$ and $x_2(t)$ measured from their respective static equilibrium positions. The transverse displacements of the right and the left cantilever wings are represented as $w_r(s, t)$ and $w_l(s, t)$ with s indicating the distance along the wing centerline measured from the support location.

The stiffness and the damping of the shock strut and the tires are modeled as nonlinear. The type of nonlinearity used here is a cubic polynomial in displacement and velocity respectively for the restoring and damping forces.

$$F_k = k_1 x + k_2 x^3 \tag{3.04a}$$

$$F_d = c_1 \dot{x} + c_2 \dot{x}^3 \tag{3.04b}$$

The dot over a variable implies derivative with respect to the temporal variable. In this representation the anti-symmetry of the restoring force and damping force is retained. If it is not so the spring and the damper do not function in the same manner for positive and negative forces. There may also be several other representations of the restoring force and damping which maintain their anti-symmetry. We use the representation given above.

3.4 System Equations of Motion

The Equations of motion of the system shown in fig (3.1) can be obtained by using the Extended Hamilton's Principle, which is given as

$$\delta \int_{t_1}^{t_2} (T + W) dt = 0 \tag{3.05}$$

where, $T(q_k, \dot{q}_k)$ – Kinetic Energy of the system with q_k representing the generalized coordinates of the system and $\dot{q}_k$ representing the generalized velocities of the system.

Eq. 3.05 can be rewritten as $\int_{t_1}^{t_2} (\delta T + \delta W) dt = 0$ (3.06)

δW is the virtual work done by the applied forces. In general the virtual work done by the applied forces can be divided into two parts the virtual work done by the conservative and the non-conservative generalized forces.

$$\delta W = \delta W_c + \delta W_{nc} \tag{3.07}$$

where, ,

δW_c - Virtual work done by the conservative forces.

δW_{nc} - Virtual work done by the non – conservative forces.

The work done by the conservative forces can be expressed in the form

$$\delta W_c = -\delta V \tag{3.08}$$

where, V is the potential energy of the system and is a function of q_k the generalized coordinates of the system.

Eq. 3.08 gets transformed in the following form

$$\int_1^2 (\delta T - \delta V + \delta W_{nc}) dt = 0 \tag{3.09}$$

This can be written as

$$\int_1^2 (\delta L + \delta W_{nc}) dt = 0 \tag{3.10}$$

where, L is the 'Lagrangian' of the system given as

$$L = (T(q_k, \dot{q}_k) - V(q_k)) \tag{3.11}$$

The δW_{nc} comprises of the virtual work done by the non-conservative external forces and the virtual work done by the damping forces.

$$\delta W_{damp} = \frac{\partial R}{\partial \dot{q}_k} \tag{3.12}$$

where, R is the Raleigh's dissipative function.

The system equations can be developed by analyzing the system into two parts. The system is divided into the discrete elements and the two continuous members.

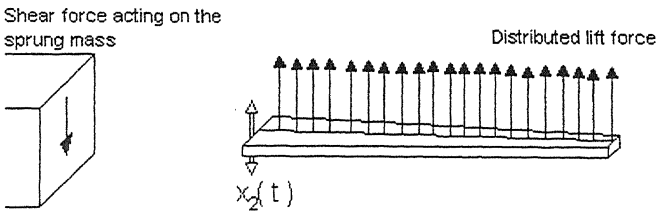

Fig(3.2) Separation of the discrete and continuous systems

The kinetic energy (T) of the discrete part of the system is given as

$$T_{disc} = \frac{1}{2} m_{us} \dot{x}_1^2 + \frac{1}{2} m_s \dot{x}_2^2 \tag{3.13}$$

And, the kinetic energy due to the two continuous systems with base excitation is given as

$$T_{cont} = \int_0^{l_w} \left(\frac{1}{2} \rho(s_l) A(s_l) \left(\dot{w}_l + \dot{x}_2 \right)^2 \right) ds_l + \int_0^{l_w} \left(\frac{1}{2} \rho(s_r) A(s_r) \left(\dot{w}_r + \dot{x}_2 \right)^2 \right) ds_r \tag{3.14}$$

where,

m_{us} – Mass of the Un-sprung mass.

m_s – Mass of the Sprung mass.

$\rho(s_i)$ – Density of the wing's material as a function of distance from the root.

$A(s_i)$ – Area of cross-section of the wing as a function of distance from the root.

l_w – Length of the wing.

i – Left (l) or Right (r) wing of the aircraft.

The potential energy (V_{disc}) of the discrete system is given as

$$V_{disc} = \frac{1}{2}k_{us1}(x_1 - y)^2 + \frac{1}{4}k_{us2}(x_1 - y)^4 + \frac{1}{2}k_{s1}(x_2 - x_1)^2 + \frac{1}{4}k_{s2}(x_2 - x_1)^4 \quad (3.15)$$

where,

k_{us1}, k_{us2} – coefficients corresponding to the un-sprung mass's nonlinear spring.

c_{us1}, c_{us2} – coefficients corresponding to the un-sprung mass's nonlinear damper

k_{s1}, k_{s2} – coefficients corresponding to the sprung mass's nonlinear spring.

c_{s1}, c_{s2} – coefficients corresponding to the sprung mass's nonlinear damper.

The Strain Energy (Π) of the continuous system is due to the bending of the cantilever wings. These strain energies corresponding to the left and right wings of the aircraft and are given as

$$\prod = \int_V \left(\frac{1}{2}\sigma_{ij}\,\varepsilon_{ij}\right) dV \quad (3.16)$$

where,

V – Volume of the material.

σ_{ij} – Stresses induced in the body

ε_{ij} – Strain induced in the members.

In computing the strain energy of the beam, the following assumptions are used

1. Linear strain displacement relations..
2. There is linear relationship between stress and strain.
3. The cantilever beam is assumed to be loaded only in the transverse direction and there are no applied axial loads.

$$\prod = \int_V \left(\frac{1}{2}\sigma_{ij}\,\varepsilon_{ij}\right) dV = \frac{1}{2}\int_V (\sigma_{ss}\,\varepsilon_{ss})\, dV \quad (3.17)$$

$$\sigma_{ss} = E\,\varepsilon_{ss} \quad (3.18)$$

Hence eq. 3.17 is modified as

$$\prod = \left(\frac{1}{2}\int_V (E\,\varepsilon_{ss}^2)\, dV\right) \quad (3.19)$$

The total axial displacement u_l as a function of s along the s - direction in beam is given as

$$u(s)=(u(s))_A - z\frac{d\,w(s)}{ds} \tag{3.20}$$

As per the aforementioned assumptions, since there are no axial loads, $(u(s))_A$ becomes zero, and hence, the axial strain induced in the beam is only because of the bending of the beam. Rewriting eq. 3.20 we get,

$$u(s)=-z\frac{d\,w(s)}{ds} \tag{3.21}$$

The axial strain (ε_{ss}) is given as,

$$\varepsilon_{ss}=\frac{d\,u(s)}{d\,s}=-z\frac{d^2w(s)}{ds^2} \tag{3.22}$$

Substituting eq. 3.22 into eq. 3.19 we get

$$\prod=\frac{1}{2}\int_0^{l_w}\left(\int_A E\left(-z\frac{d^2w(s)}{ds^2}\right)^2 dA\right)ds \tag{3.23}$$

The modulus of elasticity is assumed to be a function of s and not a function of the other two coordinates. The wing is assumed to be a tapered wing, hence the area of cross-section and moment of inertia are all function of s. Integrating over the area,

$$\prod=\frac{1}{2}\int_0^{l_w}\left(E(s)\,I(s)\left(\frac{d^2w(s)}{ds^2}\right)^2\right)ds=\frac{1}{2}\int_0^{l_w}\left(EI(s)\left(\frac{d^2w(s)}{ds^2}\right)^2\right)ds \tag{3.24}$$

In the model of an aircraft considered, the strain energy (Π) induced in the system will be because of the bending of the left and the right wing.

$$\prod=\frac{1}{2}\int_0^{l_w}\left(EI(s)\left(\frac{d^2w_l(s)}{ds^2}\right)^2\right)ds+\frac{1}{2}\int_0^{l_w}\left(EI(s)\left(\frac{d^2w_r(s)}{ds^2}\right)^2\right)ds \tag{3.25}$$

The Raleigh's dissipative function R_{disc} for the discrete system is given as

$$R_{disc}=\frac{1}{2}c_{us1}(\dot{x}_1-\dot{y})^2+\frac{1}{4}c_{us2}(\dot{x}_1-\dot{y})^4+\frac{1}{2}c_{s1}(\dot{x}_2-\dot{x}_1)^2+\frac{1}{4}c_{s2}(\dot{x}_2-\dot{x}_1)^4 \quad (3.26)$$

And the dissipative function for the continuous system is given as

$$R_{cont}=\frac{1}{2}\int_0^{l_w}c_{wl}(s)(\dot{w}_l+\dot{x}_2)^2\,ds+\frac{1}{2}\int_0^{l_w}c_{wr}(s)(\dot{w}_r+\dot{x}_2)^2\,ds \quad (3.27)$$

Using the Extended Hamilton's principle the equations of motion are derived and are as follows:

$$m_{us}\ddot{x}_1+c_{us1}(\dot{x}_1-\dot{y})+c_{us2}(\dot{x}_1-\dot{y})^3+k_{us1}(x_1-y)+k_{us2}(x_1-y)^3=$$
$$c_{s1}(\dot{x}_2-\dot{x}_1)+c_{s2}(\dot{x}_2-\dot{x}_1)^3+k_{s1}(x_2-x_1)+k_{s2}(x_2-x_1)^3 \quad (3.28a)$$

$$m_s\ddot{x}_2+c_{s1}(\dot{x}_2-\dot{x}_1)+c_{s2}(\dot{x}_2-\dot{x}_1)^3+k_{s1}(x_2-x_1)+k_{s2}(x_2-x_1)^3=$$
$$-\frac{\partial}{\partial s_l}\left(EI(s_l)\left(\frac{\partial^2 w_l}{\partial s_l^2}\right)\right)\Bigg|_{s_l=0}-\frac{\partial}{\partial s_r}\left(EI(s_r)\left(\frac{\partial^2 w_r}{\partial s_r^2}\right)\right)\Bigg|_{s_r=0} \quad (3.28b)$$

$$\frac{\partial^2}{\partial s_i^2}\left[EI(s_i)\frac{\partial^2 w_i}{\partial s_i^2}\right]+m_{wi}(s_i)\ddot{w}_i+c_{wi}(s_i)\dot{w}_i=-\left(m_{wi}(s_i)\ddot{x}_2+c_{wi}(s_i)\dot{x}_2\right)+V_{wi}(s_i,t)$$
$$i=l,r \quad (3.28c)$$

The eqs. 3.28a, 3.28b and 3.28c correspond to the coupled equations of motion for the system model adopted.

The lift distribution on the wing surface ($V_{wi}(s_i,t)$) is assumed to be of elliptical distribution and hence the lift on the wing can be expressed as Shevell [19]

$$V_{wi}(s_i,t)=L_0\,v(t)^2\left[1-\left(\frac{s}{l_w}\right)^2\right]^{1/2} \quad (3.29)$$

Where,

$$L_0=\frac{\rho_a C_L S_w}{2\pi l_w} \quad (3.30)$$

In which ρ_a is the density of air, C_L is the lift coefficient, S_w is the wing surface area and l_w is the semi wing span.

Chapter 4

Solution Technique

The equations of motion (eqs. 3.28a, 3.28b, 3.28c) for the model described in the last chapter have been developed by using the extended Hamilton's principle. These equations are coupled set of ordinary and partial differential equations.

The response of the model to combined deterministic and random excitation can be obtained by solving the above set of equations. These equations are solved by using a combination FEM in space for the cantilever wings and FDM in time based analysis. The details of the solution technique are presented in this chapter.

For the ease of handling the eqs 3.28a, 3.28b and 3.28c are expressed in terms of their relative displacements. The following substitutions are made in the equations appropriately,

$$x_1 - y \Rightarrow u_1 \tag{4.01a}$$

$$x_2 - x_1 \Rightarrow u_2 \tag{4.01b}$$

The modified system equations take form ,

$$(m_1+m_2)\ddot{u}_1 + m_2\ddot{u}_2 + c_{us1}\dot{u}_1 + c_{us2}\dot{u}_1^3 + k_{us1}u_1 + k_{us2}u_1^3 = -\frac{\partial}{\partial s_l}\left(EI(s_l)\left(\frac{\partial^2 w_l}{\partial s_l^2}\right)\right)\Bigg|_{s_l=0} - \frac{\partial}{\partial s_r}\left(EI(s_r)\left(\frac{\partial^2 w_r}{\partial s_r^2}\right)\right)\Bigg|_{s_r=0} - (m_1+m_2)\ddot{y}$$

(4.02a)

$$m_1\ddot{u}_1 + m_2\ddot{u}_2 + c_{s1}\dot{u}_2 + c_{s2}\dot{u}_2^3 + k_{s1}u_2 + k_{s2}u_2^3 = -\frac{\partial}{\partial s_l}\left(EI(s_l)\left(\frac{\partial^2 w_l}{\partial s_l^2}\right)\right)\Bigg|_{s_l=0} - \frac{\partial}{\partial s_r}\left(EI(s_r)\left(\frac{\partial^2 w_r}{\partial s_r^2}\right)\right)\Bigg|_{s_r=0} - m_2\ddot{y}$$

(4.02b)

$$\frac{\partial^2}{\partial s_i^2}\left[EI(s_i)\frac{\partial^2 w_i}{\partial s_i^2}\right] + m_{wi}(s_i)\ddot{w}_i + c_{wi}(s_i)\dot{w}_i + \left(m_{wi}(s_i)\ddot{u}_1 + c_{wi}(s_i)\dot{u}_1\right)$$
$$+\left(m_{wi}(s_i)\ddot{u}_2 + c_{wi}(s_i)\dot{u}_2\right) = -\left(m_{wi}(s_i)\ddot{y} + c_{wi}(s_i)\dot{y}\right) + F_{wi}(s_i,t)$$
$$(i = l, r) \quad (4.02c)$$

It can be seen that the response variables of interest are transformed from $x_1(t), x_2(t), w_l(s,t)$ and $w_r(s,t)$ to the variables $u_1(t), u_2(t), w_l(s,t)$ and $w_r(s,t)$. Without any loss of generality, the response can be split up into their deterministic mean and the zero mean random part.

$$u_1 = u_{m1} + u_{r1} \quad (4.03a)$$

$$u_2 = u_{m2} + u_{r2} \quad (4.03b)$$

$$w_i = w_{i\,m1} + w_{i\,r1}, i = l, r \quad (4.03c)$$

The track profile is also divided into two parts, that is the deterministic mean part and the zero mean random part as given by eq. 3.01

$$y(\xi(t)) = y_m(\xi(t)) + y_r(\xi(t)) \quad (4.03d)$$

In the present study, it is assumed that the random part of the response is smaller in magnitude compared to the mean response. That is

$$u_{m1} >> u_{r1} \quad (4.04a)$$

$$u_{m2} >> u_{r2} \quad (4.04b)$$

$$w_{im1} >> w_{i\,r1}, i = l, r \quad (4.04c)$$

This assumption is valid with deterministic initial conditions, when the mean excitation is much larger than the zero mean random input. Substituting eqs. 4.03a, 4.03b, 4.03c, 4.03d) in eqs. 4.02a, 4.02b, 4.02c and expanding the same, we get two sets of differential equations. A set of nonlinear differential equations to determine the deterministic part of the response of the structure and a set of linear differential equations in the random part

of the response of the structure. The equations to determine the deterministic part of the response is given as.

$$(m_1+m_2)\ddot{u}_{m1}+m_2\ddot{u}_{m2}+c_{us1}\dot{u}_{m1}+c_{us2}\dot{u}_{m1}^3+k_{us1}u_{m1}+k_{us2}u_{m1}^3=$$
$$-\frac{\partial}{\partial s_l}\left(EI(s_l)\left(\frac{\partial^2 w_{lm}}{\partial s_l^2}\right)\right)\Bigg|_{s_l=0}-\frac{\partial}{\partial s_r}\left(EI(s_r)\left(\frac{\partial^2 w_{rm}}{\partial s_r^2}\right)\right)\Bigg|_{s_r=0}-(m_1+m_2)\ddot{y}_m \qquad (4.05a)$$

$$m_1\ddot{u}_{m1}+m_2\ddot{u}_{m2}+c_{s1}\dot{u}_{m2}+c_{s2}\dot{u}_{m2}^3+k_{s1}u_{m2}+k_{s2}u_{m2}^3=$$
$$-\frac{\partial}{\partial s_l}\left(EI(s_l)\left(\frac{\partial^2 w_{lm}}{\partial s_l^2}\right)\right)\Bigg|_{s_l=0}-\frac{\partial}{\partial s_r}\left(EI(s_r)\left(\frac{\partial^2 w_{rm}}{\partial s_r^2}\right)\right)\Bigg|_{s_r=0}-m_2\ddot{y}_m \qquad (4.05b)$$

$$\frac{\partial^2}{\partial s_i^2}\left[EI(s_i)\frac{\partial^2 w_{im}}{\partial s_i^2}\right]+m_{wi}(s_i)\ddot{w}_{im}+c_{wi}(s_i)\dot{w}_{im}+\left(m_{wi}(s_i)\ddot{u}_{m1}+c_{wi}(s_i)\dot{u}_{m1}\right)$$
$$+\left(m_{wi}(s_i)\ddot{u}_{m2}+c_{wi}(s_i)\dot{u}_{m2}\right)=-\left(m_{wi}(s_i)\ddot{y}_m+c_{wi}(s_i)\dot{y}_m\right)+V_{wi}(s_i,t)$$
$$i=l,r \qquad (4.05c)$$

The equations corresponding to the random part of the response of the structure are assumed to be linear differential equations and are given as.

$$(m_1+m_2)\ddot{u}_{r1}+m_2\ddot{u}_{r2}+(c_{us1}+3c_{us2}\dot{u}_{m1}^2)\dot{u}_{r1}+(k_{us1}+3k_{us2}u_{m1}^2)u_{r1}=$$
$$-\frac{\partial}{\partial s_l}\left(EI(s_l)\left(\frac{\partial^2 w_{lr}}{\partial s_l^2}\right)\right)\Bigg|_{s_l=0}-\frac{\partial}{\partial s_r}\left(EI(s_r)\left(\frac{\partial^2 w_{rr}}{\partial s_r^2}\right)\right)\Bigg|_{s_r=0}-(m_1+m_2)\ddot{y}_r \qquad (4.06a)$$

$$m_1\ddot{u}_{r1}+m_2\ddot{u}_{r2}+(c_{s1}+3c_{s2}\dot{u}_{m2}^2)\dot{u}_{r2}+(k_{s1}+3k_{s2}u_{m2}^2)u_{r2}=$$
$$-\frac{\partial}{\partial s_l}\left(EI(s_l)\left(\frac{\partial^2 w_{lr}}{\partial s_l^2}\right)\right)\Bigg|_{s_l=0}-\frac{\partial}{\partial s_r}\left(EI(s_r)\left(\frac{\partial^2 w_{rr}}{\partial s_r^2}\right)\right)\Bigg|_{s_r=0}-m_2\ddot{y}_r \qquad (4.06b)$$

$$\frac{\partial^2}{\partial s_i^2}\left[EI(s_i)\frac{\partial^2 w_{ir}}{\partial s_i^2}\right]+m_{wi}(s_i)\ddot{w}_{ir}+c_{wi}(s_i)\dot{w}_{ir}+\left(m_{wi}(s_i)\ddot{u}_{r1}+c_{wi}(s_i)\dot{u}_{r1}\right)$$
$$+\left(m_{wi}(s_i)\ddot{u}_{r2}+c_{wi}(s_i)\dot{u}_{r2}\right)=-\left(m_{wi}(s_i)\ddot{y}_r+c_{wi}(s_i)\dot{y}_r\right)$$
$$i=l,r \qquad (4.06c)$$

4.1 Mean Part of Response

The deterministic part of the total response of the model gives us the mean of the response. This is obtained from the assumption that the excitation is a sum of a deterministic mean profile of the road superimposed by a zero-mean random process.

To evaluate the mean response of the model we first need to find the variational form for the equation of motion for the cantilever wings. This is done by using the principle of virtual work. That is we multiply eq. 4.06c with a virtual displacement $\delta \tilde{w}_{im}$, $i = l, r$. Then it is integrated over the entire length of the cantilever wing. The integration is carried out by parts the first term of the equation, to obtain the weak form of the term and the corresponding boundary conditions. Eq. 4.06c takes the following form.

$$\int_0^{l_w}\left[EI(s_i)\frac{\partial^2 w_{im}}{\partial s_i^2}\right]\frac{\partial^2 \delta\tilde{w}_{im}}{\partial s_i^2}ds_i + \left(\frac{\partial}{\partial s_i}\left(EI(s_i)\frac{\partial^2 w_{im}}{\partial s_i^2}\right)\delta\tilde{w}_{im}\right)\Bigg|_0^{l_w} - \left(\left(EI(s_i)\frac{\partial^2 w_{im}}{\partial s_i^2}\right)\frac{\partial(\delta\tilde{w}_{im})}{\partial s_i}\right)\Bigg|_0^{l_w}$$

$$+ \int_0^{l_w} m_{wi}(s_i)\ddot{w}_{im}\,\delta\tilde{w}_{im}ds_i + \int_0^{l_w} c_{wi}(s_i)\dot{w}_{im}\delta\tilde{w}_{im}\,ds_i$$

$$+ \int_0^{l_w}(m_{wi}(s_i)\ddot{u}_{m1} + c_{wi}(s_i)\dot{u}_{m1})\delta\tilde{w}_{im}\,dsi + \int_0^{l_w}(m_{wi}(s_i)\ddot{u}_{m2} + c_{wi}(s_i)\dot{u}_{m2})\delta\tilde{w}_{im}\,ds_i$$

$$= -\int_0^{l_w}(m_{wi}(s_i)\ddot{y}_m + c_{wi}(s_i)\dot{y}_m)\delta\tilde{w}_{im}\,ds_i + \int_0^{l_w} V_{wi}(s_i,t)\delta\tilde{w}_{im}\,ds_i$$

$$i = l, r \tag{4.07}$$

Assuming the solution form for the w_{im}

$$w_{im}(t,s_i) = \sum_j w_{im}^j(t)N_j(s_i),\ i = l,r \tag{4.08}$$

Hence,

$$\delta w_{im}(t,s_i) = \sum_j \delta w_{im}^j(t)N_j(s_i),\ i = l,r \tag{4.09}$$

where $N_j(s_i)$s are the shape functions. Hermite cubic polynomials are chosen as the shape functions so that thee elements are c^1 continuous elements. In the choice of the shape

functions the number of nodes per element is chosen as 2 and the number of degrees of freedom per node is also 2. They are the transverse displacement and the slope at the nodes. The shape functions are given as follows.

$$N_j^1 = \frac{1}{4}\left(2 - 3\eta + \eta^3\right) \tag{4.10a}$$

$$N_j^2 = \frac{l_e}{8}\left(1 - \eta - \eta^2 + \eta^3\right) \tag{4.10b}$$

$$N_j^3 = \frac{1}{4}\left(2 + 3\eta - \eta^3\right) \tag{4.10c}$$

$$N_j^4 = \frac{l_e}{8}\left(-1 - \eta + \eta^2 + \eta^3\right) \tag{4.10d}$$

where, η is the natural coordinate of the element over which integration is done. The domain of the wing is discretized into number of elements. The index 'j' indexes over all the elements of the domain. And by substituting eq. 4.09 and eq. 4.10 in eq. 4.08 and dividing the integral into summation of smaller integrals gives the following scheme

$$\int_0^{l_w}[\bullet] \Rightarrow \sum_j \left(\int_{s_{j1}}^{s_{j2}}[\bullet] \right) \tag{4.11}$$

where, s_{j1} and s_{j2} correspond to the starting and the ending coordinate of the element 'j' under integration. Using the principles of FEM we obtain the discretized form for the eq 4.08. In order to obtain the combined mass, damping and stiffness matrix, the nonlinear terms in the eqs. 4.06a, 4.06b are transformed into the following form.

$$(m_1 + m_2)\ddot{u}_{m1} + m_2\ddot{u}_{m2} + (c_{us1} + c_{us2}\hat{\dot{u}}_{m1}^2)\dot{u}_{m1} + (k_{us1} + k_{us2}\hat{u}_{m1}^2)u_{m1} = -\frac{\partial}{\partial s_l}\left(EI(s_l)\left(\frac{\partial^2 w_{lm}}{\partial s_l^2}\right)\right)\Bigg|_{s_l=0} - \frac{\partial}{\partial s_r}\left(EI(s_r)\left(\frac{\partial^2 w_{rm}}{\partial s_r^2}\right)\right)\Bigg|_{s_r=0} - (m_1 + m_2)\ddot{y}_m \tag{4.12a}$$

$$m_1 \ddot{u}_{m1} + m_2 \ddot{u}_{m2} + (c_{s1} + c_{s2}\hat{\dot{u}}_{m2}^2)\dot{u}_{m2} + (k_{s1} + k_{s2}\hat{u}_{m2}^2)u_{m2} =$$
$$-\frac{\partial}{\partial s_l}\left(EI(s_l)\left(\frac{\partial^2 w_{lm}}{\partial s_l^2}\right)\right)\Bigg|_{s_l=0} - \frac{\partial}{\partial s_r}\left(EI(s_r)\left(\frac{\partial^2 w_{rm}}{\partial s_r^2}\right)\right)\Bigg|_{s_r=0} - m_2\ddot{v}_m$$

(4.12b)

The terms $(c_{us1} + c_{us2}\hat{\dot{u}}_{m1}^2)$, $(c_{s1} + c_{s2}\hat{\dot{u}}_{m2}^2)$, $(k_{us1} + k_{us2}\hat{u}_{m1}^2)$ and $(k_{s1} + k_{s2}\hat{u}_{m2}^2)$ correspond to the approximate damping and stiffness coefficients in the system. The corresponding velocity and displacements, denoted with $[\hat{\cdot}]$, used in the coefficients are taken as the values in the previous time step in the sequential generation of the solution. Using eqs 4.12a and 4.12b and the discretized form of eq. 4.07 we get the set of simultaneous equations. These can be expressed in matrix notation with response vector $\{q_m\}$, mass matrix [M], damping matrix [D], stiffness matrix [K] and the right hand side force vector $\{f_m(t)\}$, as shown below.

$$[M]\{\ddot{q}_m\} + [C]\{\dot{q}_m\} + [K]\{q_m\} = \{f_m(t)\} \qquad (4.13)$$

For evaluation of the system coefficients at the first time step, the initial conditions are taken as the approximate values for the displacement and velocity. Using the Newmark's Finite Difference scheme we obtain the first approximate values of displacement, velocity and acceleration for all degrees of freedom of the system. Using these obtained values to determine the stiffness and damping coefficients, the operation is repeated for the same time step iteratively till convergence is achieved. The test for convergence is taken as the norm of the error in the displacement values of the degrees of freedom between two successive iteration results to be less than ε, where ε is a positive small quantity, selected on the basis of required accuracy.($\varepsilon = 10^{-6}$ for the present study). When the convergence is achieved the next time step is taken. The process is repeated with the displacements and velocities obtained in the previous time becoming the initial conditions.

4.2 Covariance Response

The equations that correspond to the stochastic part of the response is given in eq. 4.06a, 4.06b, 4.06c. These equations are Linear Ordinary/Partial Differential equations.

The evaluation of the random response of the system is also done through FDM. The second order statistics are calculated by extending the procedure formulated by Yadav [17] for a multi body ground vehicle to incorporate the presence of a continuous structure. The coefficients of the terms $u_{r1}, u_{r2}, \dot{u}_{r1}$ and $\dot{u}_{r2}$ in the equations above would require the knowledge of the mean value of the displacement and velocity of the model at the time instant under evaluation. This is obtained from the current time step's deterministic part of the response calculations. A flowchart showing the combined evaluation of the deterministic and stochastic calculations is shown below.

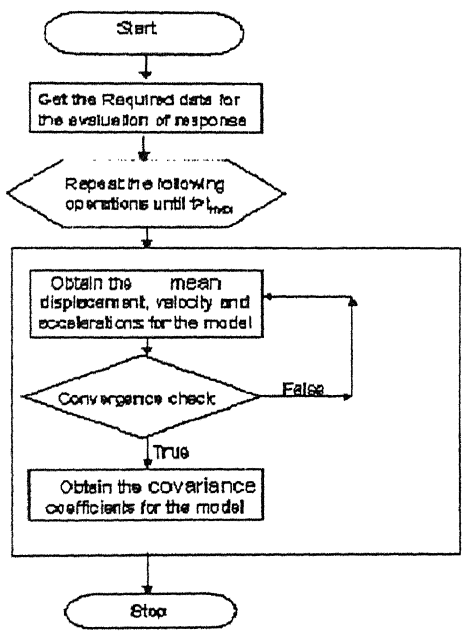

Fig. 4.1 Flow chart showing the evaluation of the response of the structure

The combined stochastic equation of the model is again put in the form of the mass, damping and the stiffness matrices with the associated right hand side force vector. It is given as

$$[M]\{\ddot{q}_r\}+[C]\{\dot{q}_r\}+[K]\{q_r\}=\{f_r(t)\} \tag{4.14}$$

Where $\{q_r\}$ correspond to the random part of the response of the model.

In the evaluation of the correlation of the response we post multiply eq. 4.14 at t_1 by $q_r^T(t_2)$ and take the expectation. The solution of the equation leads to the cross-covarianceof the response of the system at time t_1 and t_2.

$$[M]\{\ddot{\kappa}_{qq}(t_1,t_2)\}+[C]\{\dot{\kappa}_{qq}(t_1,t_2)\}+[K]\{\kappa_{qq}(t_1,t_2)\}=E[f_r(t_1)q_r^T(t_2)] \tag{4.15}$$

This would lead to the requirement of the cross-covariance between $q_r(t)$ and $f_r(t)$. To obtain this we develop the required equation by taking expectation of eq. 4.14 at time t_2 and $f^T(t_1)$.

$$[M]\{\ddot{\kappa}_{qf}(t_1,t_2)\}+[C]\{\dot{\kappa}_{qf}(t_1,t_2)\}+[K]\{\kappa_{qf}(t_1,t_2)\}=E[f_r(t_1)f_r^T(t_2)] \tag{4.16}$$

Solving eqs. 4.17 and 4.18 would eventually lead to the solution of the covariance values of the system at the time instant under evaluation.

4.3 Newmark's Finite Difference Scheme

The evaluation of the mean and the covariance of the response for the model is done by Newmark's Finite Difference Scheme (Bathe [35]). After forming the stiffness, damping and the mass matrices we initialize the displacement, velocity and acceleration initial conditions. We select the desired time step Δt for the finite difference scheme. Along with the time step, the parameters of the FD scheme α and δ are also selected to obtain integration accuracy and stability of the solution. Typically the parameters are required to satisfy the following conditions

$$\delta \geq 0.5; \qquad \alpha \geq 0.25(0.5+\delta)^2 \tag{4.19}$$

There are other constants involved in the FD scheme they are as follows,

$$a_0 = \frac{1}{\alpha \Delta t^2}; \quad a_1 = \frac{\delta}{\alpha \Delta t}; \quad a_2 = \frac{1}{\alpha \Delta t}; \quad a_3 = \frac{1}{2\alpha} - 1; \quad a_4 = \frac{\delta}{\alpha} - 1;$$

$$a_5 = \frac{\Delta t}{2}\left(\frac{\delta}{\alpha} - 2\right); \quad a_6 = \Delta t(1-\delta); \quad a_7 = \delta \Delta t \tag{4.20}$$

The effective stiffness matrix, formed at each time instant is given as follows,

$$^{(t+\Delta t)}\left[\hat{K}\right] = {}^{(t+\Delta t)}[K] + a_0\,{}^{(t+\Delta t)}[M] + a_1\,{}^{(t+\Delta t)}[C] \tag{4.21}$$

where,

$^{(t+\Delta t)}\left[\hat{K}\right]$ - Equivalent stiffness matrix at time $t+\Delta t$.

$^{(t+\Delta t)}[K]$, $^{(t+\Delta t)}[M]$, $^{(t+\Delta t)}[C]$ - Equivalent stiffness, mass and the damping matrices at time $t+\Delta t$.

The effective load vector at the current time is also evaluated using the expression given below. This requires the value of the displacements, velocities and accelerations at the previous time step.

$$^{(t+\Delta t)}\left\{\hat{R}\right\} = {}^{(t+\Delta t)}\{R\} + {}^{(t+\Delta t)}[M]\left(a_0\,{}^{t}\{u\} + a_2\,{}^{t}\{\dot{u}\} + a_3\,{}^{t}\{\ddot{u}\}\right) + {}^{(t+\Delta t)}[C]\left(a_1\,{}^{t}\{u\} + a_4\,{}^{t}\{\dot{u}\} + a_5\,{}^{t}\{\ddot{u}\}\right) \tag{4.22}$$

$^{t}\{u\}$ - Displacement response vector at time t.

$^{t}\{\dot{u}\}$ - Velocity response vector at time t.

$^{t}\{\ddot{u}\}$ - Acceleration response vector at time t.

$^{(t+\Delta t)}\left\{\hat{R}\right\}$ - Equivalent force vector at time $t+\Delta t$.

$^{(t+\Delta t)}\{R\}$ - Force vector at time $t+\Delta t$.

Since the equivalent stiffness matrix and the equivalent force vector are obtained, we can solve for the response of the system at time $t+\Delta t$ using the following expression,

$$^{(t+\Delta t)}\left[\hat{K}\right]\,{}^{(t+\Delta t)}\{u\} = {}^{(t+\Delta t)}\left\{\hat{R}\right\} \tag{4.23}$$

After solving for the displacements at time $(t+\Delta t)$, this data is used to calculate the velocities and accelerations at time $(t+\Delta t)$, using the following expressions.

$$^{(t+\Delta t)}\{\ddot{u}\} = a_0\left(^{(t+\Delta t)}\{u\} - {}^{t}\{u\}\right) - a_2\,{}^{t}\{\dot{u}\} - a_3\,{}^{t}\{\ddot{u}\} \tag{4.24a}$$

$$^{(t+\Delta t)}\{\dot{u}\} = {}^{t}\{\dot{u}\} + a_6\,{}^{t}\{\ddot{u}\} + a_7\,{}^{(t+\Delta t)}\{\ddot{u}\} \tag{4.24b}$$

Thus the response displacement, velocity and acceleration are evaluated and the solution marches a step to $(t+\Delta t)$. This process is continued till $t = t_{max}$ is achieved.

Chapter 5

Results and Discussions

The present study aims at obtaining the response of an aircraft for a track induced random excitation during constant and variable velocity runs. As described earlier the wings of the aircraft are modeled as flexible continuous members with non-uniform distributed parameters. Results have been presented in three sections. The first section deals with the vehicle track responses during the uniform velocity taxi run. The second section deals with the accelerating take off run of the aircraft and the last section deals with the decelerating landing run of the aircraft.

The flight vehicle considered for the study is a mid-sized Fighter-Trainer aircraft. The following data have been used for the generation of the results.

Total mass of the Aircraft	:	9500 Kgs
Sprung-mass	:	9000 Kgs
Un-sprung-mass	:	500 Kgs
Spring Constants of the Shock Strut.		
Linear coefficient (k_{s1})	:	300 N/m
Non-Linear Coefficient (k_{s2})	:	90000 N/m
Damping Constants of the Shock Strut.		
Linear coefficient (c_{s1})	:	19000 N s/m
Non-Linear Coefficient (c_{s2})	:	28500 N s/m
Spring Constants of the Tire.		
Linear coefficient (k_{us1})	:	1750 N/m
Non-Linear Coefficient (k_{us2})	:	250000 N/m
Damping Constants of the Tire.		

Linear coefficient (c_{us1}) : 28500 N s/m

Non-Linear Coefficient (c_{us2}) : 38000 N s/m

The wings of the aircraft are modeled as a cantilever beam with varying sectional properties along the length. The wing parameters and their variation are as given below [18].

Mass per unit length : $m_0(1-0.39\,(s/l_w))$

m_0 - Mass per unit length at root : 27 kg/m

Moment of Inertia along the length : $EI_0(1-1.11(s/l_w)+0.3(s/l_w)^2)$

EI_0 - MI of the wing at Root : $1.926 * 10^7$ N m^2

Damping per unit length : $c_0(1-0.39\,(s/l_w))$

c_0 - Damping per unit length at root : 27000 N s/m

The mean track profile is taken as a single frequency harmonically curved shape with zero slope

$$y(\xi) = a\,Cos(\nu\,\xi) \tag{5.01}$$

where, a is the amplitude of the track and ν is the wave number of the harmonic function.

Amplitude of the track (a) : 0.005 m

Wave number of the harmonic function (ν) : $\frac{2\pi}{50}$ rad./m

This is a generic form and superimposition of such terms can be used to model any given track shape.

The zero mean random track unevenness, as stated earlier, must posses a correlation function whose first and second derivatives are continuous. The random process is assumed to be a homogenous in space. The form of the correlation function of the random process is chosen as follows.

$$\Phi_{yy}(\xi) = \sigma^2 e^{-\alpha\xi^2} \tag{5.02}$$

The values for the parameters σ and α are taken from Yadav [17] as 0.01 and 0.005 respectively.

A parameter study has been carried out by varying the nonlinear stiffness coefficient from -5% to +5% about the nominal value. Another parameter study has been done to evaluate the effect of damping varying it from +100% to -50% about the nominal value.

Sections 5.1.1, 5.2.1 and 5.3.1 present the second order statistics for the taxi, take-off and landing runs respectively. Each run has been studied with three forward motion patterns. Variation in nonlinear spring stiffness is considered for all the tree motion patterns for each run while the variations in the damping coefficient has been studied only with the extreme case in each type of runs.

5.1 Taxi Run

5.1.1 Variation in non-linear stiffness coefficients

The effect of variation in the nonlinear stiffness coefficient is observed in this section for taxi run. For the case of the taxi run, the aircraft is assumed to move forward at constant velocity. This corresponds to a situation where the vehicle, moving at constant speed over a smooth surface, suddenly encounters a rough terrain at t = 0, without any change in the forward velocity. The simulation of the taxi run is done for 3 cases: Taxi runs at 40 Km/hr, 60 Km/hr and 80 Km/hr. The response behavior for the taxi runs are presented graphically for a time interval of 20 s. The results have been presented for the responses of the un-sprung mass, the sprung mass and the discretized wing tip with initial conditions are assumed to be zero for displacement and zero velocity in the vertical direction. Figures 5.01 to 5.06 are for taxi velocity of 40 km/hr, figures 5.07 to 5.12 are for the taxi velocity of 60 km/hr and finally figures 5.13 to 5.18 are for the aircraft's taxi velocity of 80 km/hr.

The figures 5.01, 5.07 and 5.13 show the plots of the mean displacements of the un-sprung mass, the sprung mass and the wing tip for the three taxi velocities. The mean displacement rises with time because of the lift acting on the wings. It then steadies to oscillate about the new mean position. The transient oscillation of the system dampens out quickly. The amount of initial rise in the values of the displacement response increases with the increase in the taxiing velocity. The standard deviations of the displacement of the un-sprung mass, sprung mass and the wing tip are shown in figures 5.02, 5.08 and 5.14. The plots illustrate an initial high dispersion in the displacement. This dispersion decreases or dampens as time progresses. The graphs indicate a distinct time period that decreases with increase in the taxi velocity. In each period the standard deviation shows the form of a half sine wave. The effect of the change in the nonlinear spring coefficient is very small and barely noticeable for both the mean and the SD of displacement response.

The mean velocity (figs 5.03, 5.09 and 5.15) and the standard deviation (figs 5.04, 5.10 and 5.16) of the response have some similarity with the displacement response pattern. There is an initial rise in the mean velocity of the un-sprung mass, the sprung mass and the wing tip. These come down as time progresses and continue to have small amplitude oscillations about the zero mean. There is an initial rise in the amplitude of the velocities' standard deviation which, after initial transience follows a pattern similar to the displacement response. The effect of the change in the non-linear stiffness coefficients, like in the displacement response, is very small.

The taxi run acceleration response mean and standard deviation are presented in figures 5.05, 5.11 and 5.17 and 5.06, 5.12 and 5.18 respectively for the three taxi velocities. The mean response show an initial high value that comes down and then has very small undulations about the zero mean. The initial acceleration of the un-sprung mass and the sprung mass increases as the taxiing velocity increases. The acceleration plot of the cantilever

wings shows a superimposed high frequency small amplitude oscillation decaying with time. This is attributed to the high stiffness value of the structure. The SD of the acceleration response indicates sinusoidal humps as in the displacement and velocity response. Here too the plot of the SD of the acceleration of the wing tip shows a high frequency oscillation with amplitude decaying with time. The variation in nonlinear stiffness has little effect on the acceleration response.

5.1.2 Variation in damping coefficients

The mean and SD of displacement, velocity and acceleration responses of the un-sprung mass, the sprung mass and the wing tip during the taxi run of 80 km/hr have been presented as graphs in figures 5.19 to 5.24.

The large variation in the damping coefficients has a profound effect on the mean displacement of the un-sprung mass, the sprung mass and the wing tip (fig. 5.19). The mean displacement plot expectedly shows heavy oscillations for a decrease in the damping coefficients. The transient oscillations dominate for a longer time with the low value of damping coefficients. An increase in the damping coefficients shows a faster decay in the transient oscillations of the system. The SD of the displacements response (figure 5.20) shows two attributes. One is the frequency and the other is the amplitude of oscillation of the response. Both are inversely proportional to the damping of the system. That is, as the damping coefficient is increased the frequency and amplitude of oscillation decrease

Observation similar to the displacement mean response can be made for the mean velocity response. The amplitude and the frequency increases as the damping decreases. The mean velocity plot of the un-sprung mass, the sprung mass and the wing tip are shown in the figure (5.21).

The SD of the velocity of the un-sprung mass, the sprung mass and the wing tip (figure 5.22) show same attributes as the displacement SD.

The mean acceleration plot (figure 5.23) shows a pattern similar to the displacement and velocity response. There is a small change in the amplitude of the plot and frequency of the plot because of the change in the damping coefficients. The mean acceleration of the wing tip has a superimposed high frequency oscillation. The SD of acceleration response is shown in figure 5.24. The SD of the acceleration of the wing tip shows a low frequency oscillation for low damping coefficients. Except for this, rest of the plots show pattern similar to displacement and velocity response.

5.2 Take-off Run

5.2.1 Variation in non-linear stiffness coefficients

The aircraft while take off must have an accelerating motion so as to attain the take off velocity. In this case the vehicle is assumed to start from rest and accelerate at a uniform rate to the take off velocity in 3 different time intervals, hence with 3 different acceleration rates. The velocity required to attain during take-off is given as 280 km/hr. The times taken to attain this velocity are taken as 20, 30 and 40 seconds. Hence the corresponding constant acceleration rates are 3.88889 m/s^2, 2.66667 m/s^2 and 1.66667 m/s^2 respectively. The un-sprung mass, the sprung mass and wing are again assumed to have zero-initial displacements and zero initial velocities.

The mean and the standard deviation of the displacement, velocity and acceleration responses of the un-sprung mass, sprung mass and the wing tip have been presented as graphs. Figures 5.25 to 5.30 are for an accelerating rate of 3.88889 m/s^2, the next 6 plots figures 5.31 to 5.36 show the responses for an accelerating rate of 2.66667 m/s^2 and the figures 5.37 to 5.42 present the responses for an accelerating rate of 1.66667 m/s^2.

Figures 5.25, 5.31 and 5.37 shows the mean displacement of the un-sprung mass, the sprung mass and the wing tip. Since the velocity of the aircraft is increasing, the lift on the wings also increases as a function of time. This is reflected as rise in the system mean from the initial level. During all the three acceleration rates, the maximum height from the ground level reached at take-off by the vehicle are the same, as the final velocity to be attained in all the 3 cases is 280km/hr. There is similarity in the pattern of the displacement SD for the response (figures 5.26, 5.32 and 5.38) while take off. A periodic pattern is apparent with sinusoidal variations having decreasing amplitude as the time progresses. The rate of decay of amplitude decreases marginally with the increase in acceleration

The change in the non-linear stiffness coefficients is small on the mean and the SD of the displacement response.

The effect of the track profile is not distinct in the mean displacement plots. This is due to the fact that the rise in the level of the aircraft due to lift produced in the wings dominates the amplitude of the response of the system. But the effect of the track mean periodicity can be clearly seen in the mean velocity and mean acceleration response being presented below.

The mean velocities' plots of the un-sprung mass, the sprung mass and the wing tip are shown in figures 5.27, 5.33 and 5.39. They are sensitive the effect of the track's mean periodic profile. The initial hump in the velocity plot can be attributed to the transient response of the system. As time progresses the frequency of oscillation of the response increases with increase in the vehicle forward velocity. The amplitude of response of the system also increases with time. However the mean velocity response dies out with the aircraft attaining a velocity that has the lift negates its weight so that ground input becomes ineffective. The SD of the velocity response (figures 5.28, 5.34 and 5.40) shows a periodic sinusoidal pattern with an initial increase in the amplitude of dispersion and later it decays

with time. The second amplitude is the largest in all the three cases. Like displacement, the velocity response also shows little sensitivity by change in the nonlinear stiffness.

The response calculation scheme is conditioned to simulate a soft take off for the aircraft. The aircraft does not loose ground contact all of a sudden; rather there would be a continuous decrease in the contact area of the tire around the point of take off. When the calculation scheme assumes sudden loss of contact, the sudden removal of the forcing function would predict a spike in the acceleration plot of the system's response. This spike in the acceleration plots reflects as impulsive force acting on the system. Hence to avoid this the track is assumed to have the following profile during the time where in the lift induced in the wings ranges between 90% and 100% of the total weight of the aircraft. This is given as follows,

$$y_m(\xi(t)) = a\, e^{-v_2 t}\, Cos\left[\nu\left(v_1 t + \tfrac{1}{2} v_2 t^2\right)\right] \qquad (5.03)$$

This scheme is applied only on the deterministic mean profile of the track and not on its random part of the track profile.

The mean acceleration plots of the response are shown in the figures 5.29, 5.35 and 5.41. The general nature of the acceleration mean is similar to the velocity mean response. The spikes are still visible in the mean acceleration plots of the aircraft's wing tip. This is because the exponential function selected to simulate the smooth take off is not fully successful. However the spike in the mean acceleration plot of the un-sprung mass and the sprung mass have been removed and its effect is reduced considerably in the acceleration plot of the wing tip. The SD of the acceleration of the aircraft's degrees of freedom and the wing tip are shown in the figures 5.30, 5.36 and 5.42. The general pattern of the acceleration response is similar to the velocity response. The effect of variation in non-linear stiffness coefficient is not strong in the acceleration mean and SD as well.

5.2.1 Variation in damping coefficients

The mean and SD of displacement, velocity and acceleration responses of the un-sprung mass, the sprung mass and the wing tip have been presented as graphs. Figures 5.43 to 5.48 are for the take of run at a constant accelerating rate of 3.88889 m/s^2.

The mean displacement of the un-sprung mass, the sprung mass and the wing tip is shown in figure 5.43. The mean displacement plot shows a variation in the plots for change in the damping coefficients in the first few seconds of acceleration. Then there is no significant change in the plot after the transients have died down. The SD of the displacement response (figure 5.44) show an increase in the amplitude and decrease in the frequency of oscillation as the coefficients of damping is reduced.

The mean velocity of the aircraft's un-sprung mass, the sprung mass and the wing tip is shown in the figure 5.45. The nature of this plot is not very different from the nature of the mean velocity of the aircraft with variation in the stiffness coefficients. There is an increase in the amplitude of oscillation and decrease in the frequency with decrease in damping. Similar observations can be made for the figure 5.46, which shows the SD of the displacement of the degrees of freedom of the aircraft and the wing tip.

The mean acceleration response is shown in the figure 5.47. The mean acceleration shows same trend as discussed earlier for the take off run (with variation in the non-linear stiffness coefficients). Low damping results in higher response magnitudes initially. The wing tip shows low sensitivity to change in damping. The SD of the acceleration does show significant change in the magnitude of the amplitude of oscillation (figure 5.48), low damping giving higher amplitudes.

5.3 Landing Run

5.3.1 Variation in non-linear stiffness coefficients

The vehicle, while landing, will have vertical sink velocity; hence it must be given as a part of the initial condition for the system dynamics. The position of the sprung mass and the un-sprung mass will not be at their static equilibrium level. The spring and the damper of the shock strut and the tires will be free with no loads acting on them. Hence negative values of initial displacements must be provided as initial conditions for the two lumped masses. The vehicle is assumed to have a sink velocity of 1 m/s and the initial displacement for the tire is given as 0.1 m and the same value is given for the shock strut's initial displacement. The sprung mass's initial velocity is assumed to have the same sink velocity of 1m/s at the point of impact with the ground. At touch down the tire first experiences the shock and it is then passed on to the super structure through the un-sprung mass.

The vehicle is simulated for three different landing runs based on the time required to full halt. The vehicle's initial glide velocity is taken as 280 km/hr. The time taken to stop are selected to be 20, 30 and 40 seconds. Hence the deceleration rates are given as 3.88889 m/s^2, 2.66667 m/s^2 and 1.66667 m/s^2 respectively.

The mean and the standard deviation of the displacement, velocity and acceleration responses of the un-sprung mass, sprung mass and the wing tip during landing run have been presented as graphs. Figures 5.49 to 5.55 are for a deceleration rate of 3.88889 m/s^2 and the next 6 plots figures 5.56 to 5.62 show the responses for a deceleration rate of 2.66667 m/s^2 and the figures 5.63 to 5.69 show the responses for a deceleration rate of 1.66667 m/s^2.

The mean displacement responses are shown in the figures 5.49, 5.56 and 5.63. There is an initial dip in the displacement plots which is not clearly seen in these plots and hence they are enlarged and shown in figures 5.50, 5.57 and 5.64. The system response has a rise in the mean displacement and then slowly the height above the ground level decreases in a small amplitude oscillatory fashion, to their mean position as the time progresses. The SD of the displacement (figures 5.51, 5.58, 5.65) of the un-sprung mass, the sprung mass and the wing tip show an initial rise in the amplitude of the dispersion and later this amplitude decays with time with a distinct periodic oscillation. The change in the non-linear stiffness coefficient has little effect on the response behavior.

The mean velocity plots are shown in figures 5.52, 5.59 and 5.66. These plots show initial high amplitude of velocity response. A distinct periodic oscillatory pattern is observed that has a rapid decrease in the amplitude. The SD of velocity response (figures 5.53, 5.60 and 5.67) can be interpreted as superposition of a linear decreasing function with a higher frequency oscillating part. The oscillation amplitude decreases with time after an initial increase. The non-linear stiffness coefficient change indicates again a little effect on the response pattern.

The Mean acceleration of the un-sprung mass, the sprung mass and the wing tip (figures 5.54, 5.61 and 5.68) show an initial spike in the acceleration caused because of the touch down. Then the oscillation of this acceleration plot decays in amplitude with increase in time. The oscillation of the wing tip shows a superimposed high frequency oscillation. But the envelope within which these high frequency oscillation is taking place decays and converges to the zero acceleration line. The SD of the acceleration of the degrees of freedom and the wing tip are shown in figure 5.55, 5.62 and 5.69. The SD shows after a small initial fluctuation a non oscillatory decay of the acceleration. This initial shallow dip in the SD can be attributed to the reduction in the contact area of the tires with the ground because of

rebound effect after touch down of the aircraft. Change in the nonlinear stiffness coefficient has a little effect on the acceleration response pattern.

5.3.2 Variation in damping coefficients

The mean and SD of displacement, velocity and acceleration responses of the un-sprung mass, the sprung mass and the wing tip have been presented as graphs. Figures 5.70 to 5.75 are for the landing run at a decelerating rate of 3.88889 m/s^2.

Same type of initial conditions, which were used for the parameter study of the aircraft with respect to varying stiffness, is also used in this parameter study. The sprung mass and the un-sprung mass have non-zero initial displacement corresponding to the extended nature of the springs and non-zero initial velocity corresponding to the sink velocity of the aircraft. The aircraft is simulated to have a decelerating rate of 3.8889 m/s^2. The sink velocity is taken as 1m/s for both the sprung mass and the un-sprung mass.

The mean displacement response for landing run of the aircraft (figure 5.70) shows the same characteristics as reported for the landing run earlier with the variation in the nonlinear stiffness. The change in the damping affects the initial transience. With the passage of time, the responses are very close. Near stoppages, however some difference in the response can be observed. The SD of the displacement is sensitive to damping (figure 5.71). The SD of displacement response for a 50% reduction in stiffness shows a large amplitude oscillation and it does not decay within the stoppage time. This is not the case with the 0% change in damping and 100% increase in damping, where in the SD displacement dampens out its oscillations with in the time frame.

The mean velocity responses are shown in figure 5.72. There is no significant change in the characteristic of the plots from the corresponding plots obtained during the parameter study of the stiffness. Lower damping results in higher response mean. The SD of

the velocity (figure 5.73) shows the comparable characteristic for 0% change and 100% increase in damping coefficients. But for 50% decrease in the damping the oscillations are strong with the amplitude decaying slowly. The oscillations do not die even when the vehicle comes to stop.

There is no significant change in the nature of the plots for the mean and SD of and the acceleration response (figures 5.74 and 5.75) compared to the case for variation in the nonlinear stiffness. The change in damping modifies the response only during the initial part of motion.

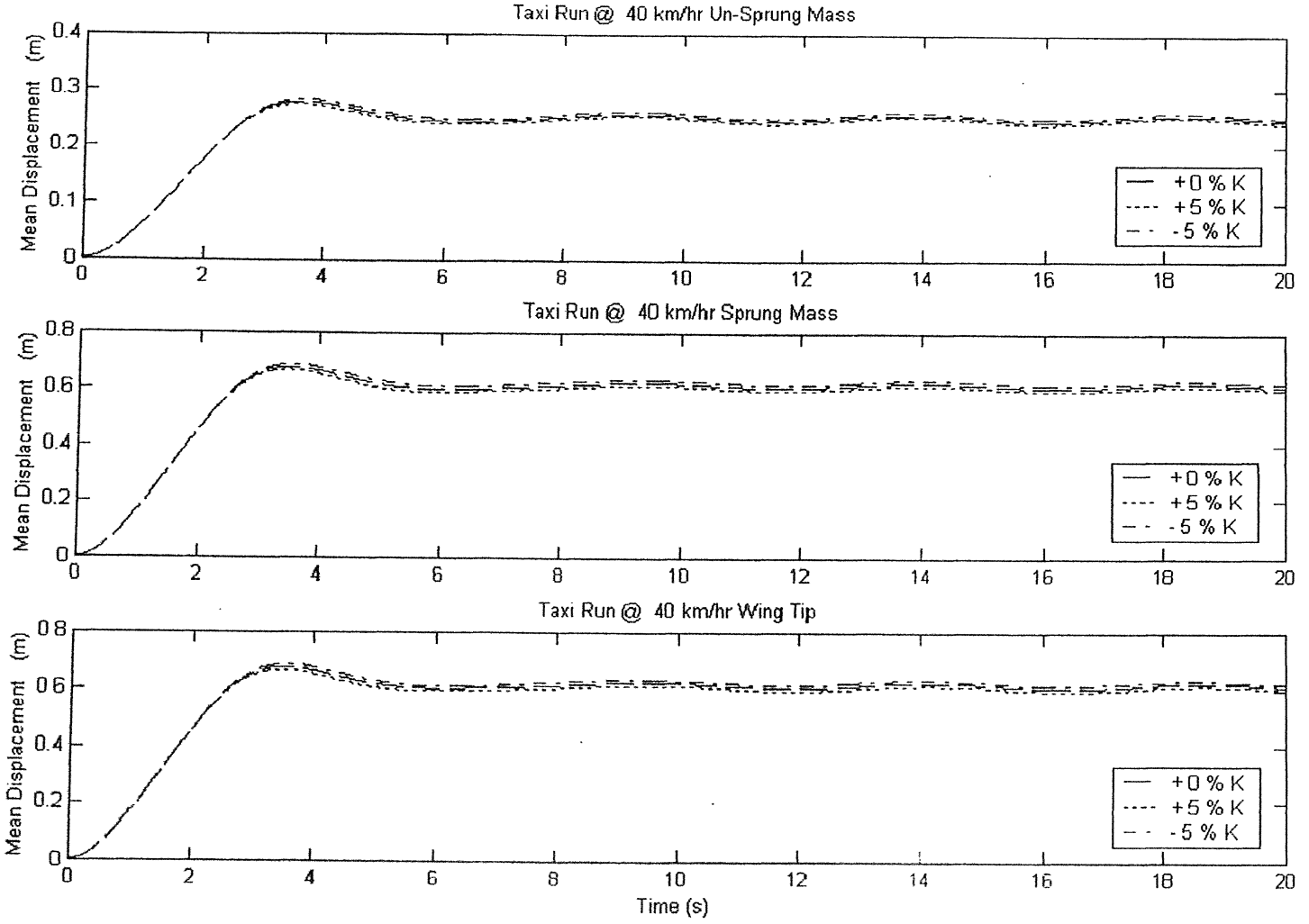

Fig 5.01 Mean displacement during taxi-run at 40 km/hr (variation in nonlinear stiffness coefficients)

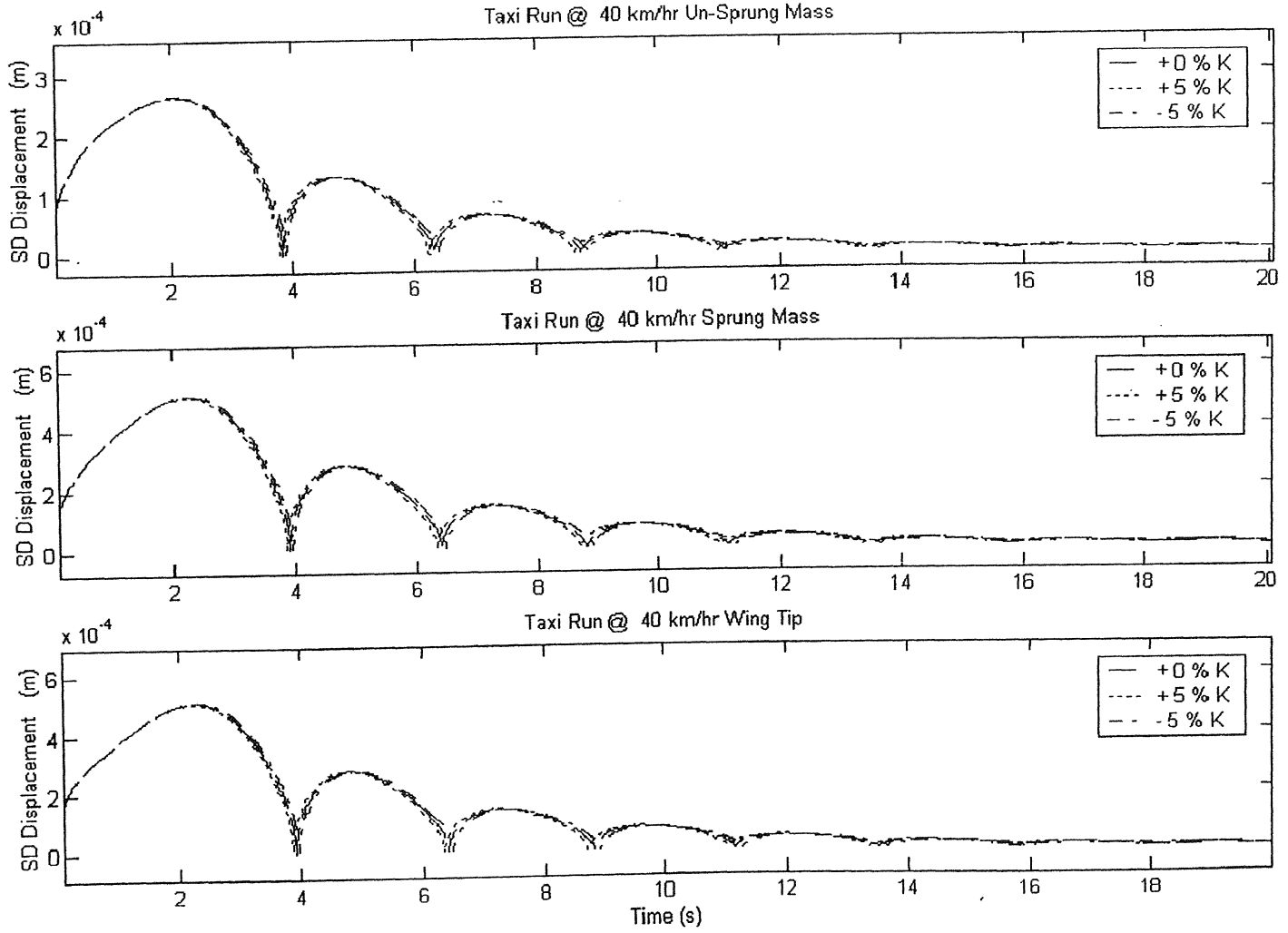

Fig 5.02 SD displacement during taxi-run at 40 km/hr (variation in nonlinear stiffness coefficients)

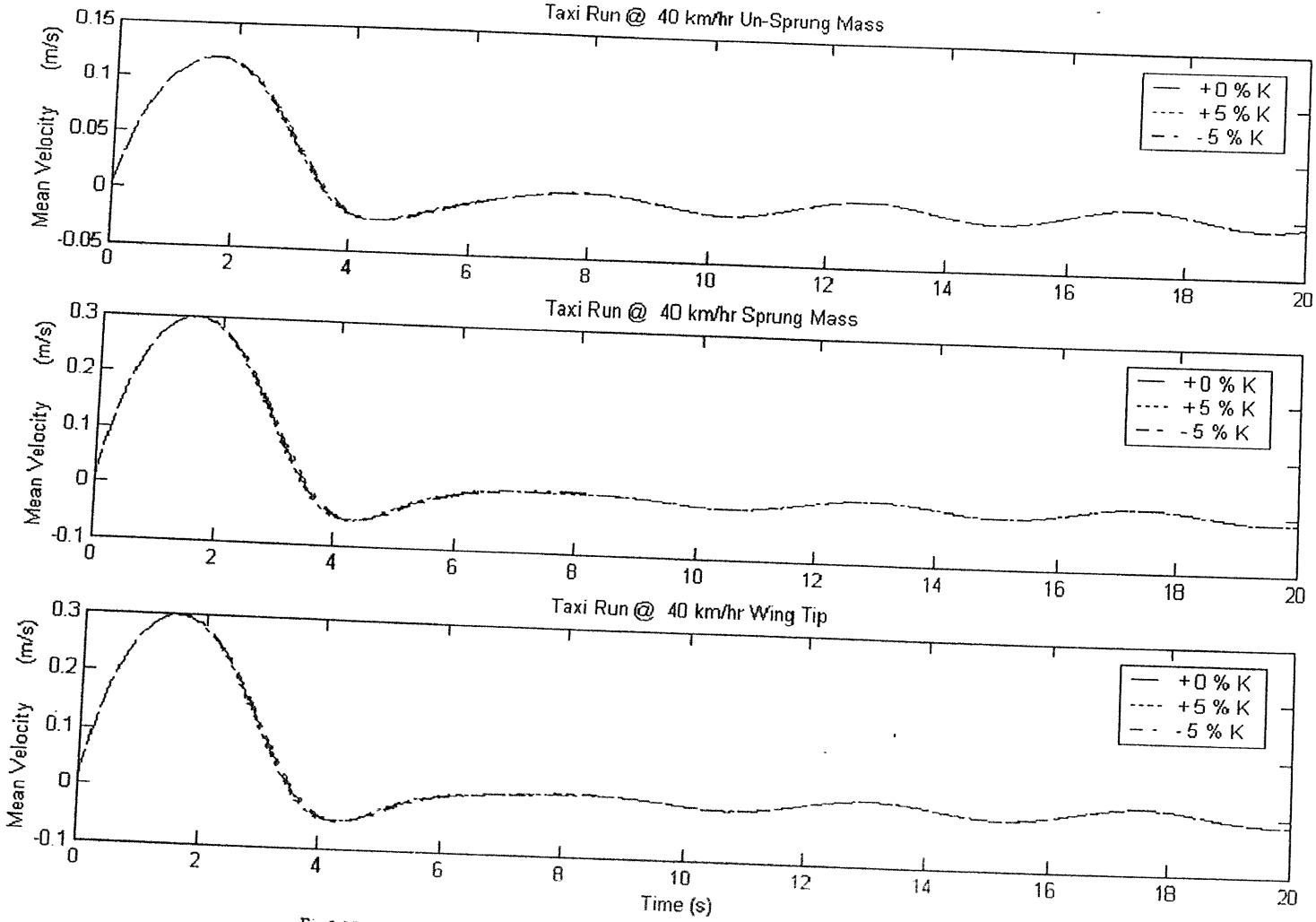

Fig 5.03 Mean Velocity during taxi-run at 40 km/hr (variation in nonlinear stiffness coefficients)

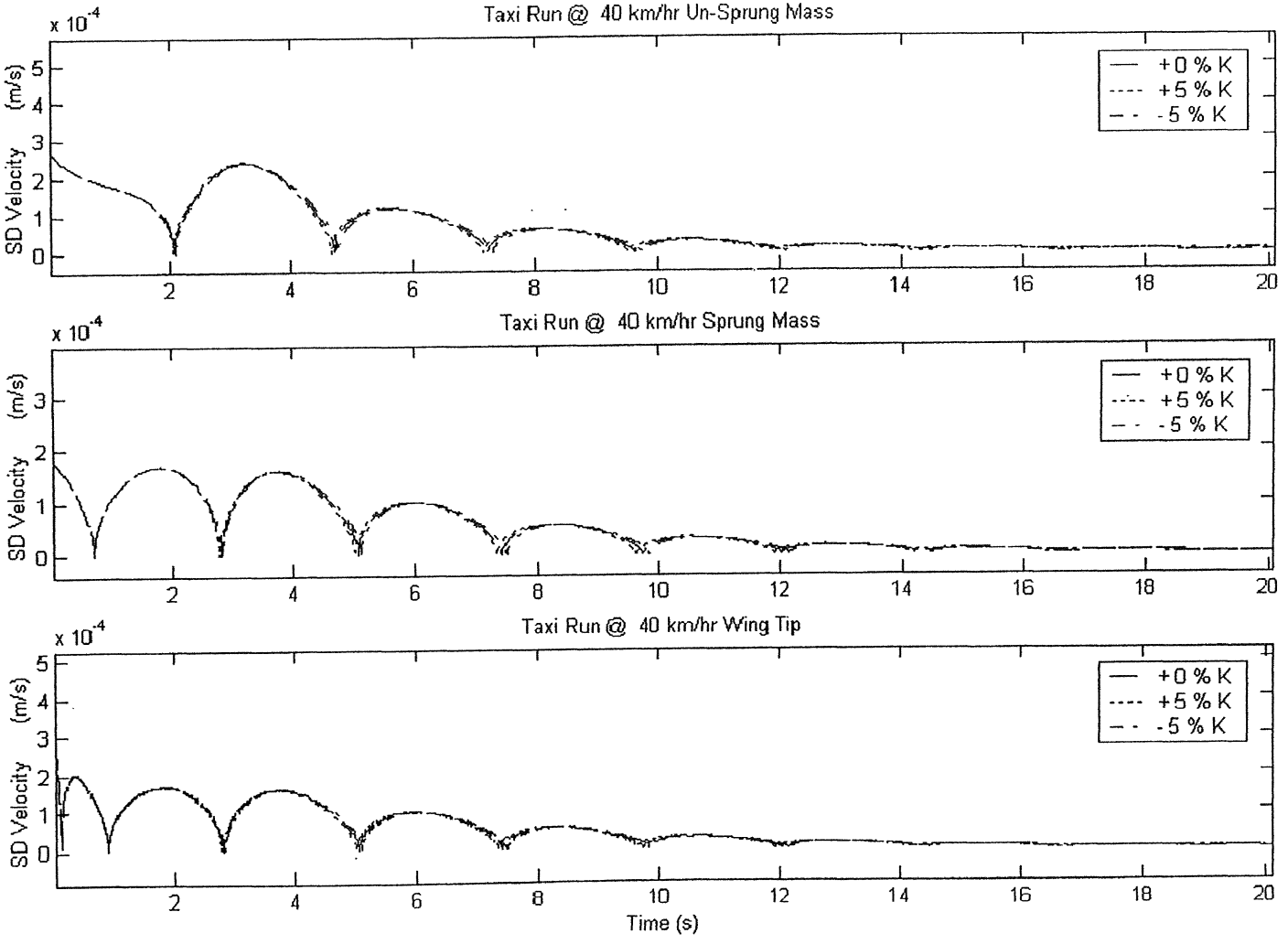

Fig 5.04 SD Velocity during taxi-run at 40 km/hr (variation in nonlinear stiffness coefficients)

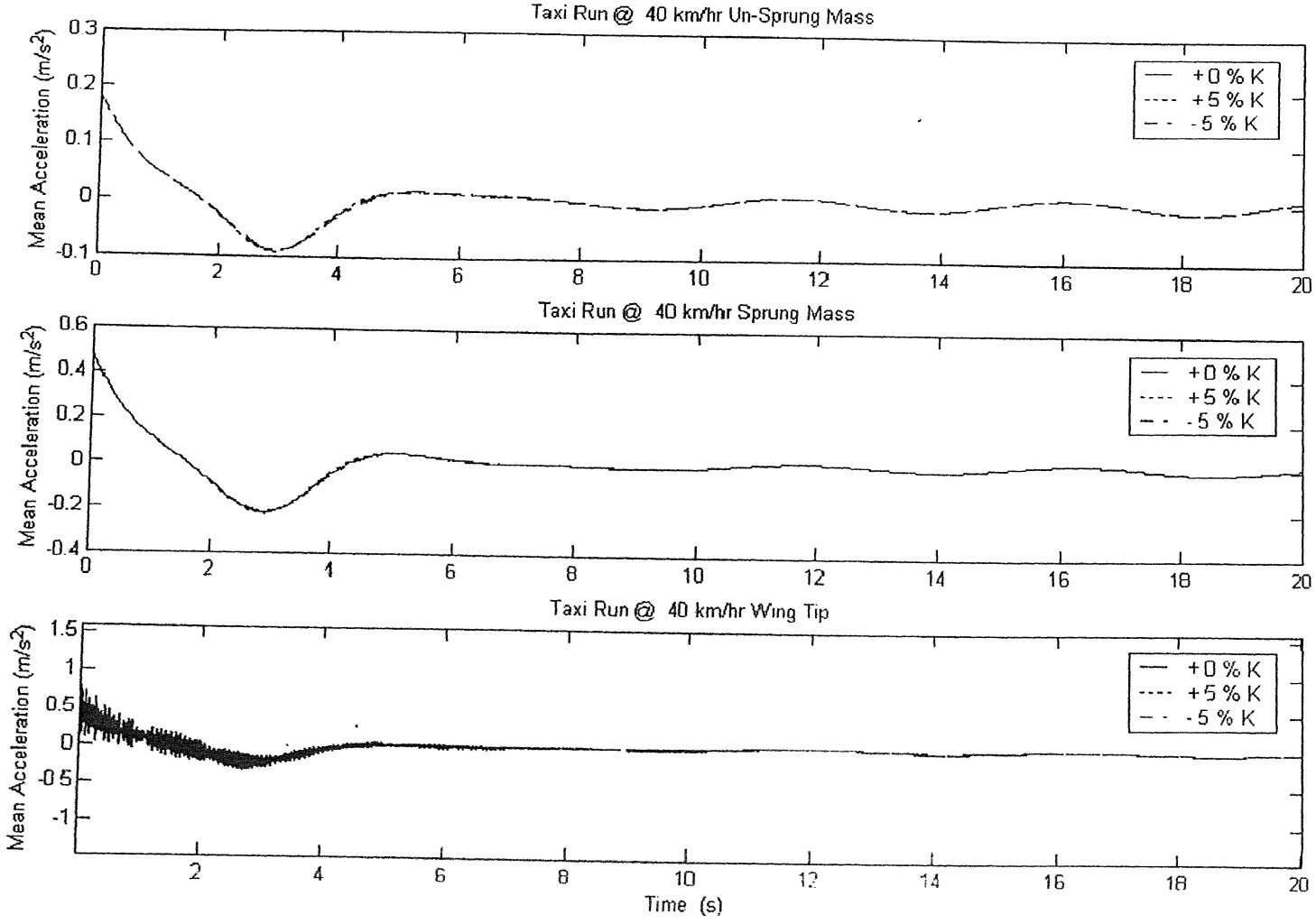

Fig 5.05 Mean acceleration during taxi-run at 40 km/hr (variation in nonlinear stiffness coefficients)

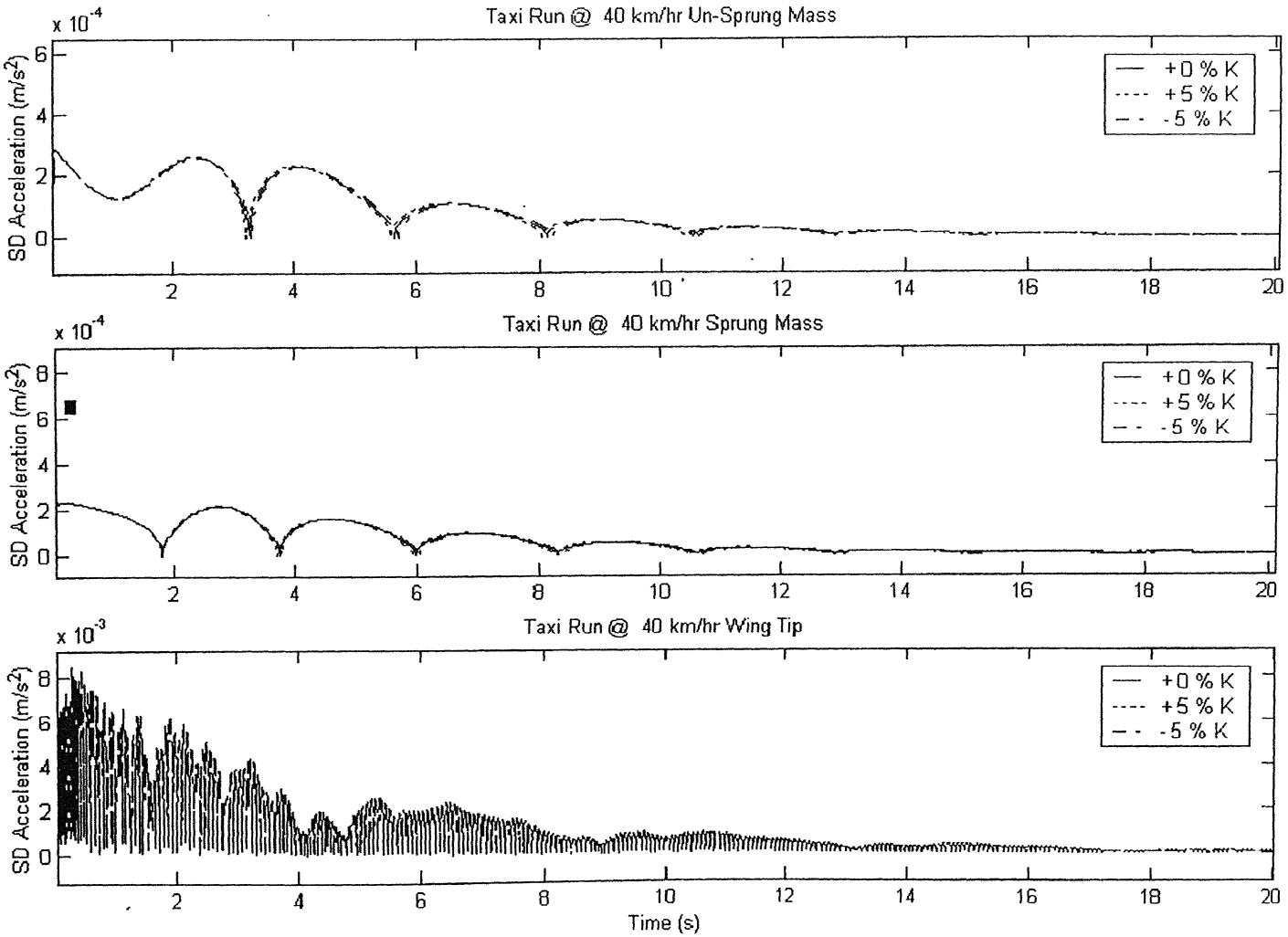

Fig 5.06 SD acceleration during taxi-run at 40 km/hr (variation in nonlinear stiffness coefficients)

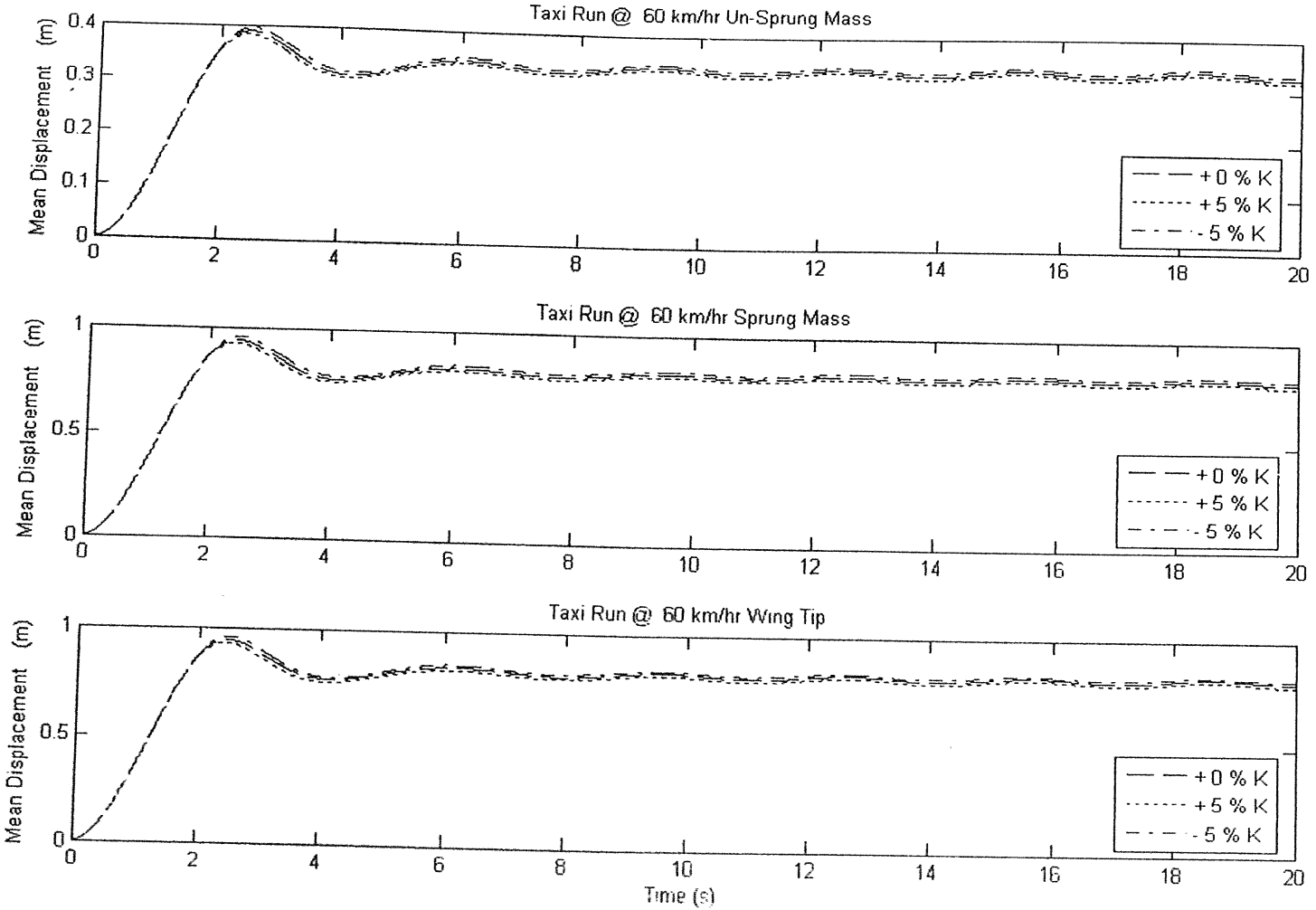

Fig 5.07 Mean displacement during taxi-run at 60 km/hr (variation in nonlinear stiffness coefficients)

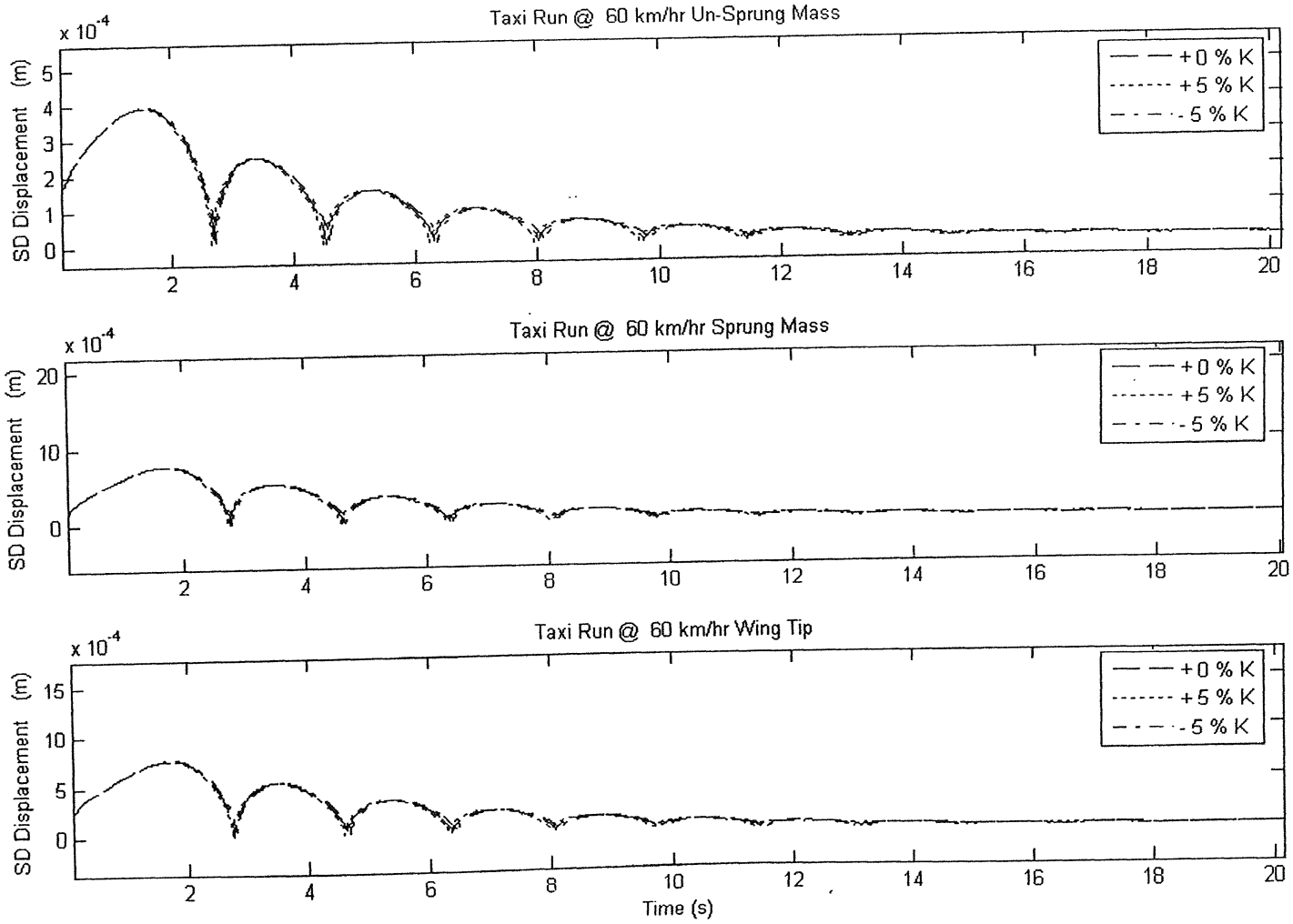

Fig 5.08 SD displacement during taxi-run at 60 km/hr (variation in nonlinear stiffness coefficients)

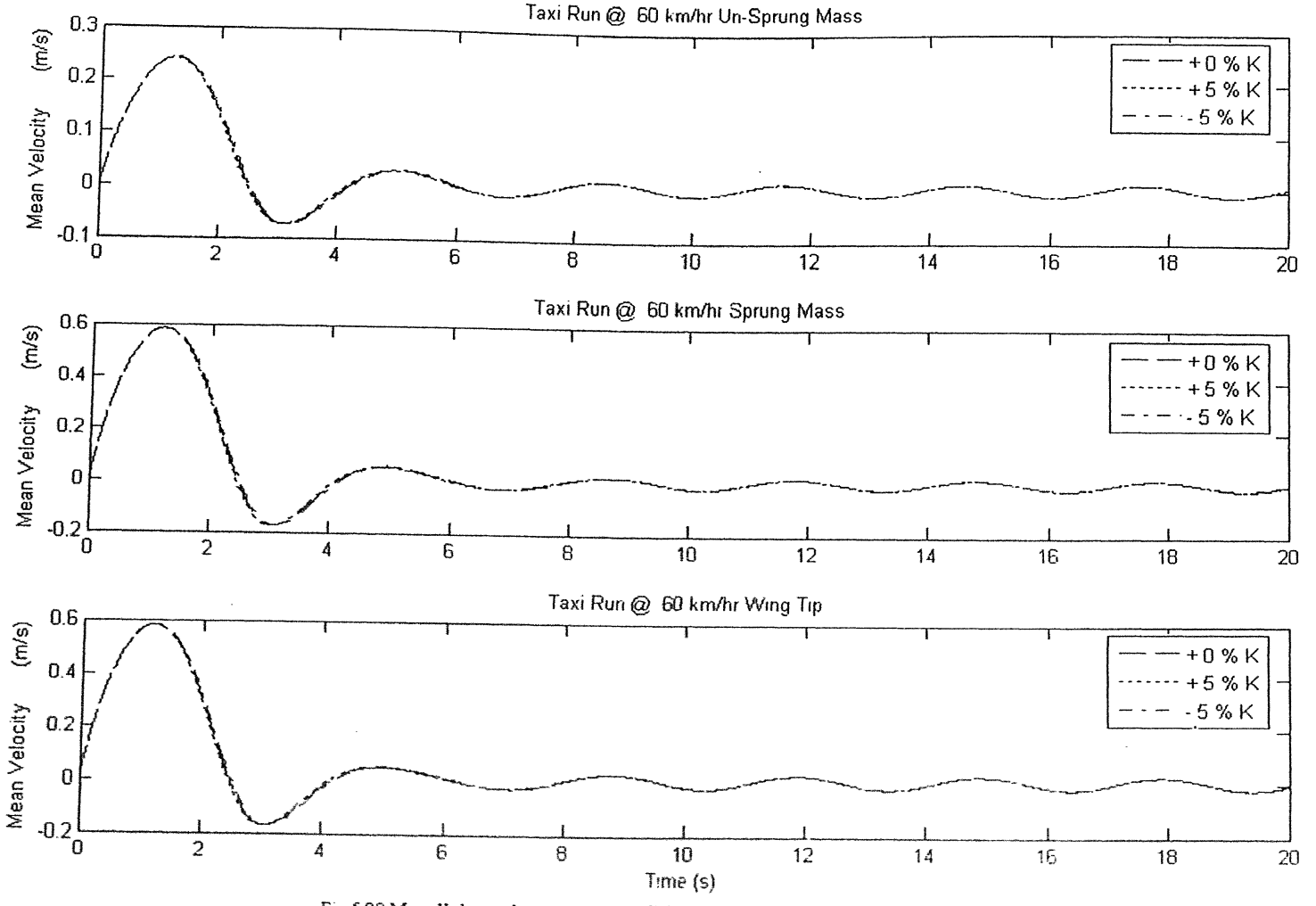

Fig 5.09 Mean Velocity during taxi-run at 60 km/hr (variation in nonlinear stiffness coefficients)

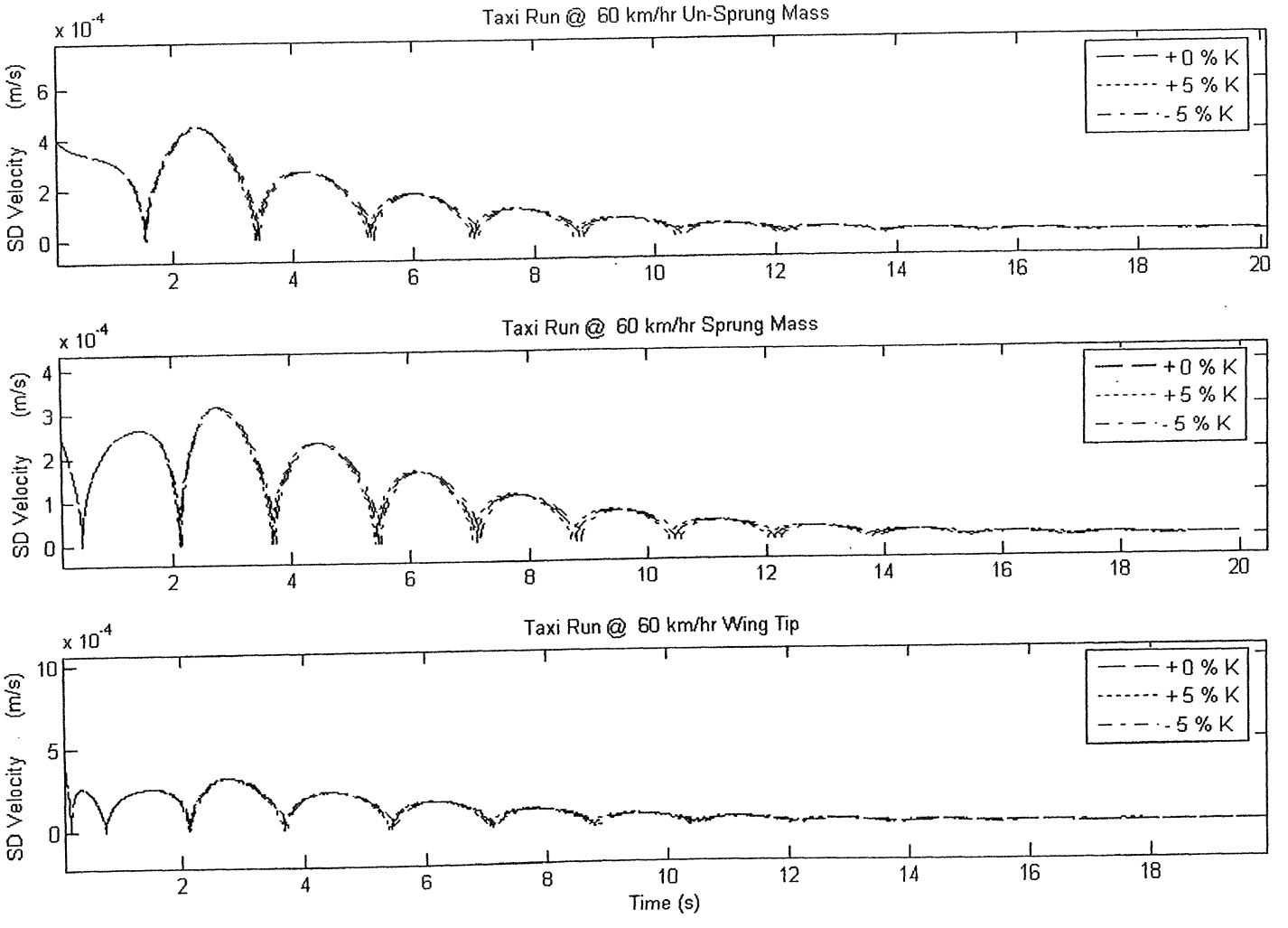

Fig 5.10 SD Velocity during taxi-run at 60 km/hr (variation in nonlinear stiffness coefficients)

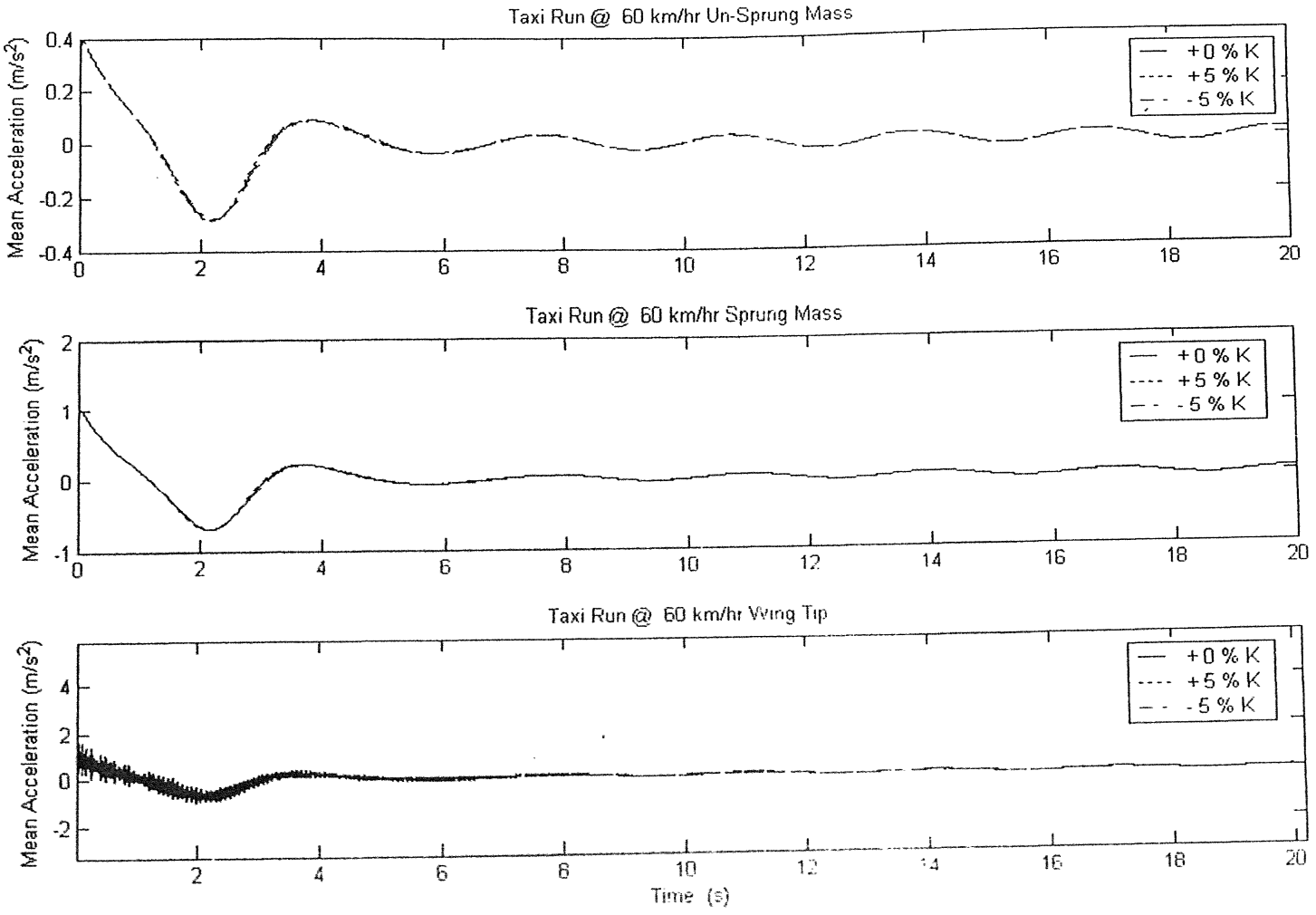

Fig 5.11 Mean acceleration during taxi-run at 60 km/hr (variation in nondimensional stiffness coefficients)

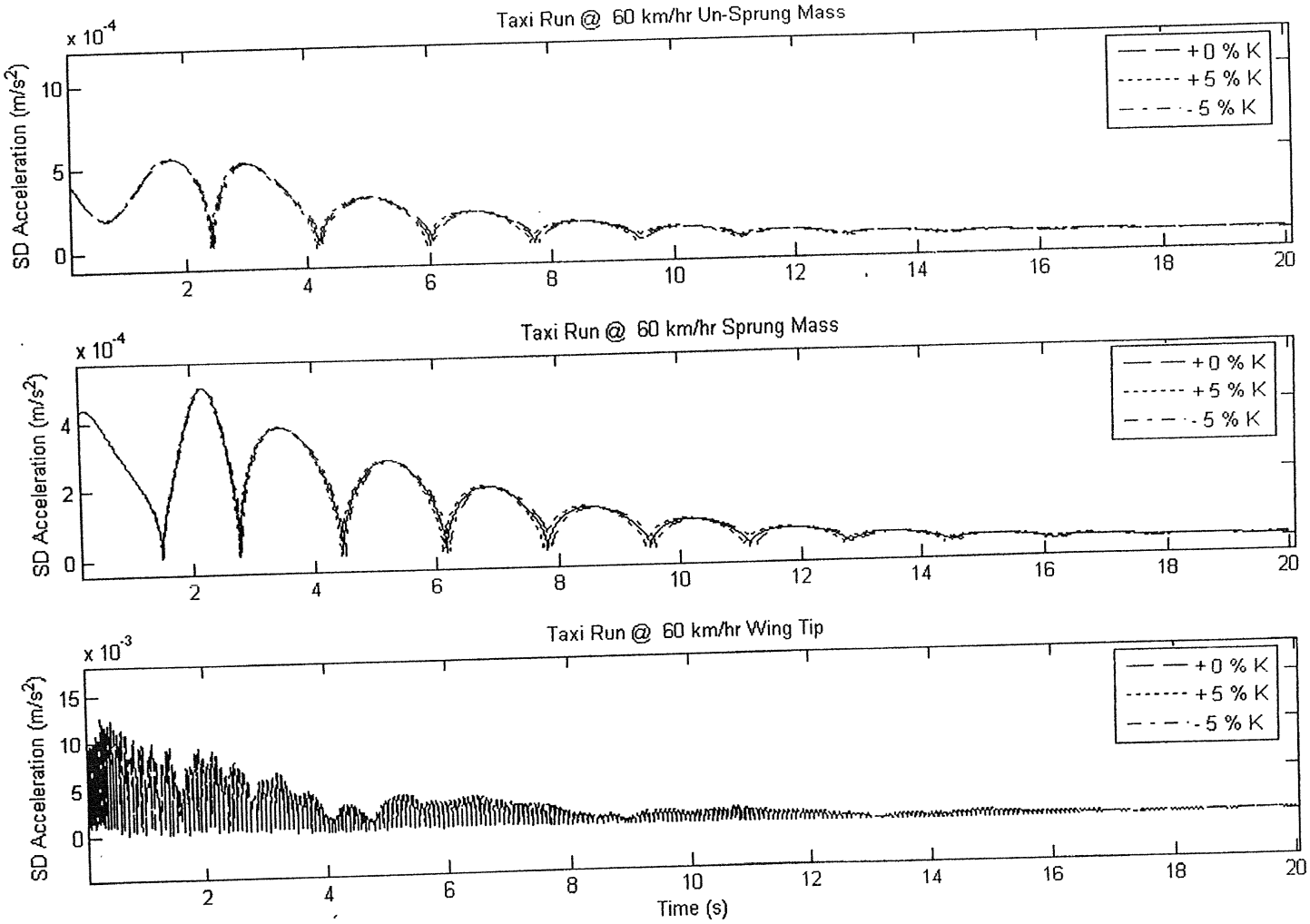

Fig 5.12 SD acceleration during taxi-run at 60 km/hr (variation in nonlinear stiffness coefficients)

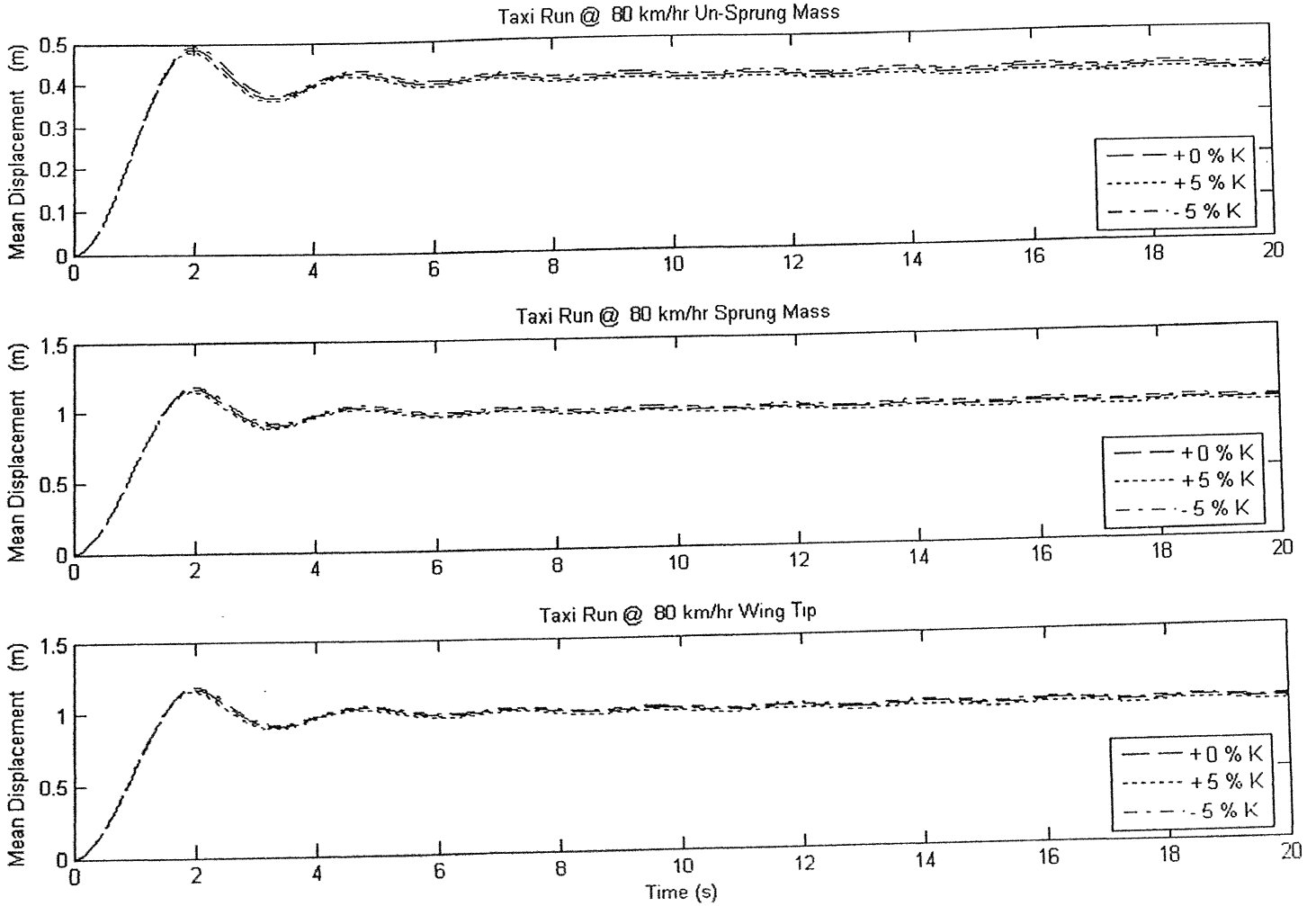

Fig 5.13 Mean displacement during taxi-run at 80 km/hr (variation in nonlinear stiffness coefficients)

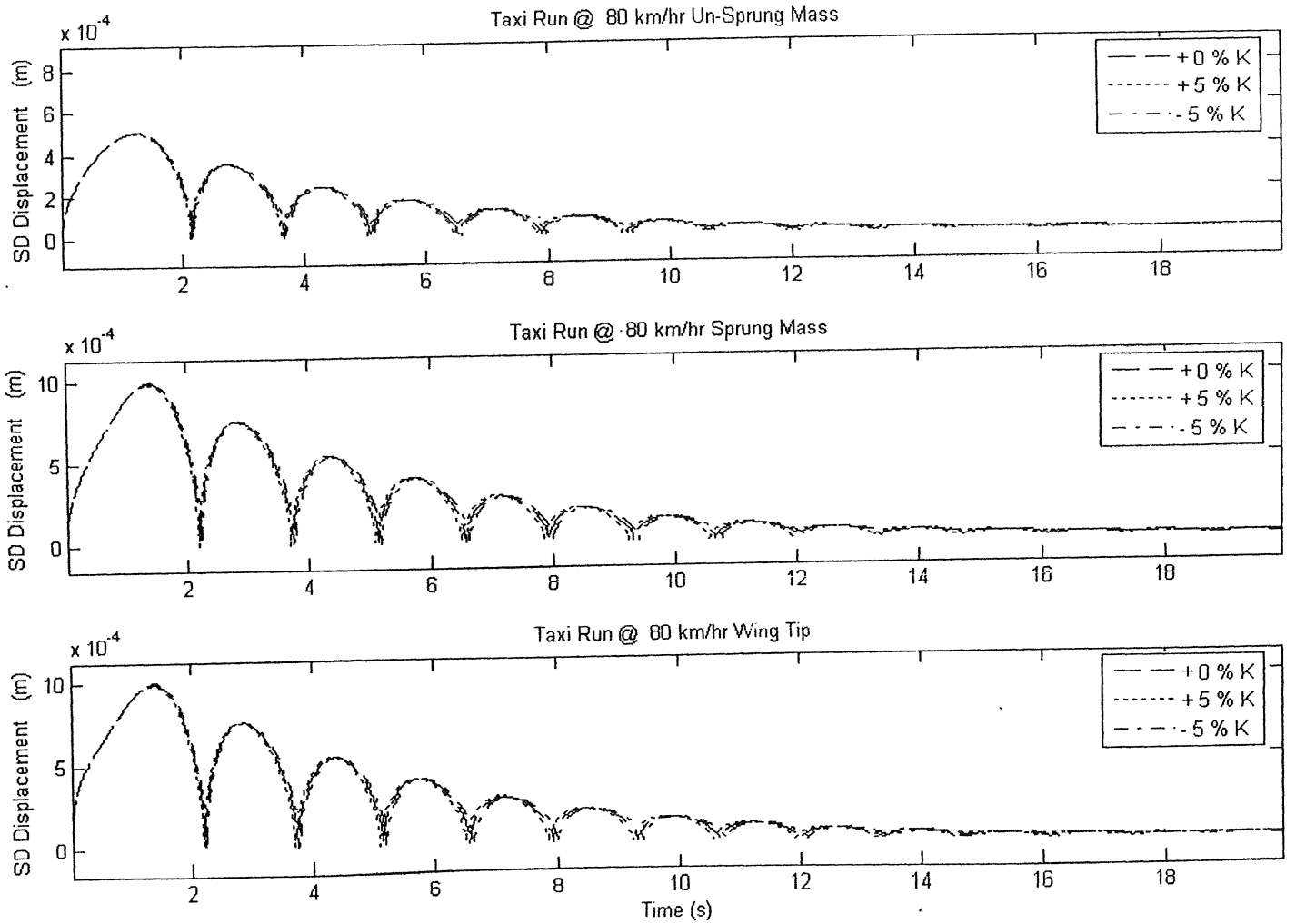

Fig 5.14 SD displacement during taxi-run at 80 km/hr (variation in nonlinear stiffness coefficients)

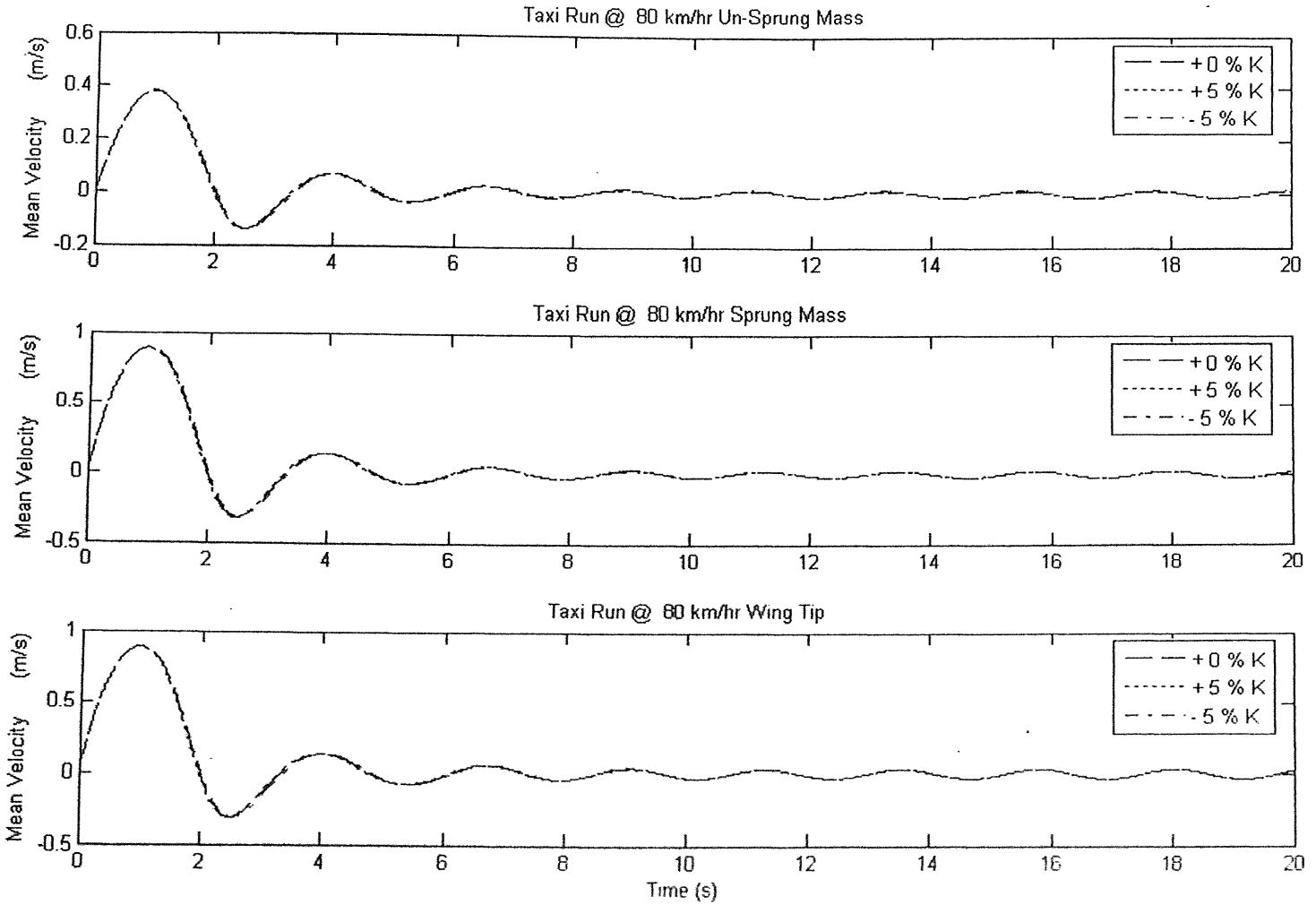

Fig 5.15 Mean Velocity during taxi-run at 80 km/hr (variation in nonlinear stiffness coefficients)

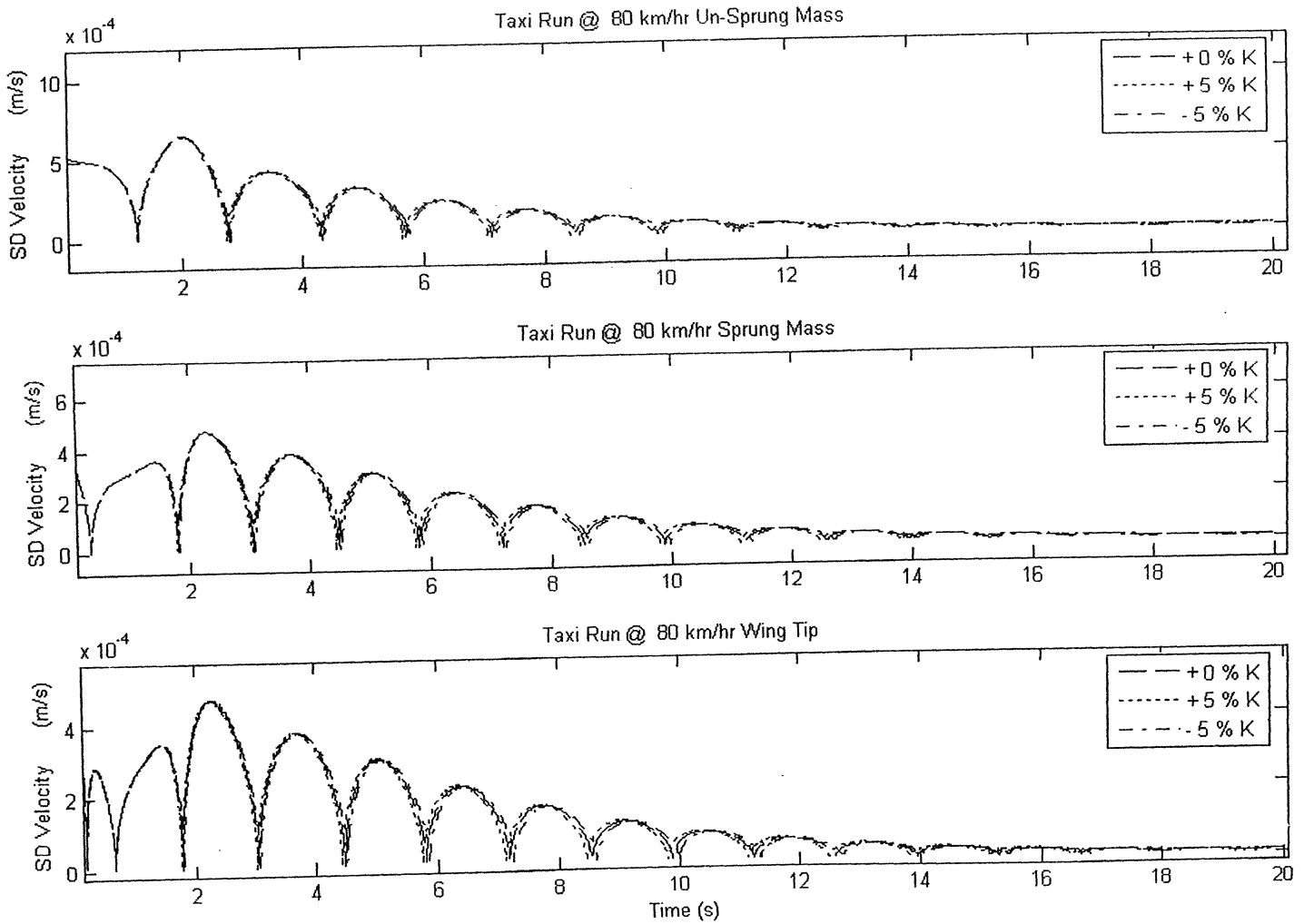

Fig 5.16 SD Velocity during taxi-run at 80 km/hr (variation in nonlinear stiffness coefficients)

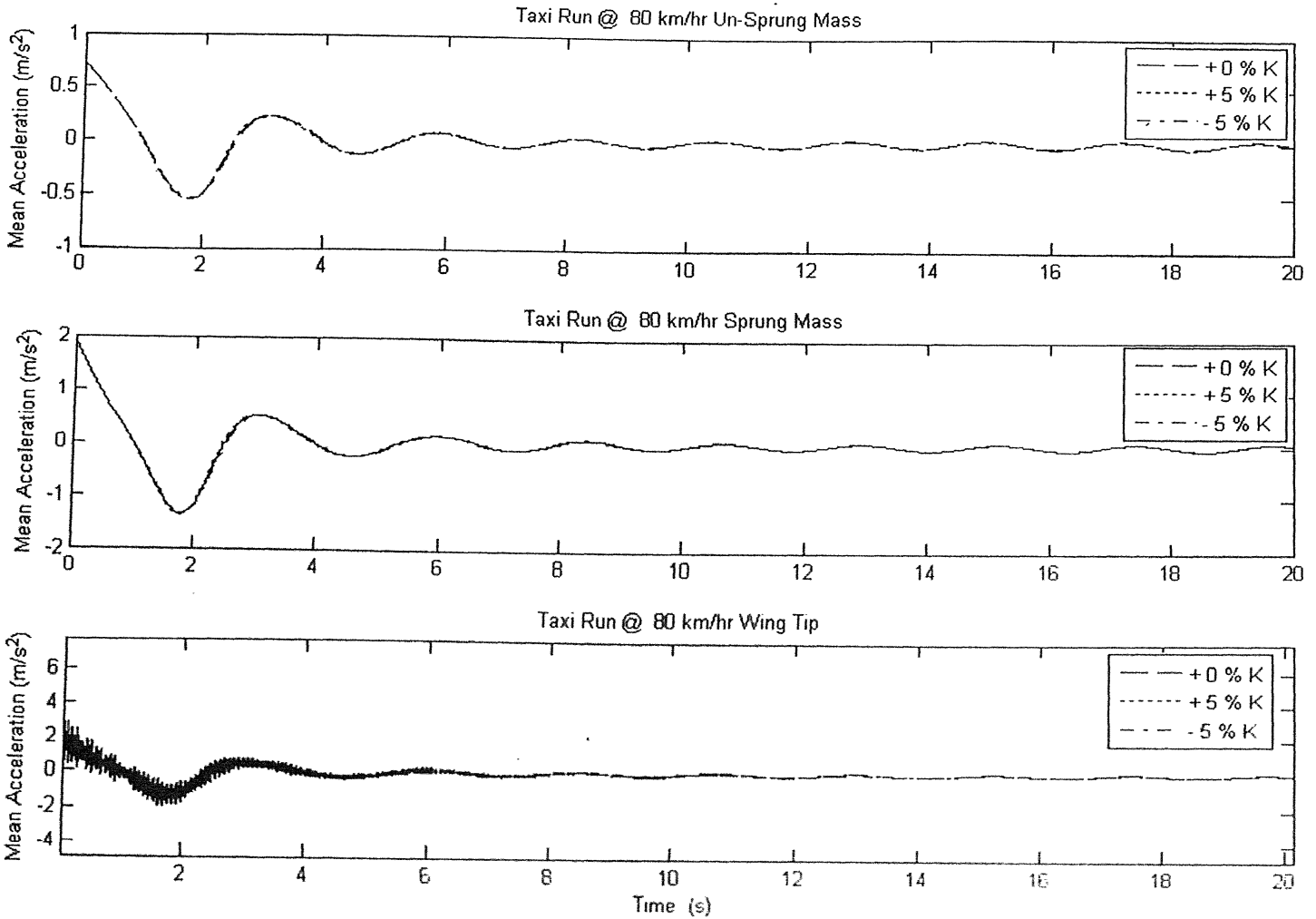

Fig 5.17 Mean acceleration during taxi-run at 80 km/hr (variation in nonlinear stiffness coefficients)

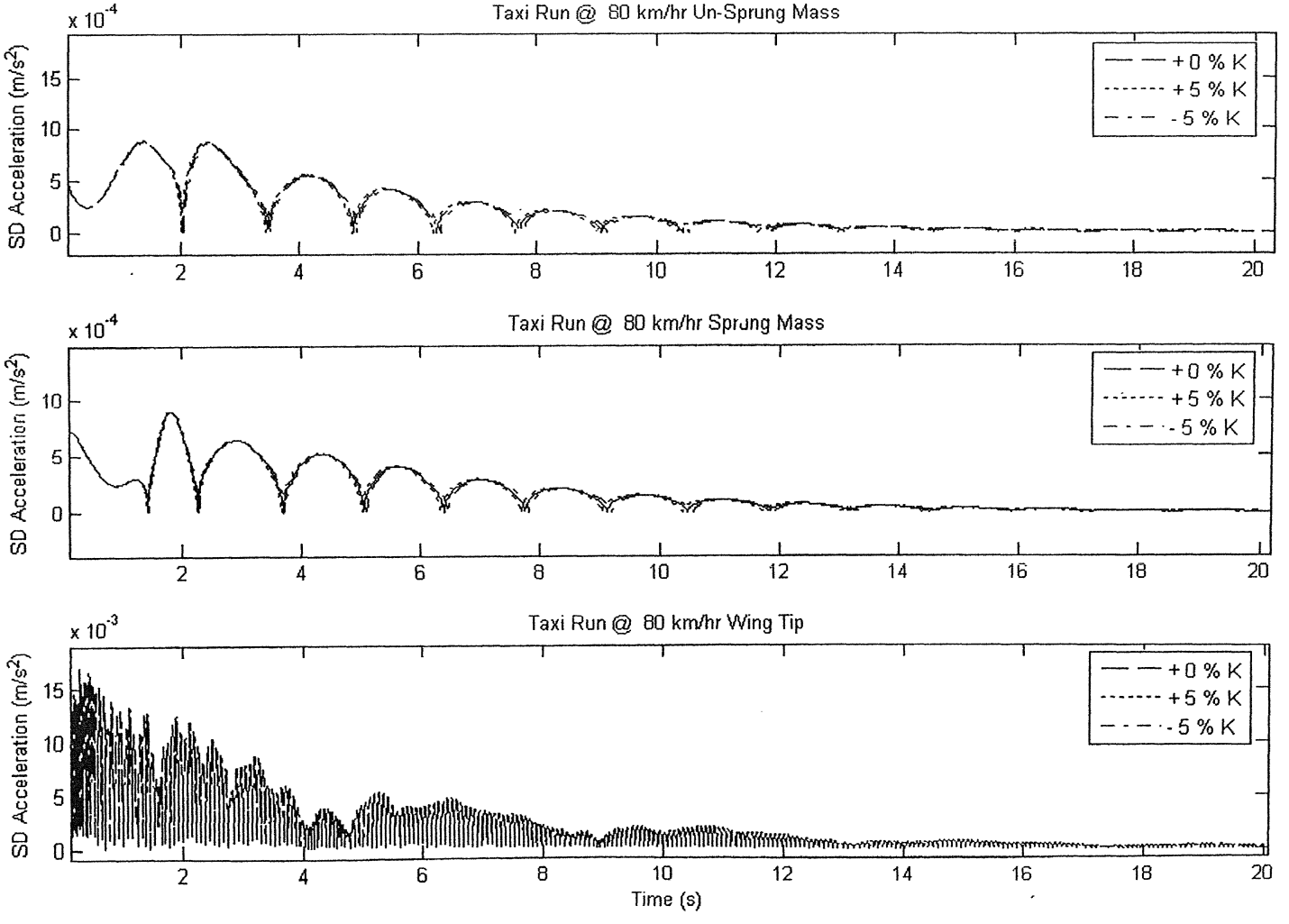

Fig 5.18 SD acceleration during taxi-run at 80 km/hr (variation in nonlinear stiffness coefficients)

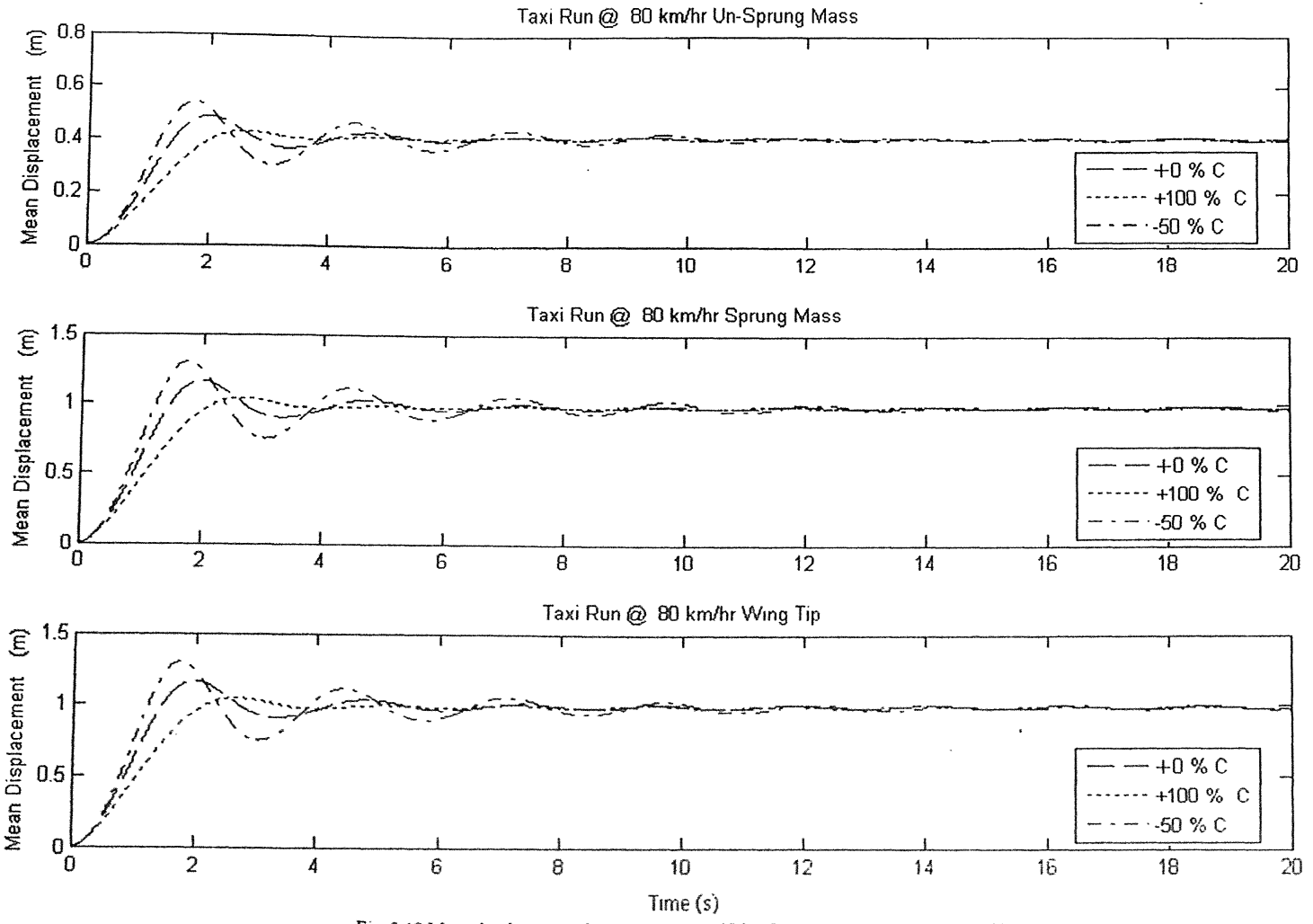

Fig 5 19 Mean displacement during taxi-run at 80 km/hr (variation in damping coefficients)

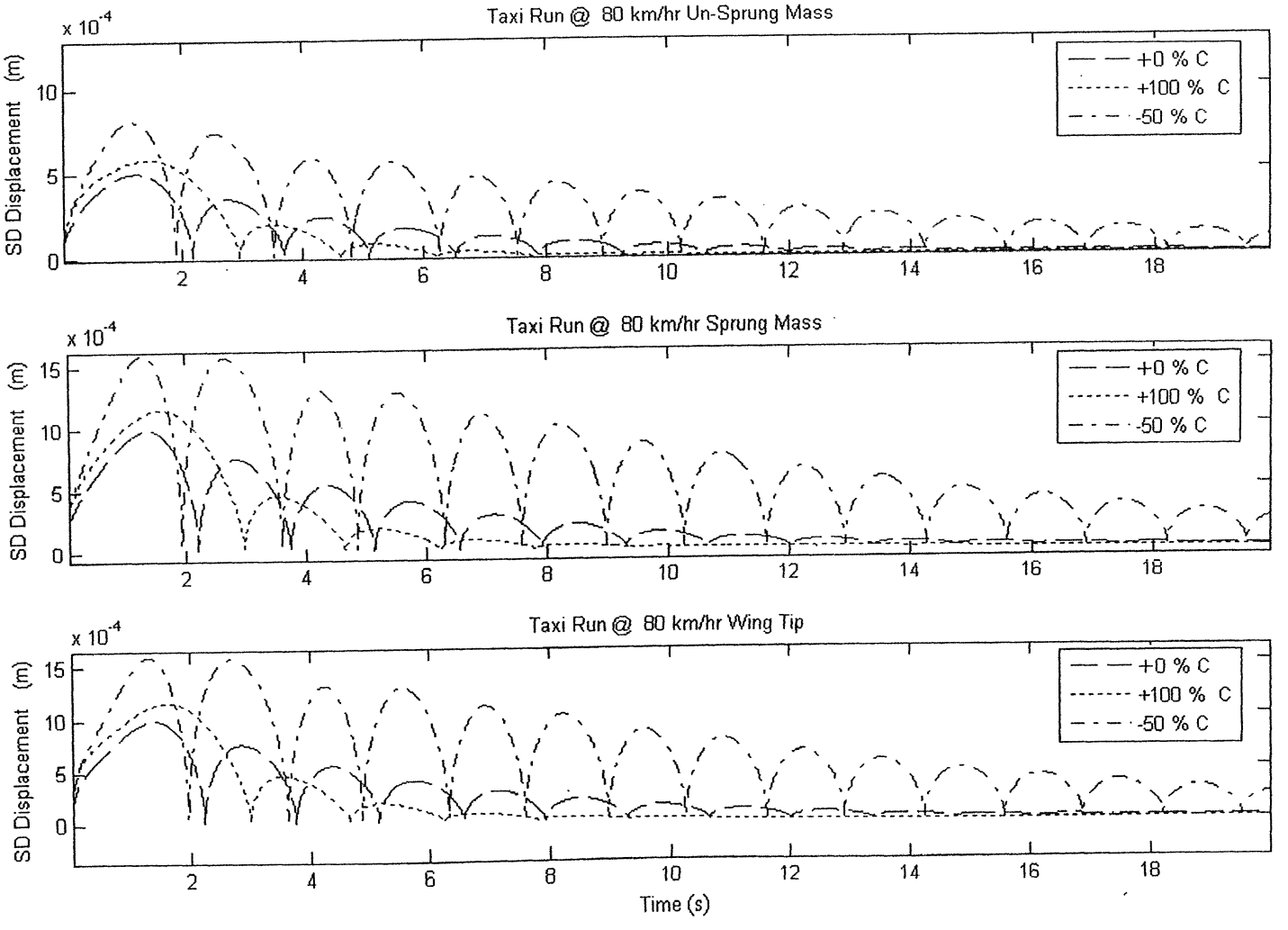

Fig 5.20 SD displacement during taxi-run at 80 km/hr (variation in damping coefficients)

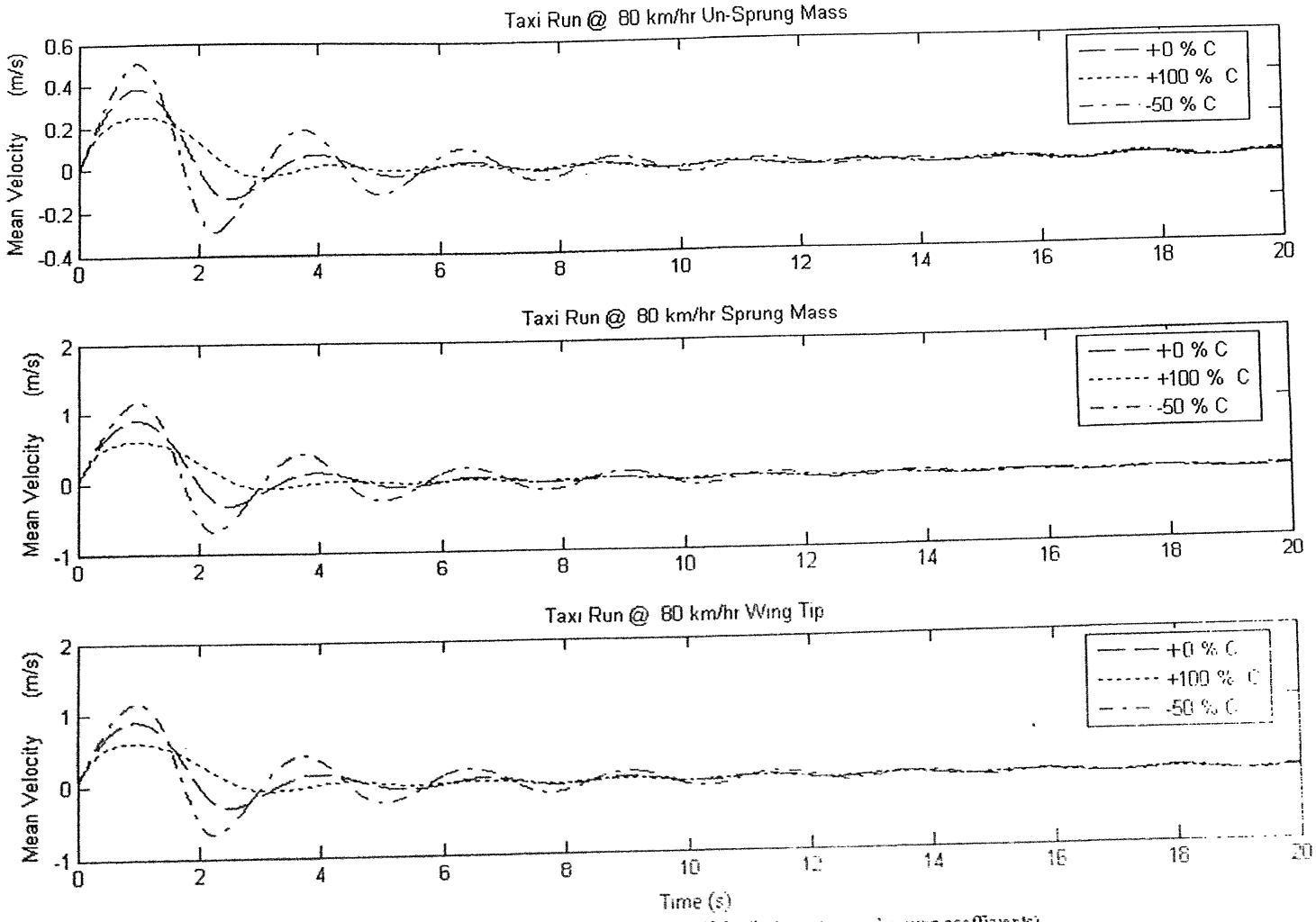

Fig 5.21 Mean Velocity during taxi-run at 80 km/hr (variation in damping coefficients)

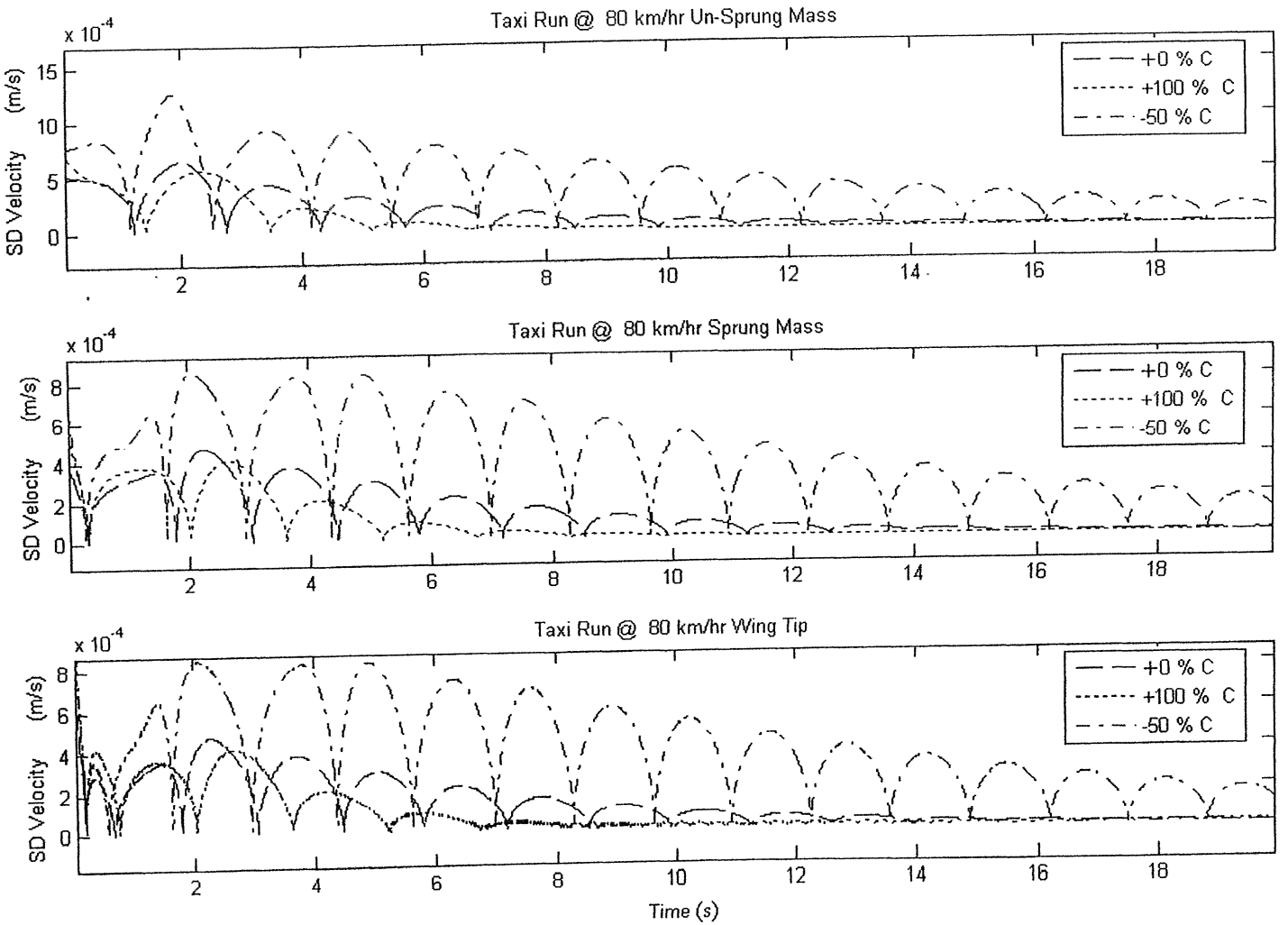

Fig 5.22 SD Velocity during taxi-run at 80 km/hr (variation in damping coefficients)

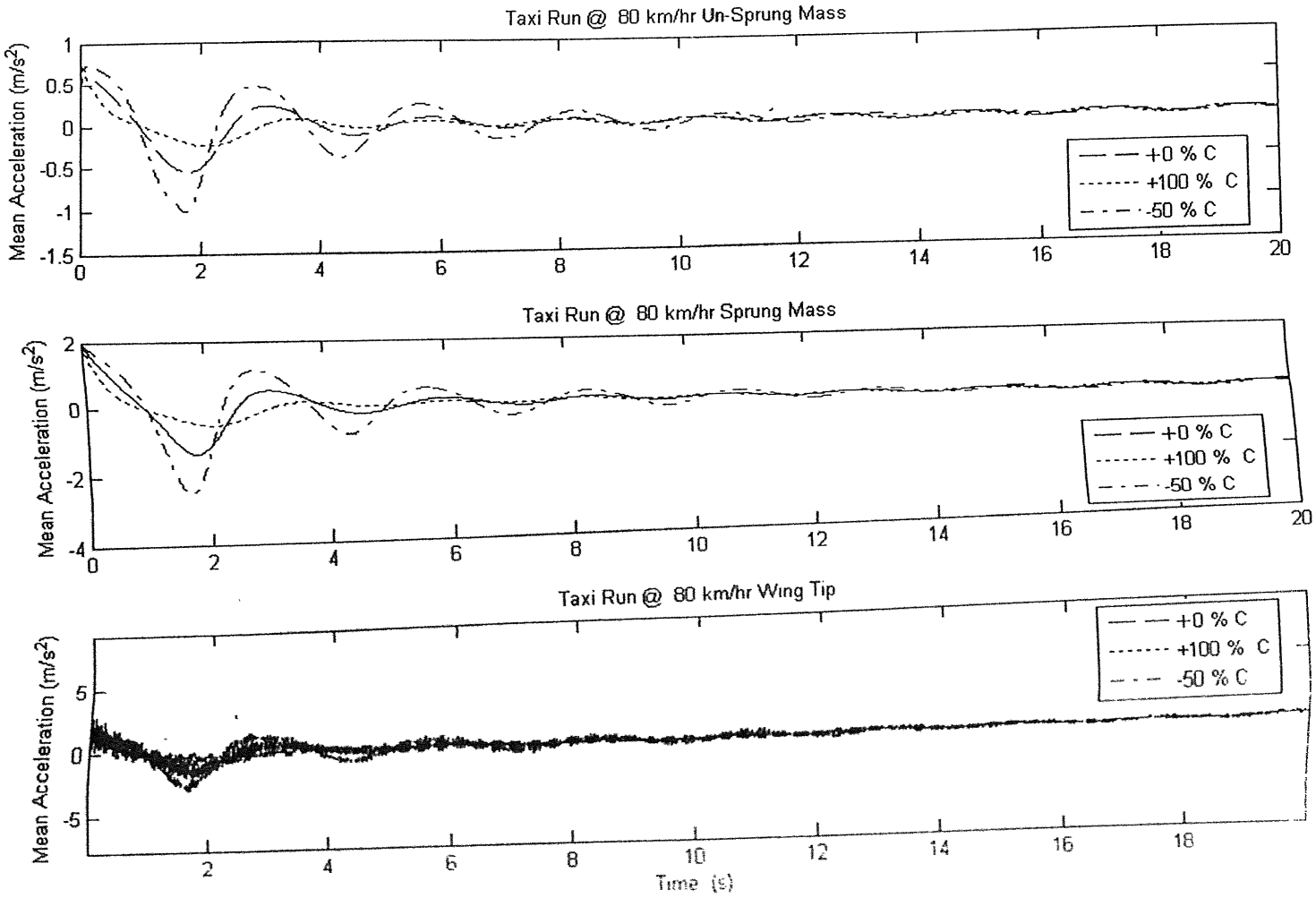

Fig 5.23 Mean acceleration during taxi-run at 80 km/hr (variation in damping coefficients)

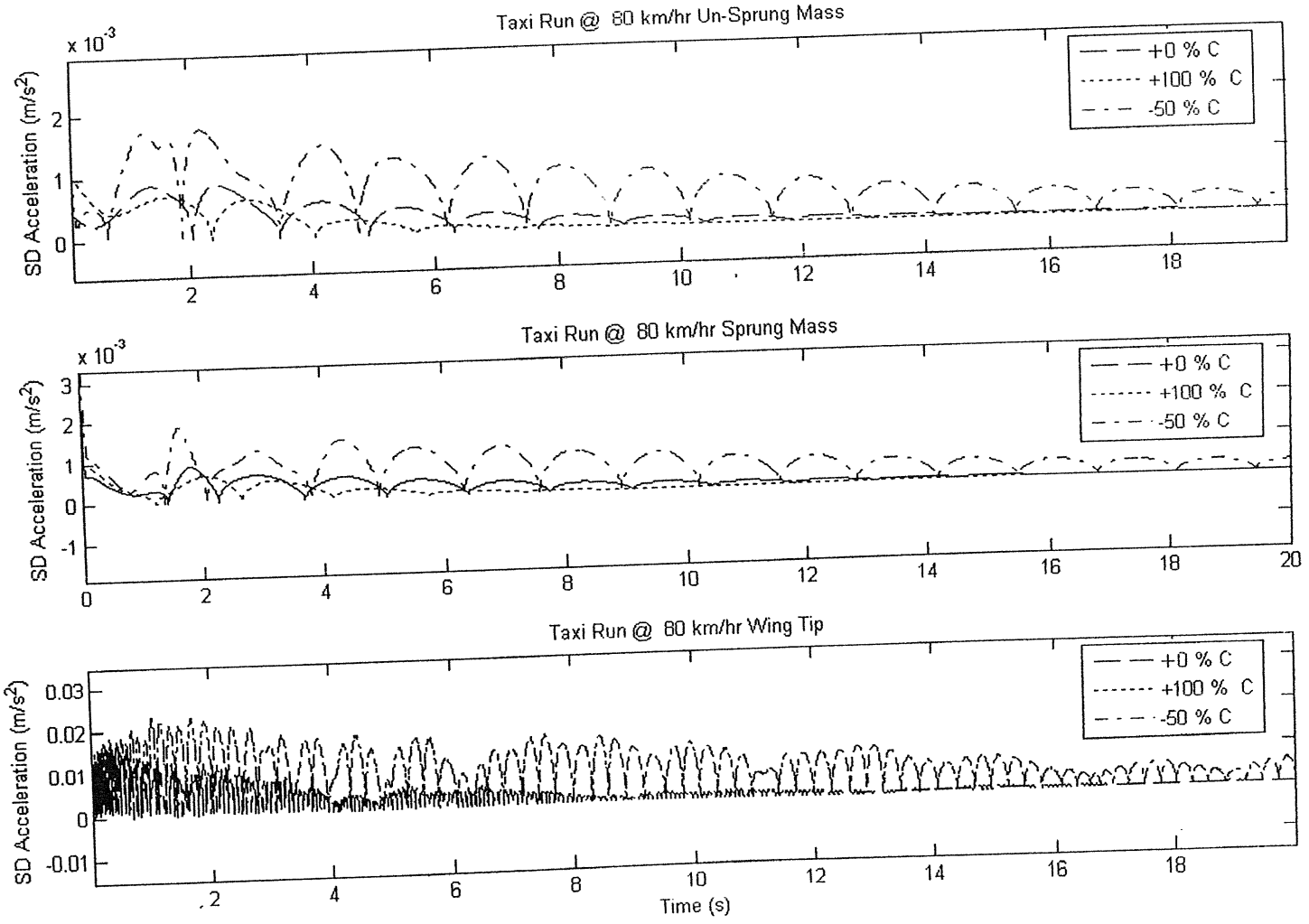

Fig 5.24 SD acceleration during taxi-run at 80 km/hr (variation in damping coefficients)

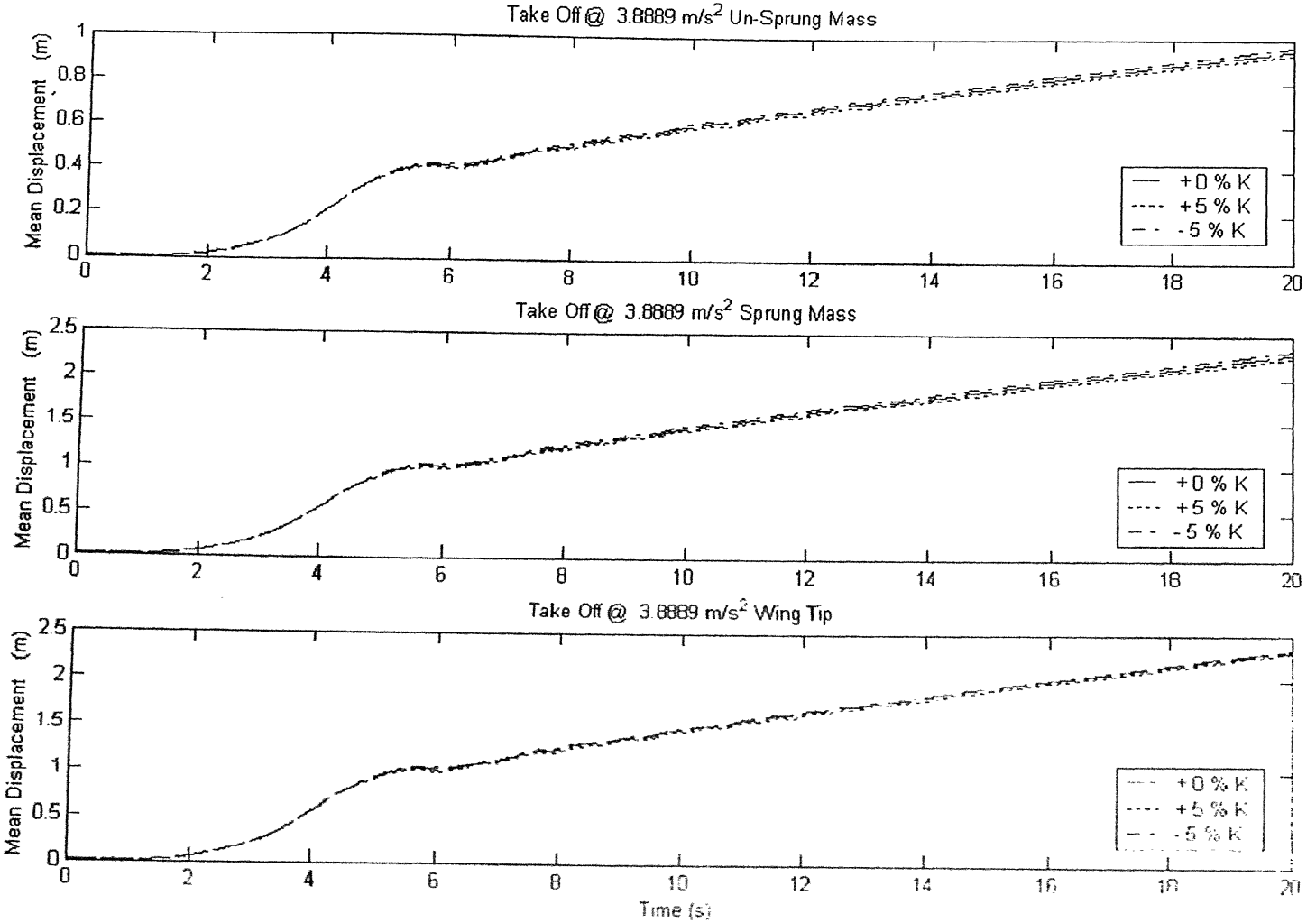

Fig 5 25 Mean displacement during take off at 3.8889 m/s² (variation in nonlinear stiffness coefficients)

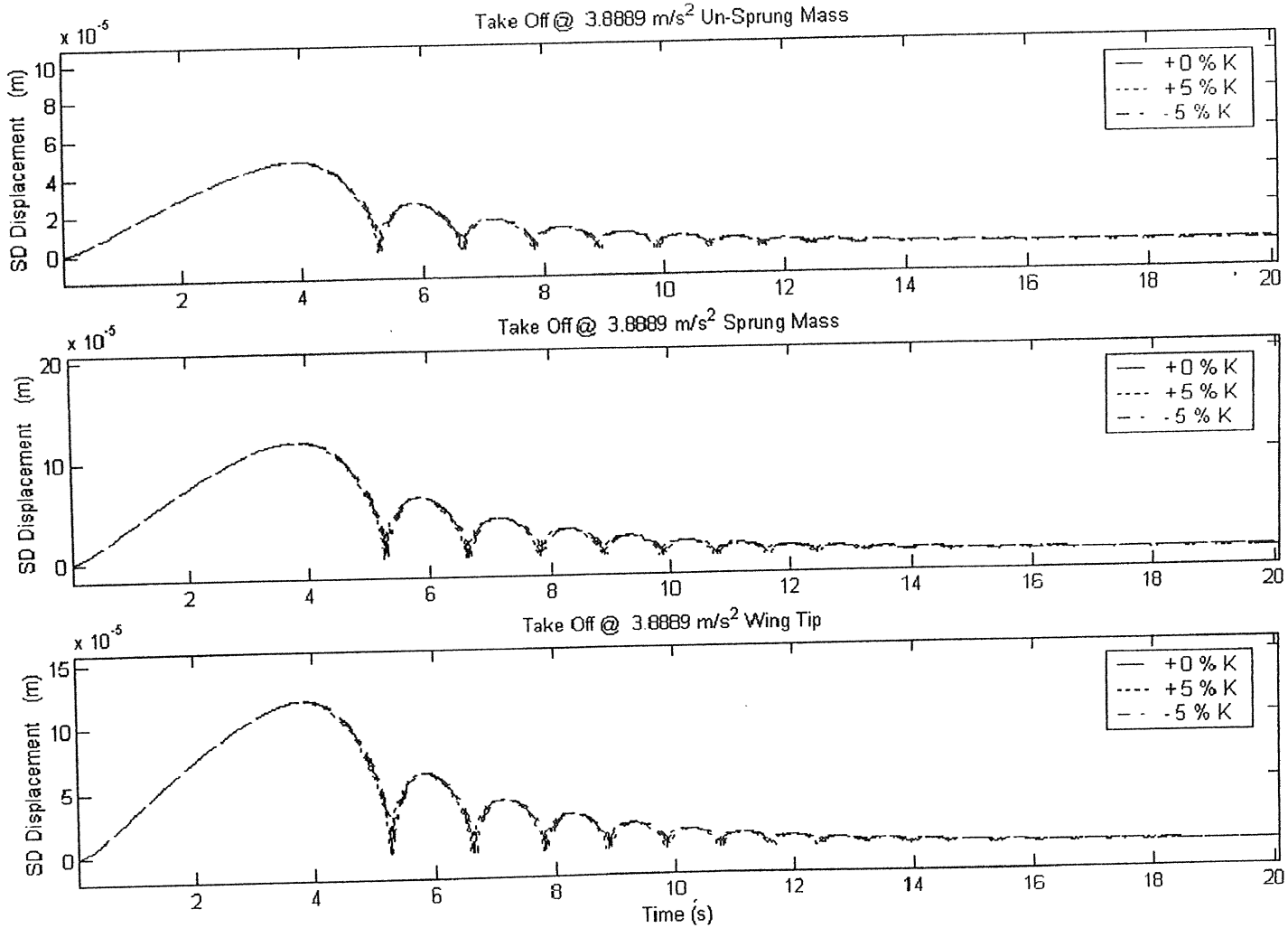

Fig 5.26 SD displacement during take off at 3.8889 m/s² (variation in nonlinear stiffness coefficients)

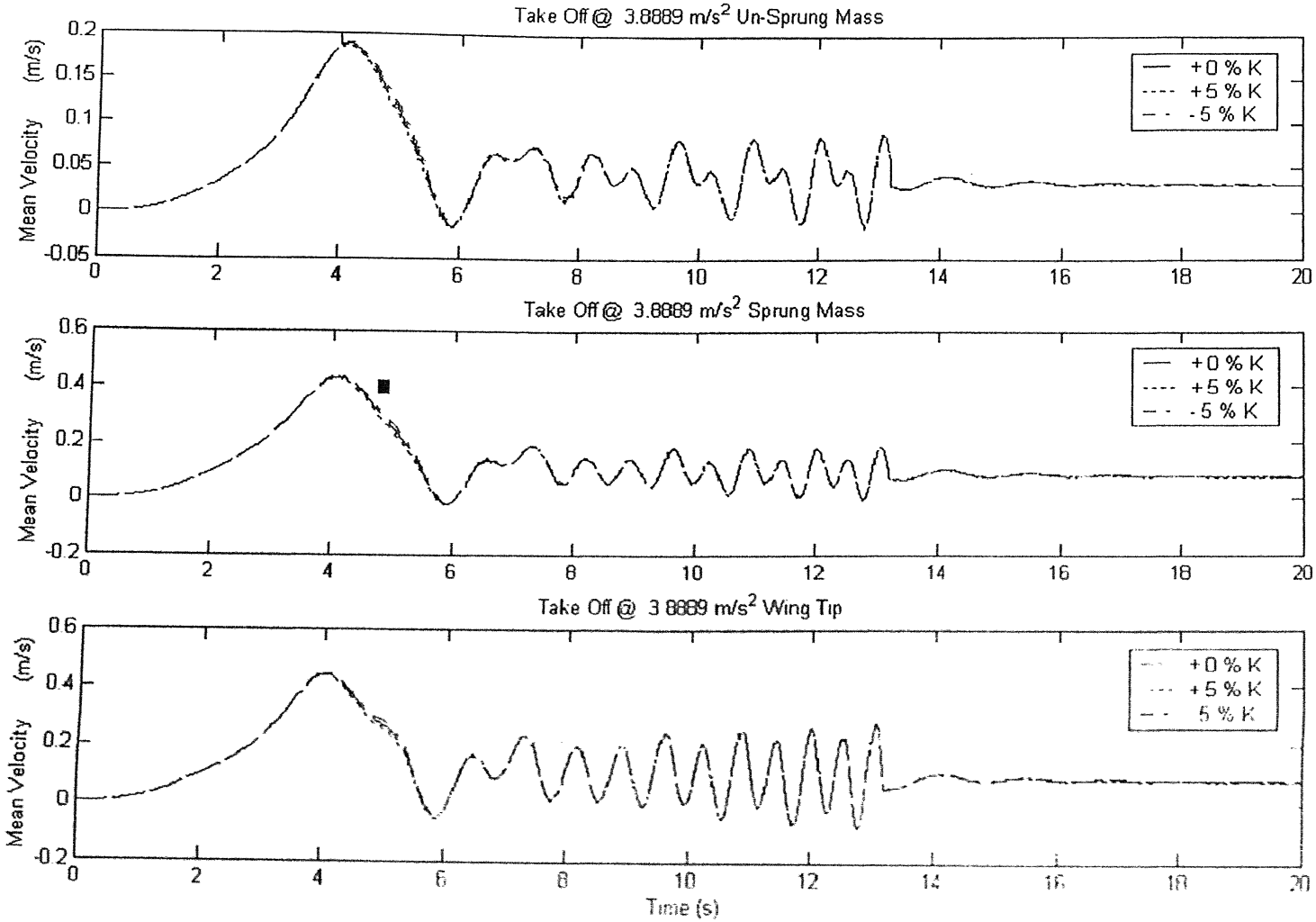

Fig 5.27 Mean Velocity during take off at 3.8889 m/s^2 (variation in nonlinear stiffness coefficients)

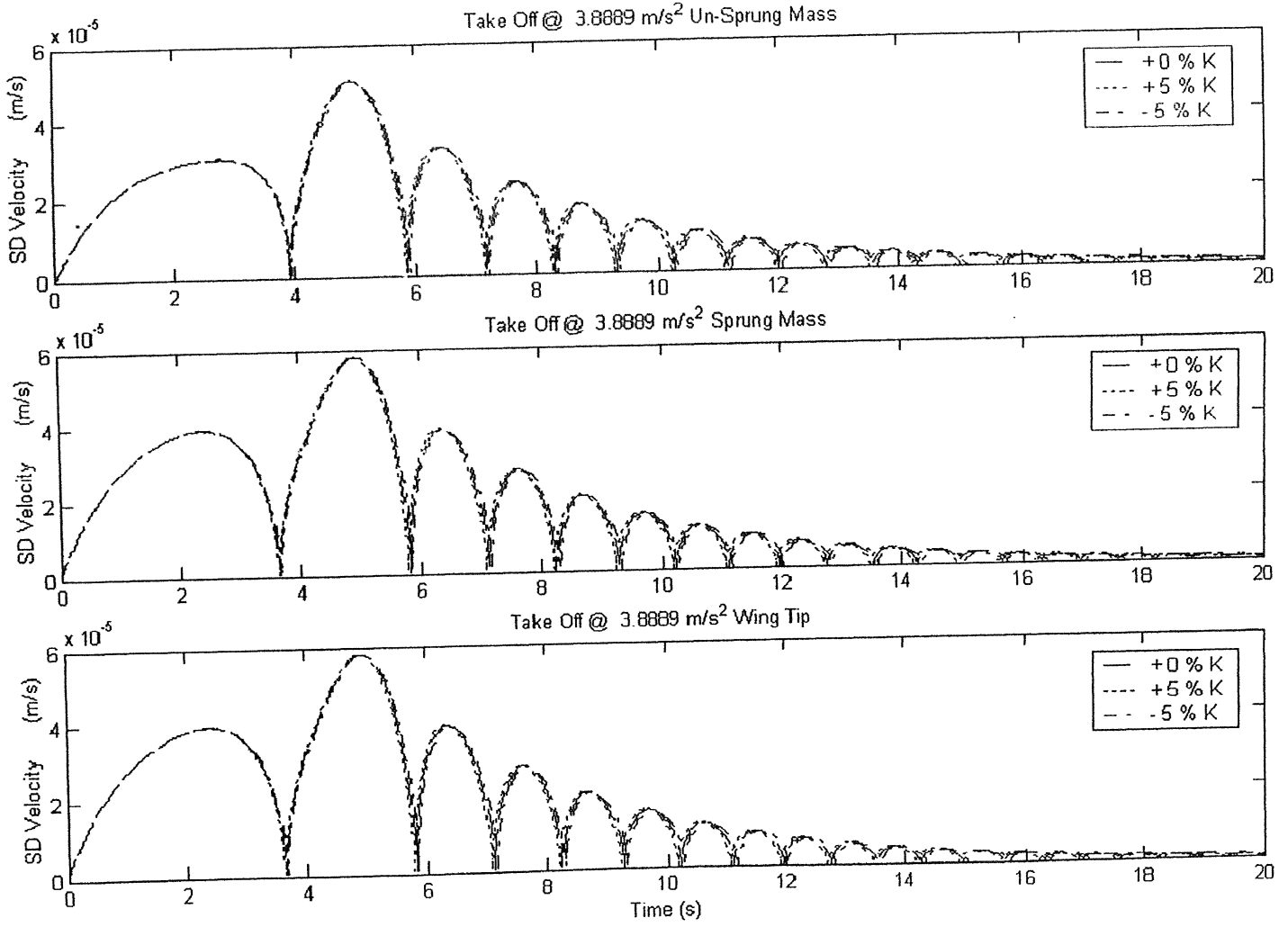

Fig 5.28 SD Velocity during take off at 3.8889 m/s^2 (variation in nonlinear stiffness coefficients)

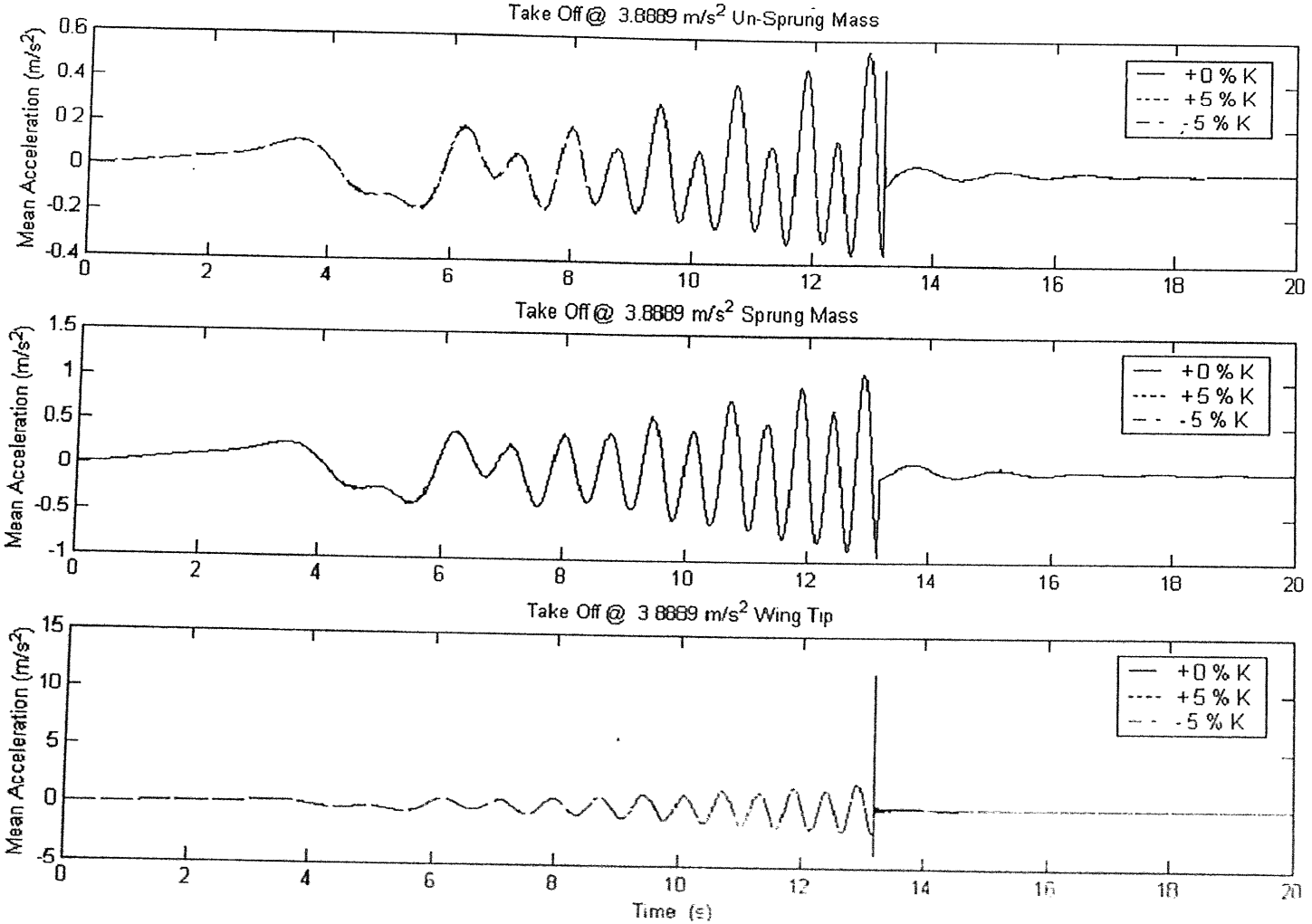

Fig 5.29 Mean acceleration during take off at 3.8889 m/s^2 (variation in nonlinear stiffness coefficients)

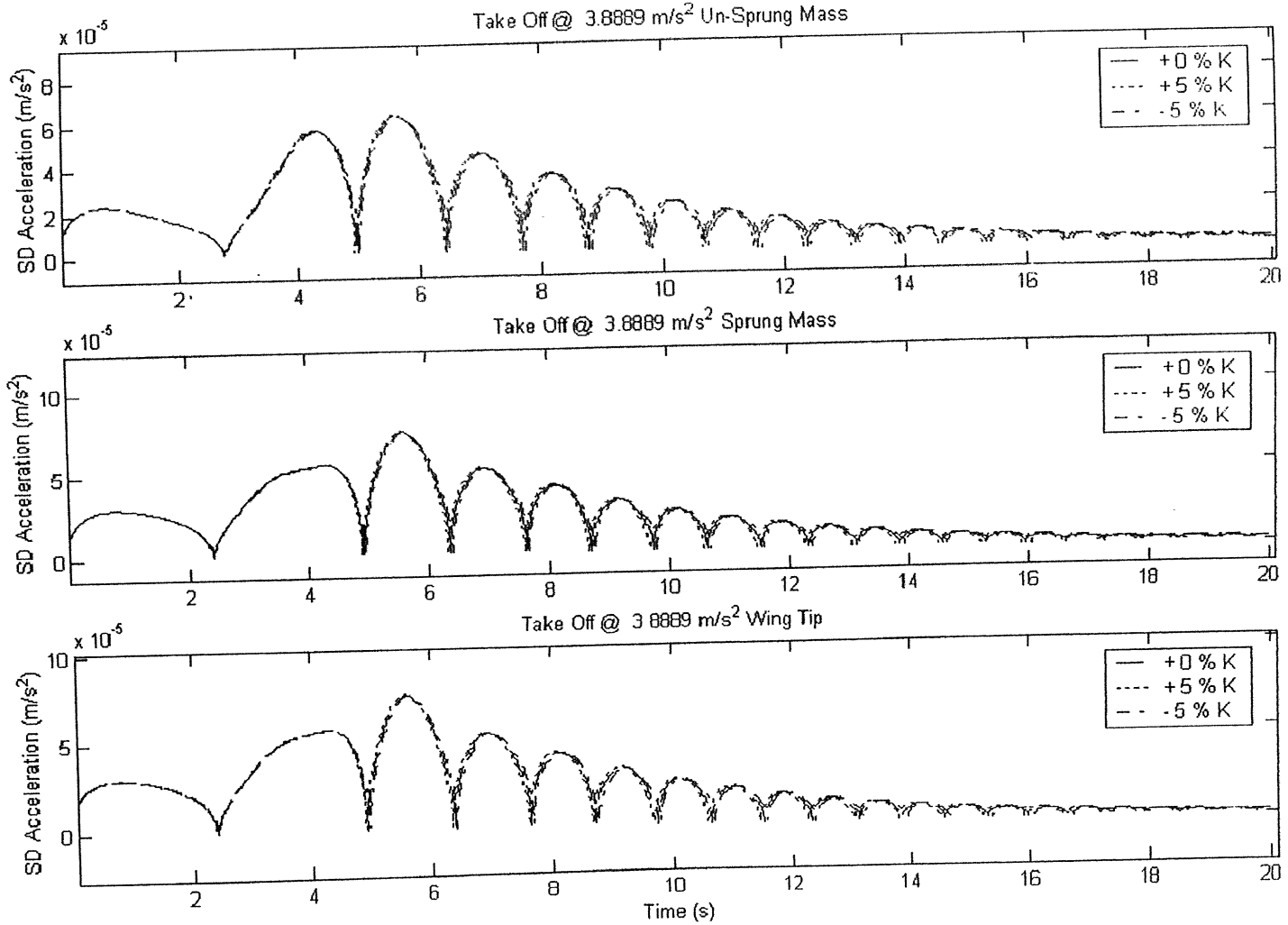

Fig 5.30 SD acceleration during take off at 3.8889 m/s² (variation in nonlinear stiffness coefficients)

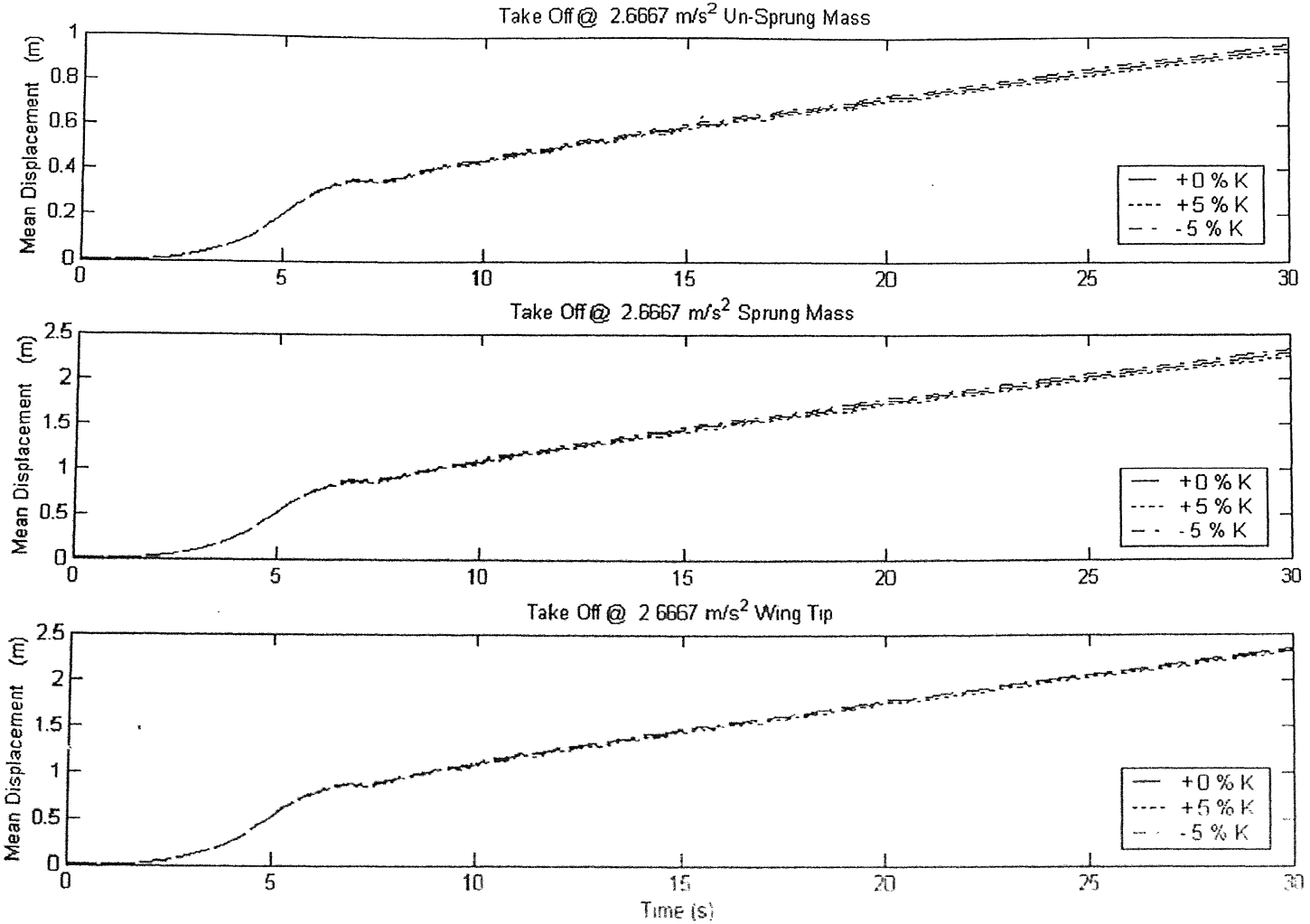

Fig 5.31 Mean displacement during take off at 2.6667 m/s^2 (variation in nonlinear stiffness coefficients)

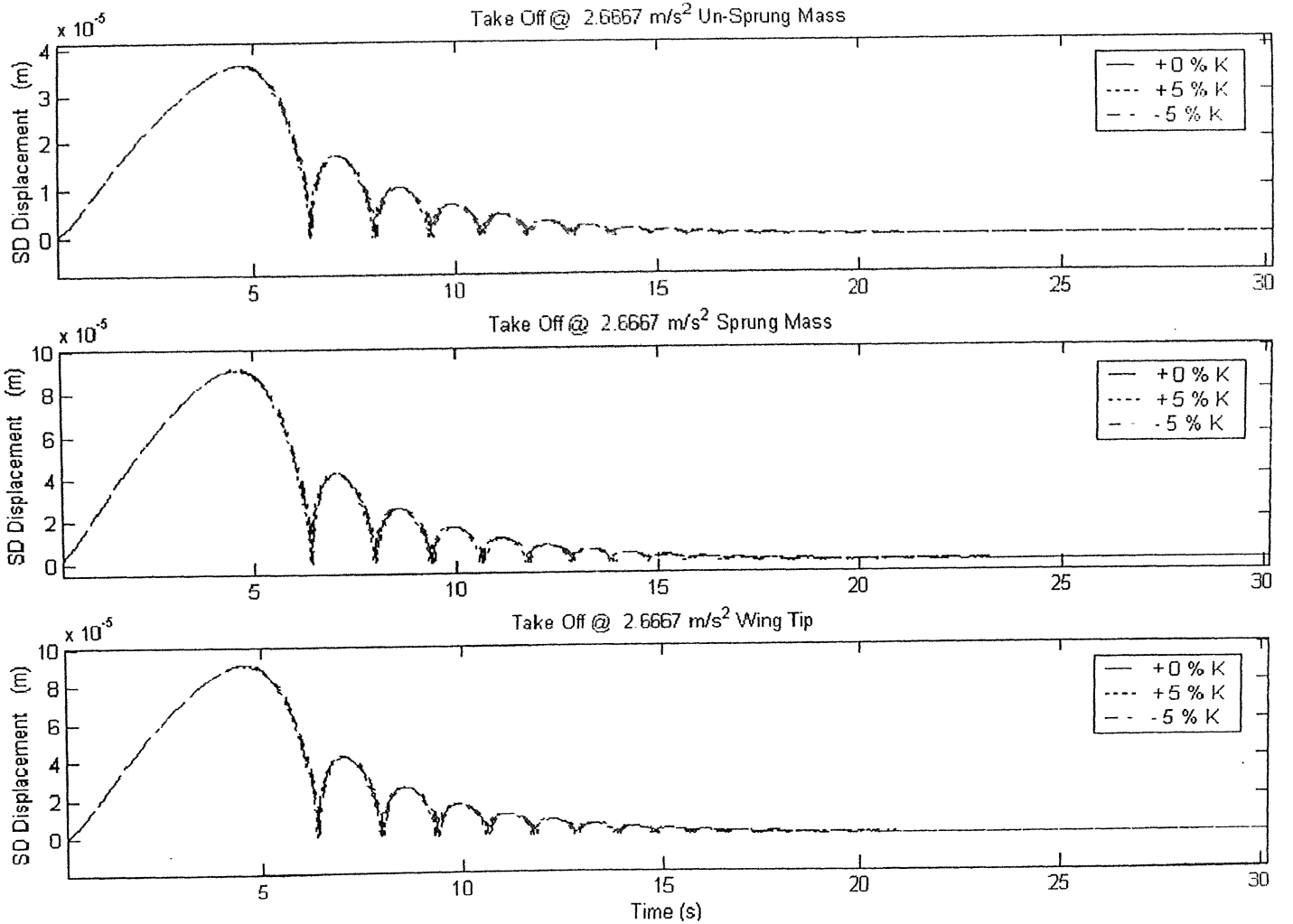

Fig 5 32 SD displacement during take off at 2 6667 m/s² (variation in nonlinear stiffness coefficients)

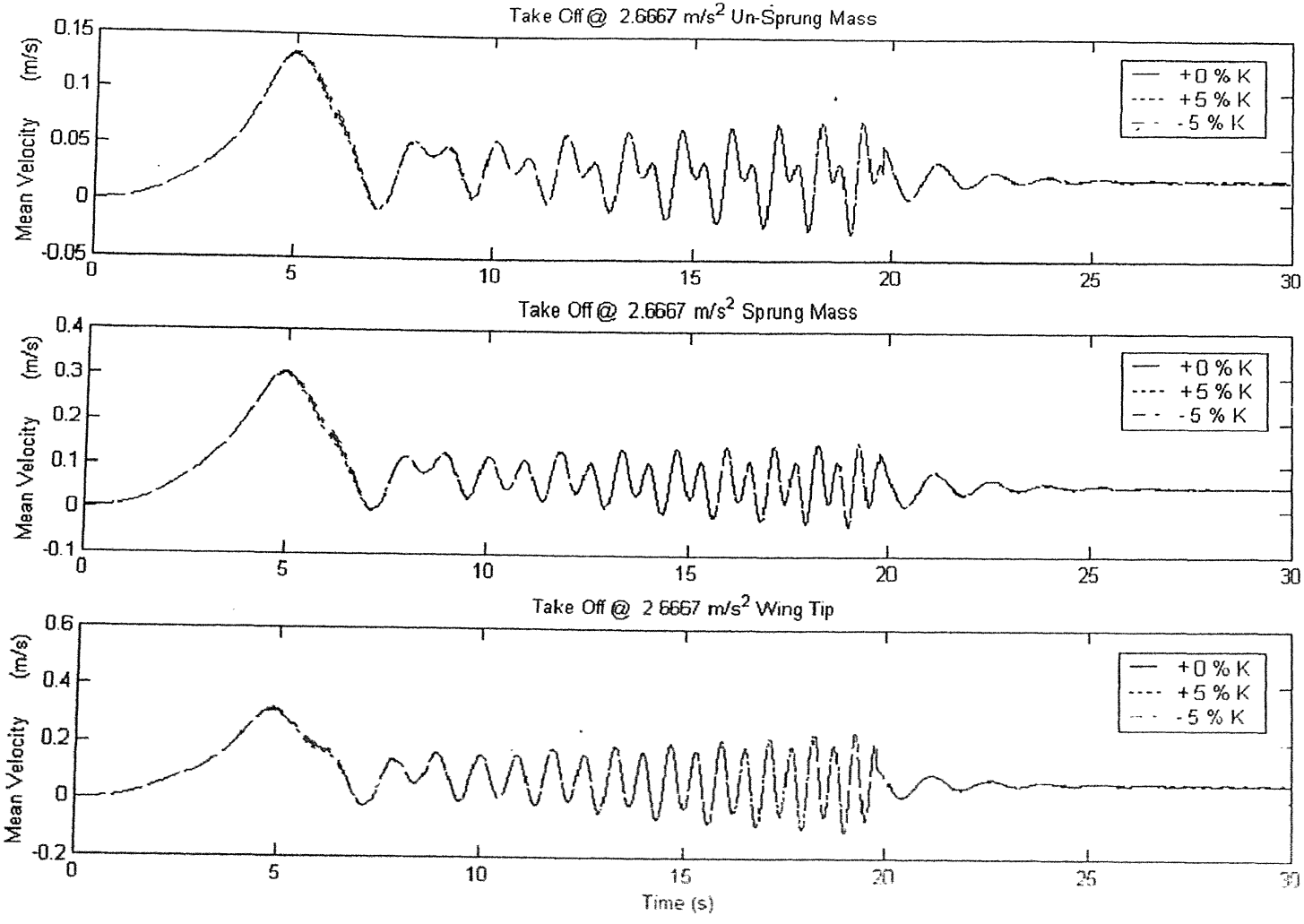

Fig. 5.33 Mean Velocity during take off at 2.6667 m/s^2 (variation in nonlinear stiffness coefficients)

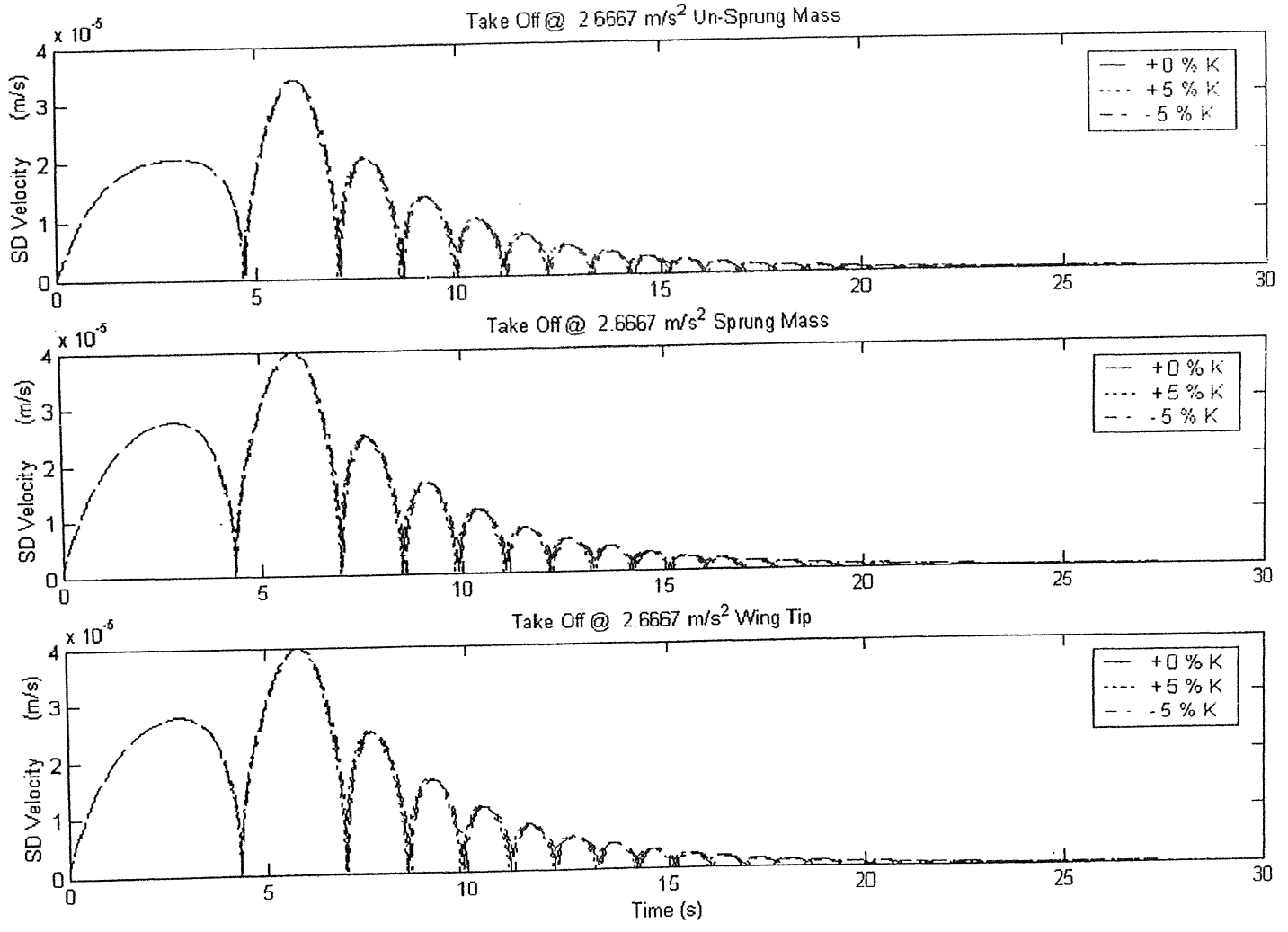

Fig 5.34 SD Velocity during take off at 2.6667 m/s² (variation in nonlinear stiffness coefficients)

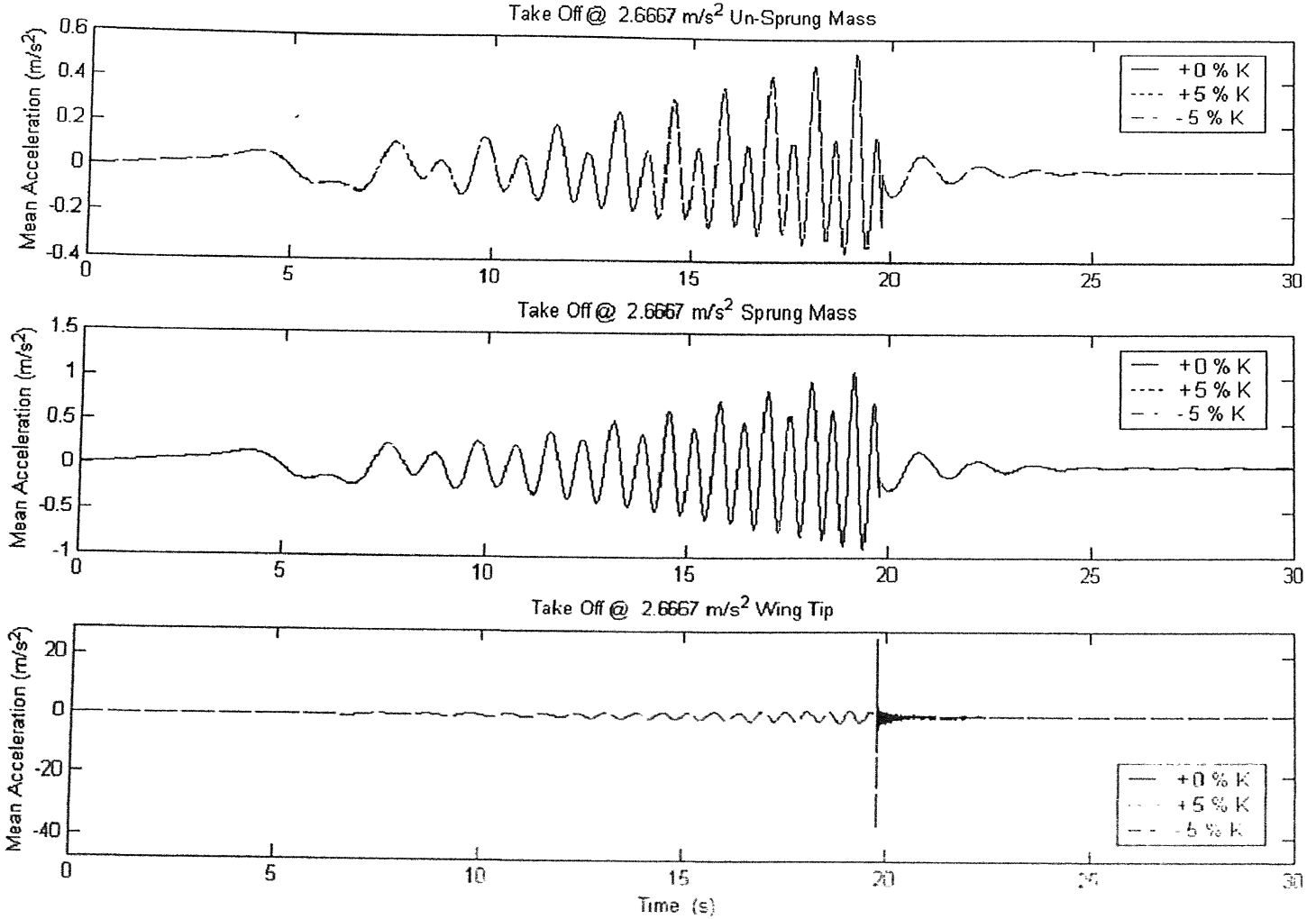

Fig 5.35 Mean acceleration during take off at 2.6667 m/s^2 (variation in nonlinear stiffness coefficients)

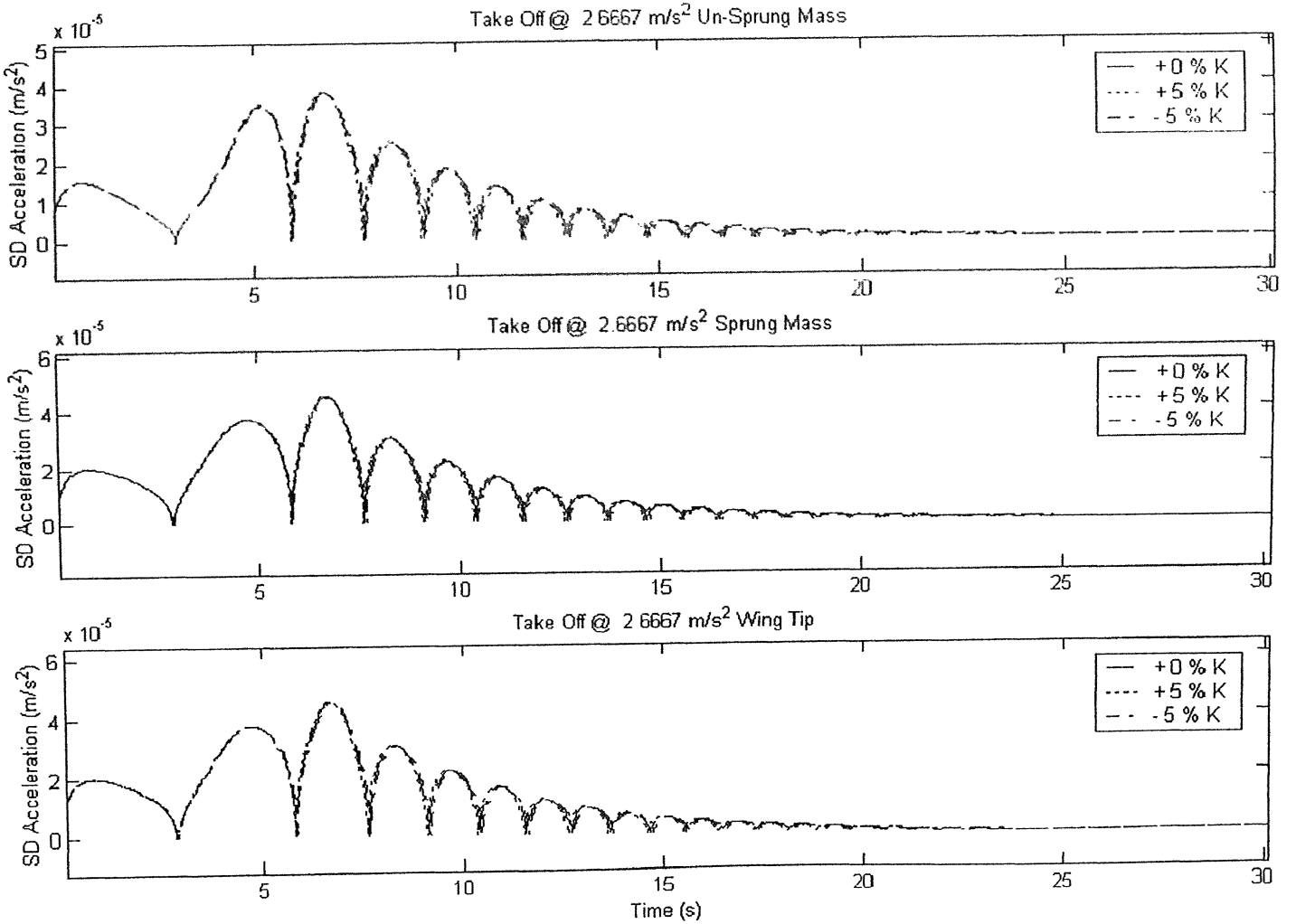

Fig 5.36 SD acceleration during take off at 2.6667 m/s^2 (variation in nonlinear stiffness coefficients)

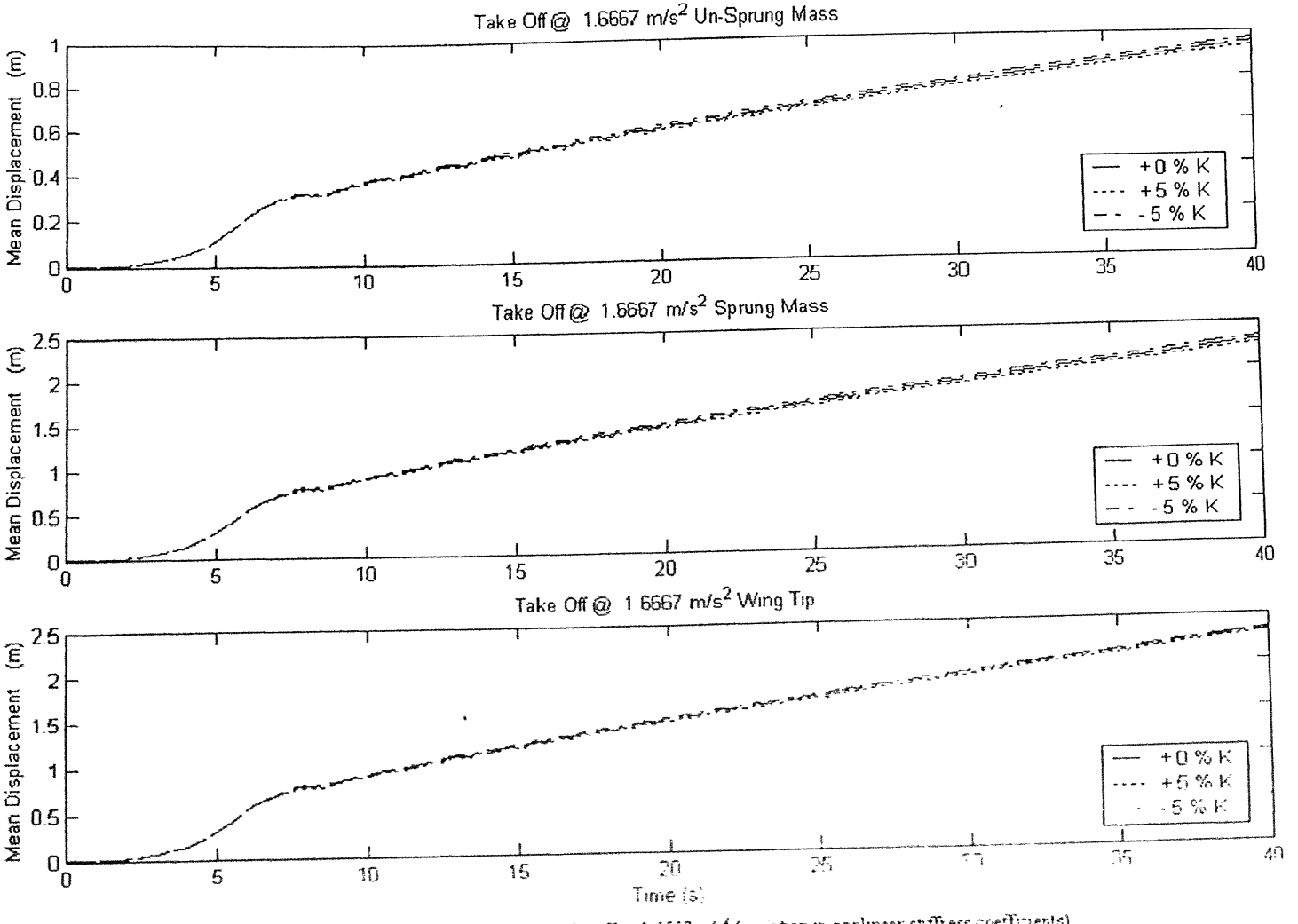

Fig 5.37 Mean displacement during take off at 1.6667 m/s² (variation in nonlinear stiffness coefficients)

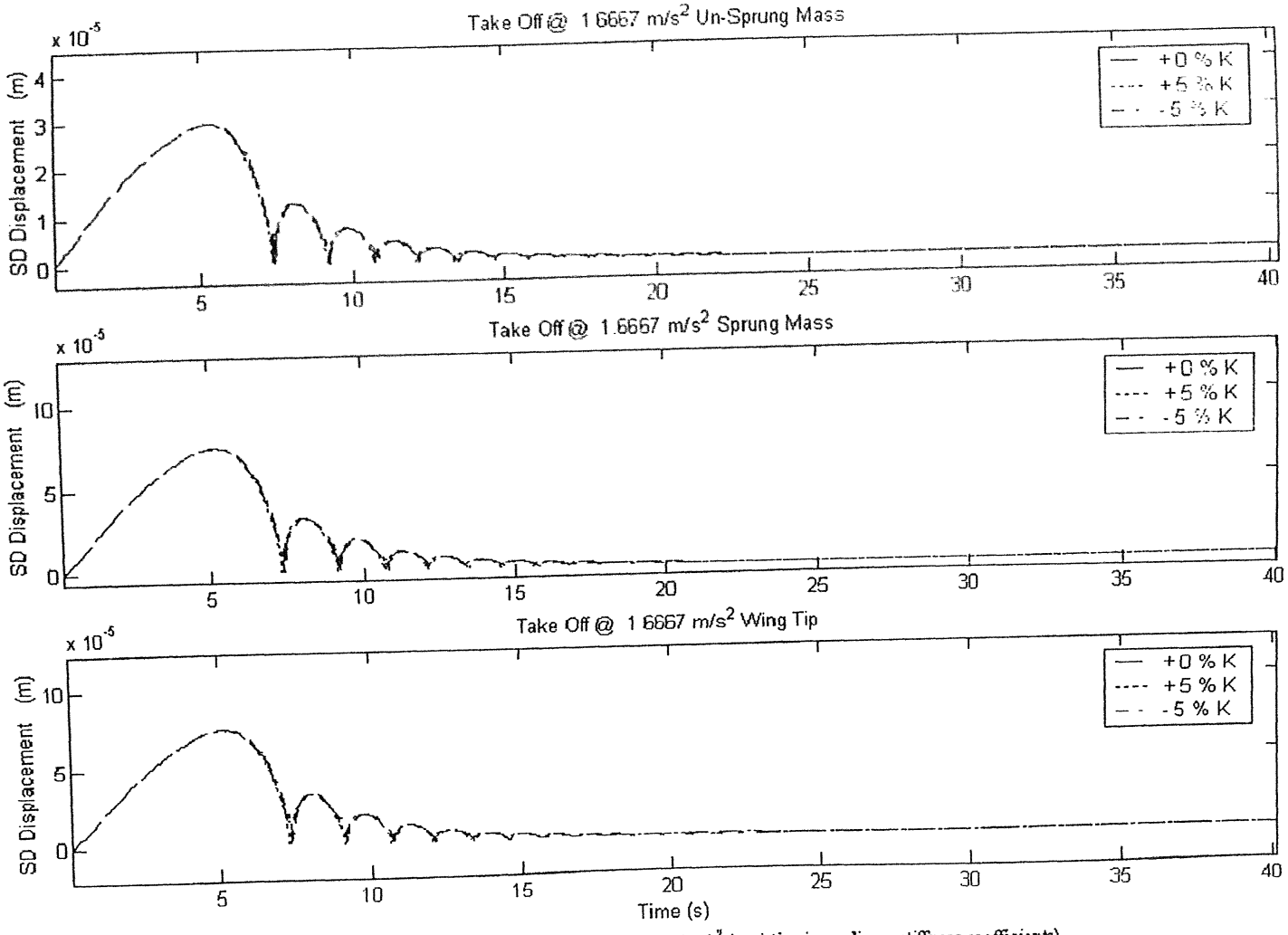

Fig 5.38 SD displacement during take off at 1.6667 m/s^2 (variation in nonlinear stiffness coefficients)

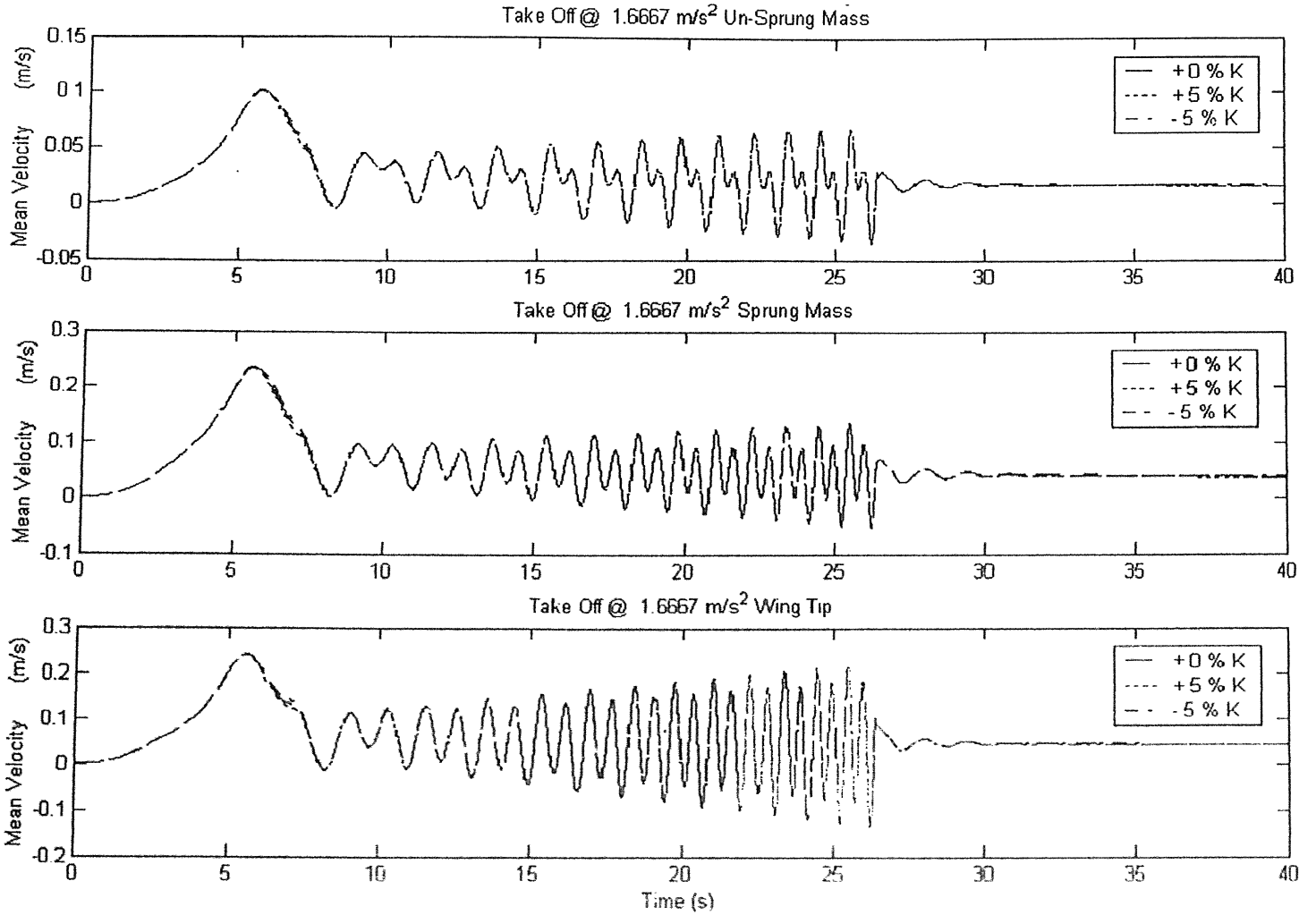

Fig 5 39 Mean Velocity during take off at 1.6667 m/s^2 (variation in nonlinear stiffness coefficients)

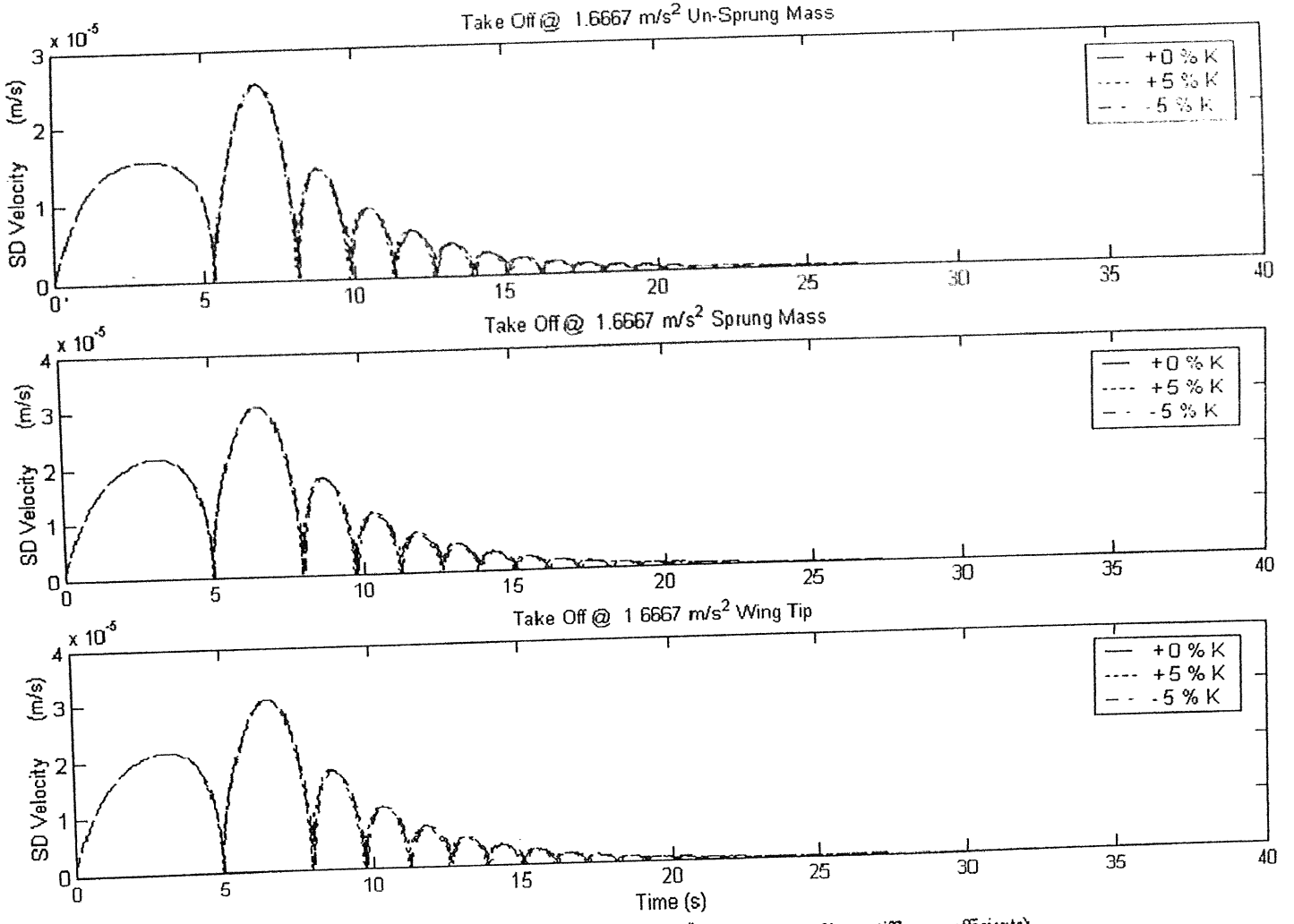

Fig 5.40 SD Velocity during take off at 1.6667 m/s^2 (variation in nonlinear stiffness coefficients)

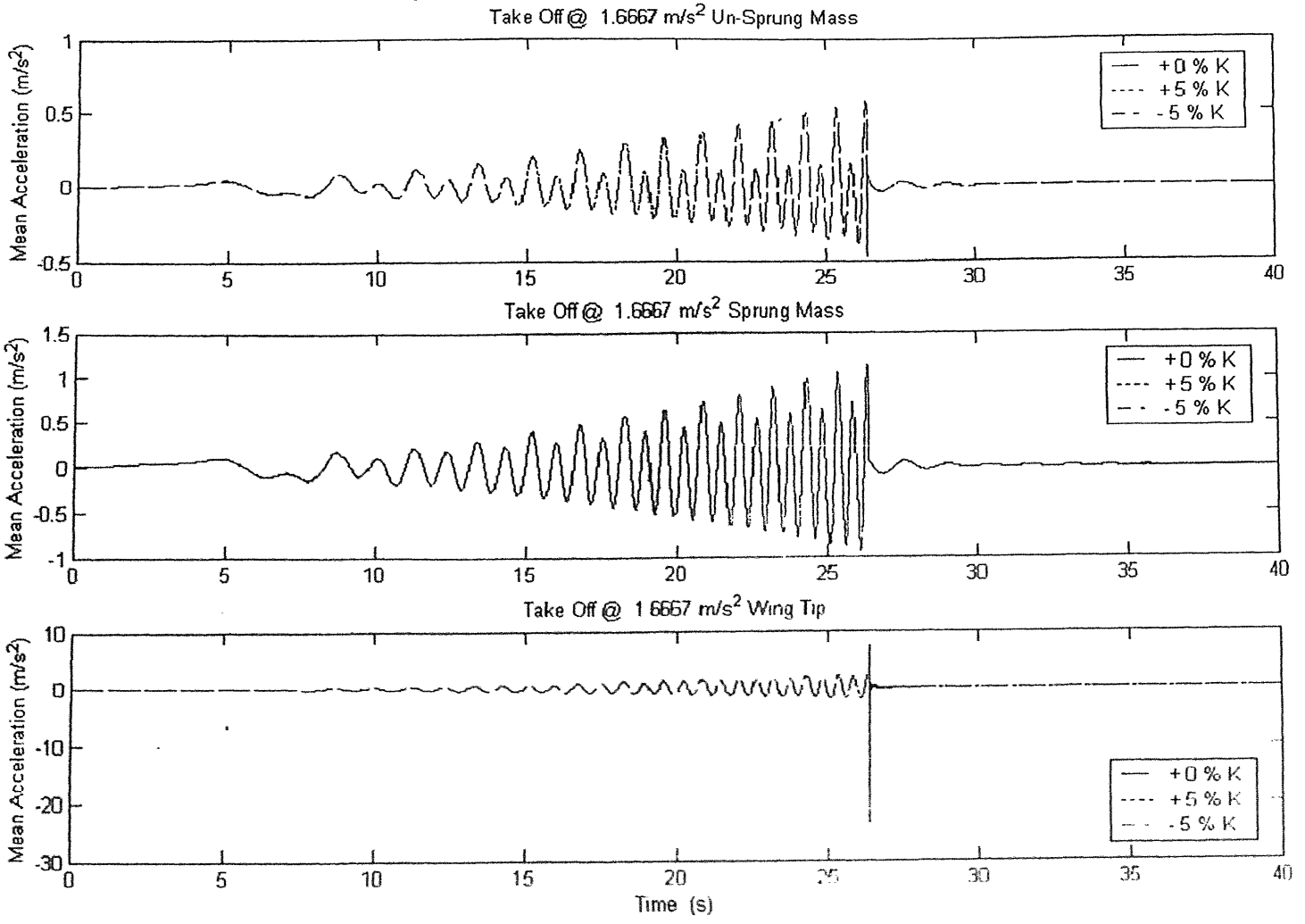

Fig 5.41 Mean acceleration during take off at 1.6667 m/s^2 (variation in nonlinear stiffness coefficients)

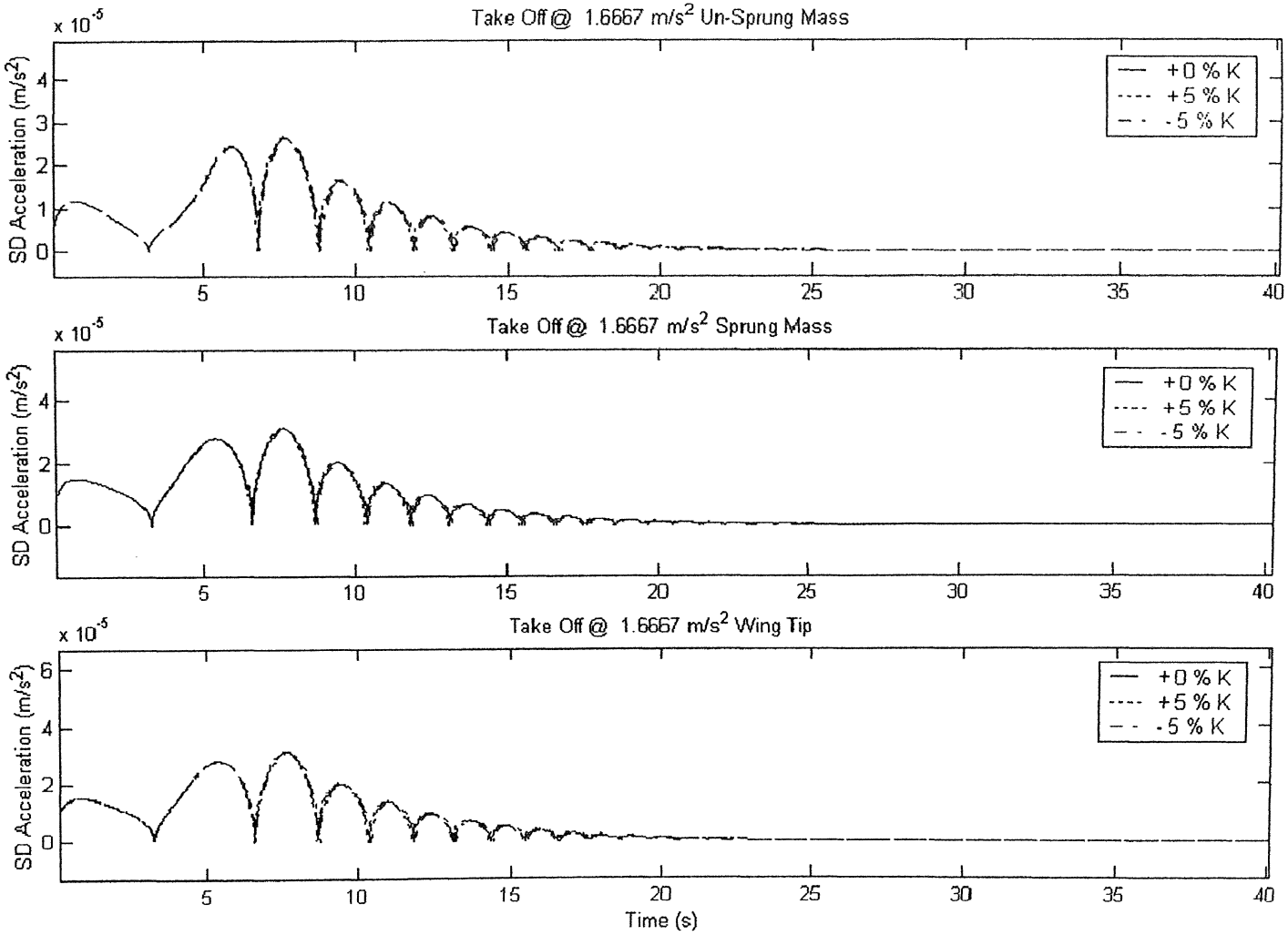

Fig 5.42 SD acceleration during take off at 1.6667 m/s^2 (variation in nonlinear stiffness coefficients)

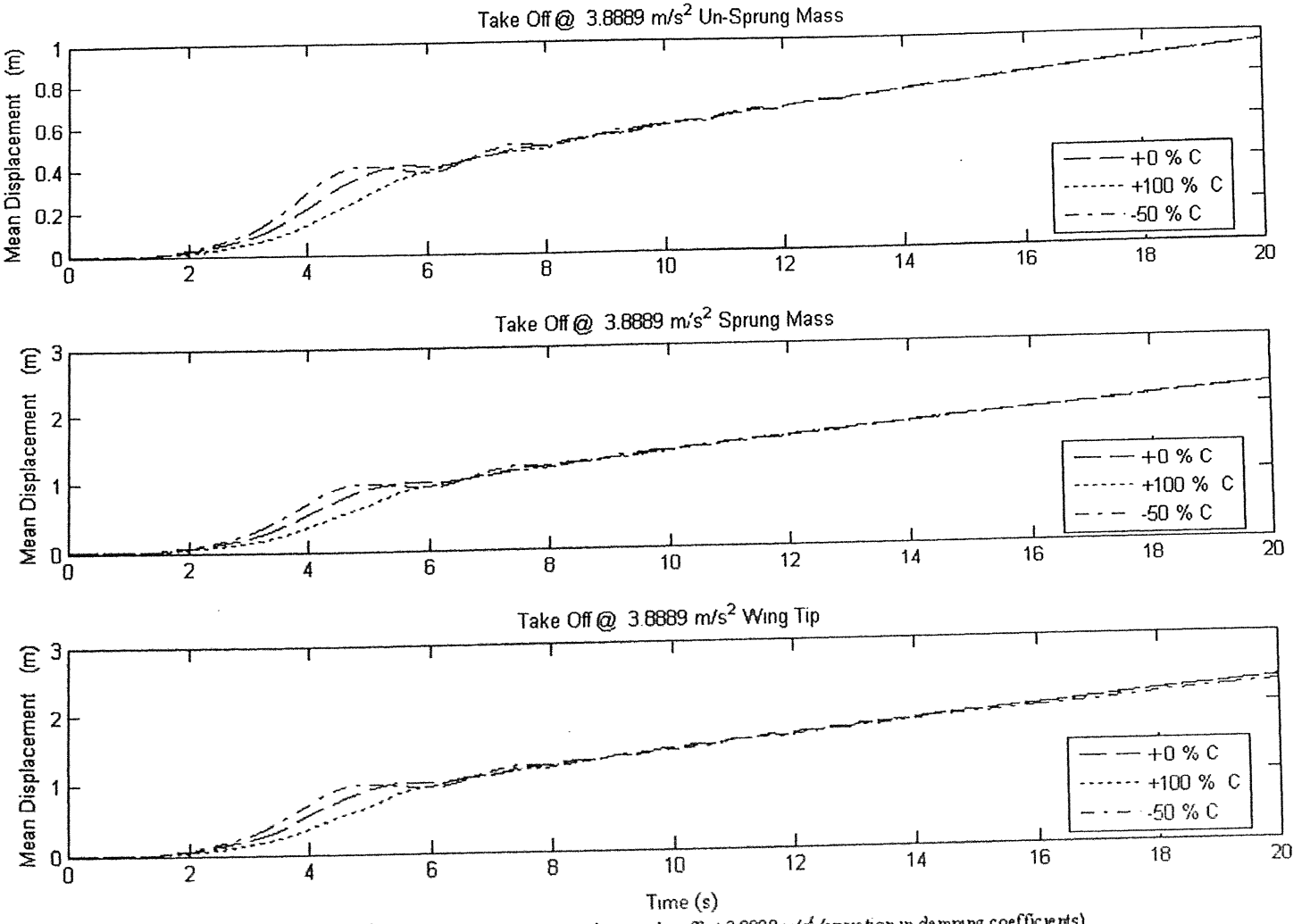

Fig 5.43 Mean displacement during take off at 3.8889 m/s^2 (variation in damping coefficients)

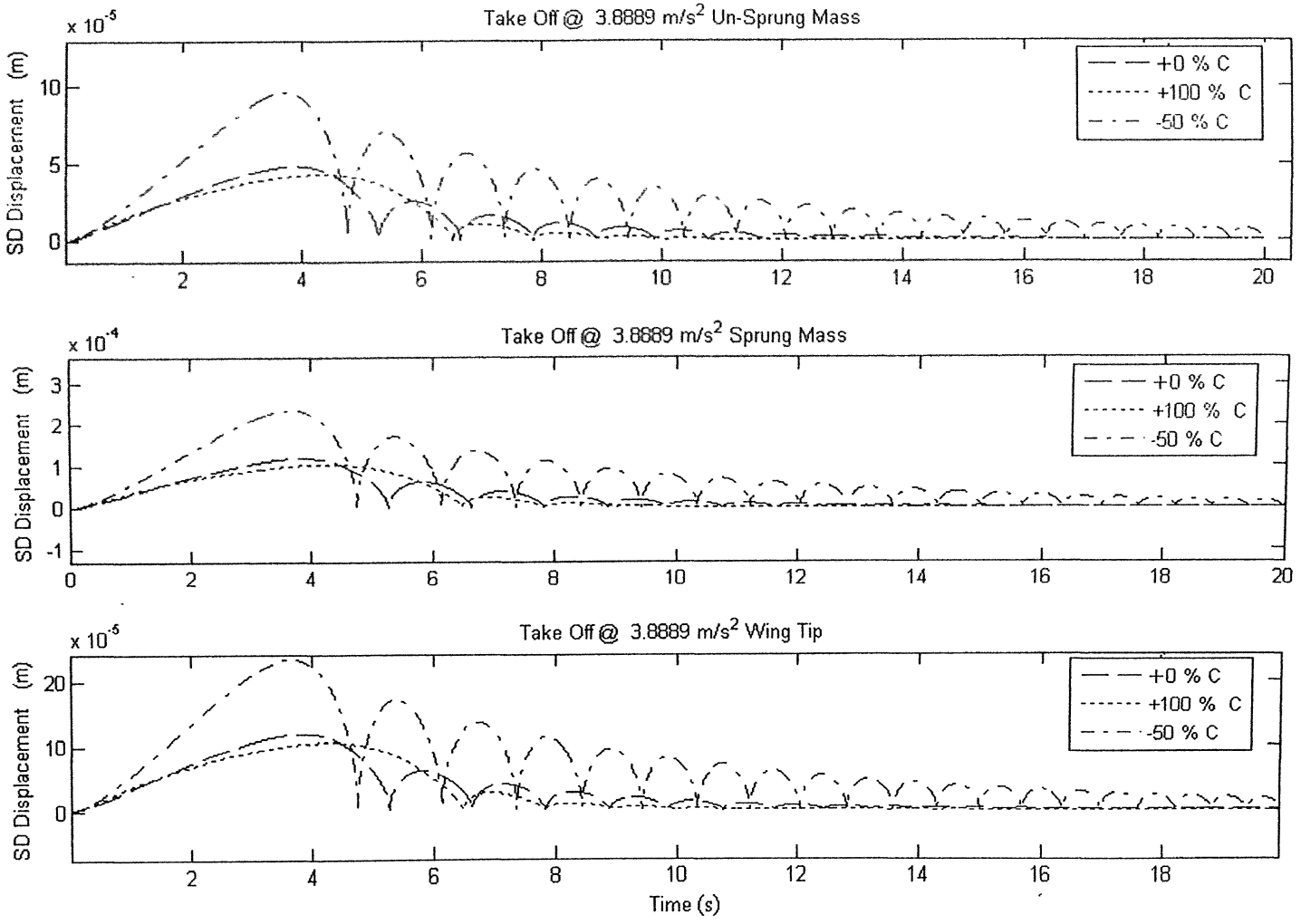

Fig 5.44 SD displacement during take off at 3.8889 m/s^2 (variation in damping coefficients)

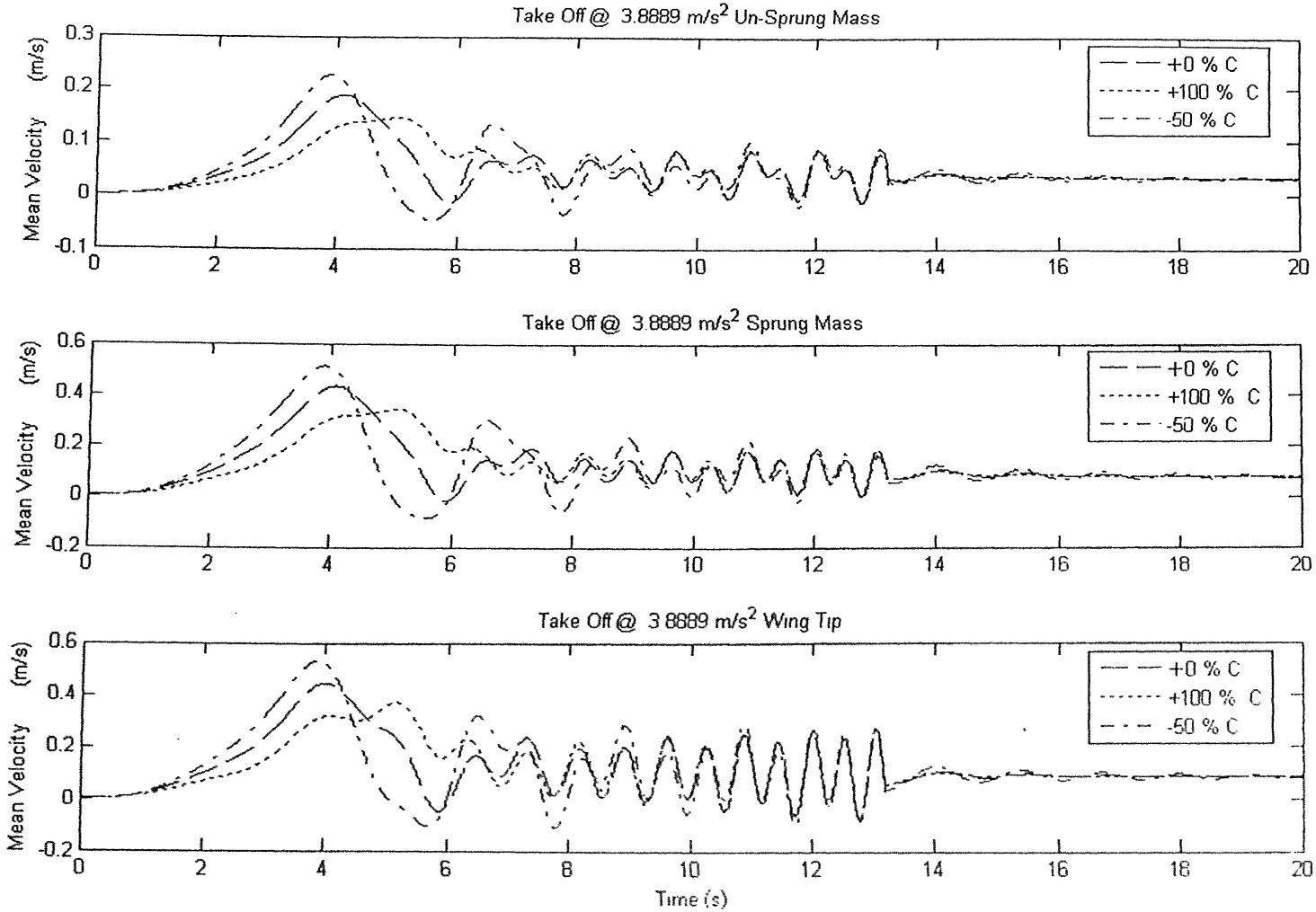

Fig 5.45 Mean Velocity during take off at 3.8889 m/s^2 (variation in damping coefficients)

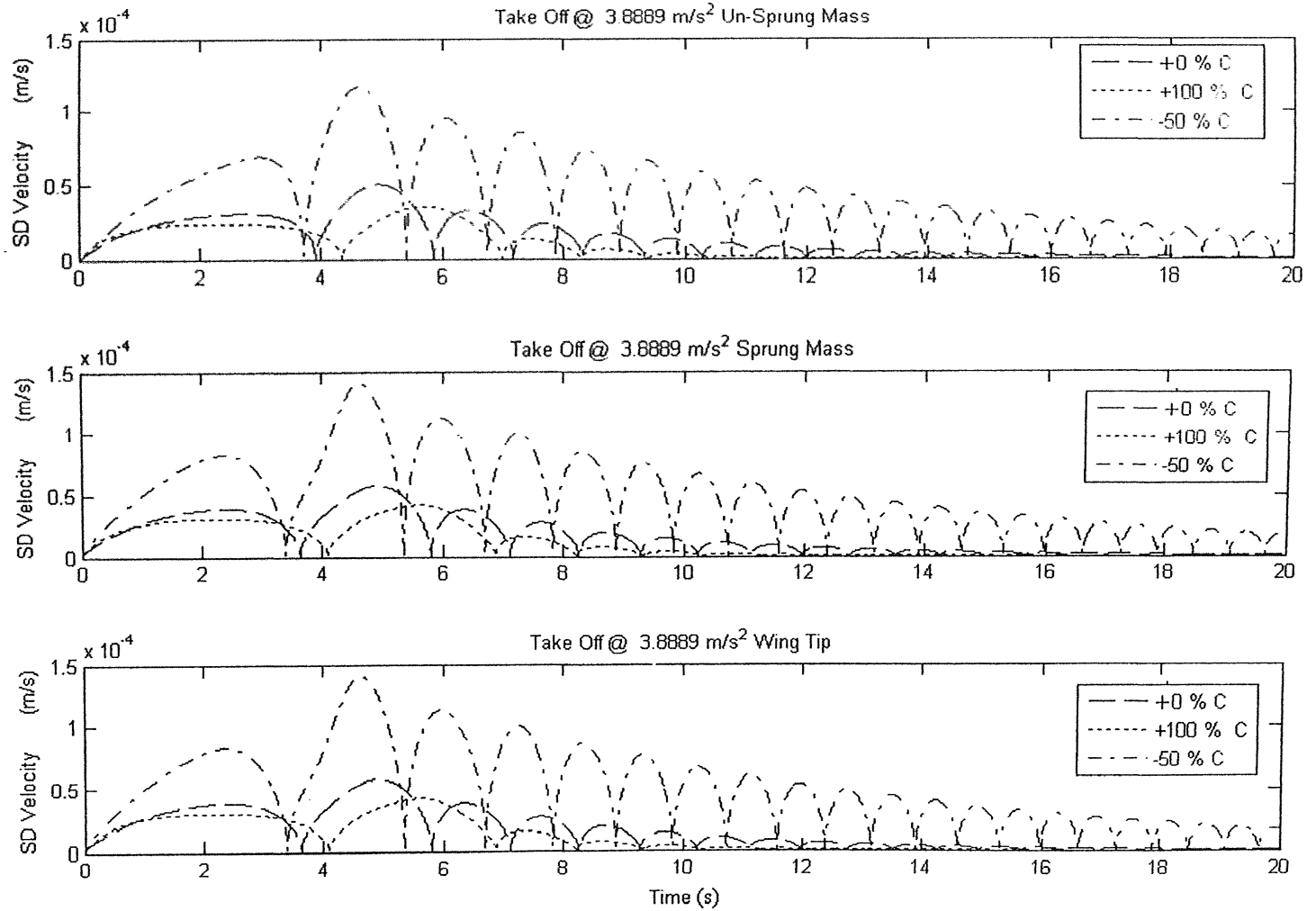

Fig 5.46 SD Velocity during take off at 3.8889 m/s² (variation in damping coefficients)

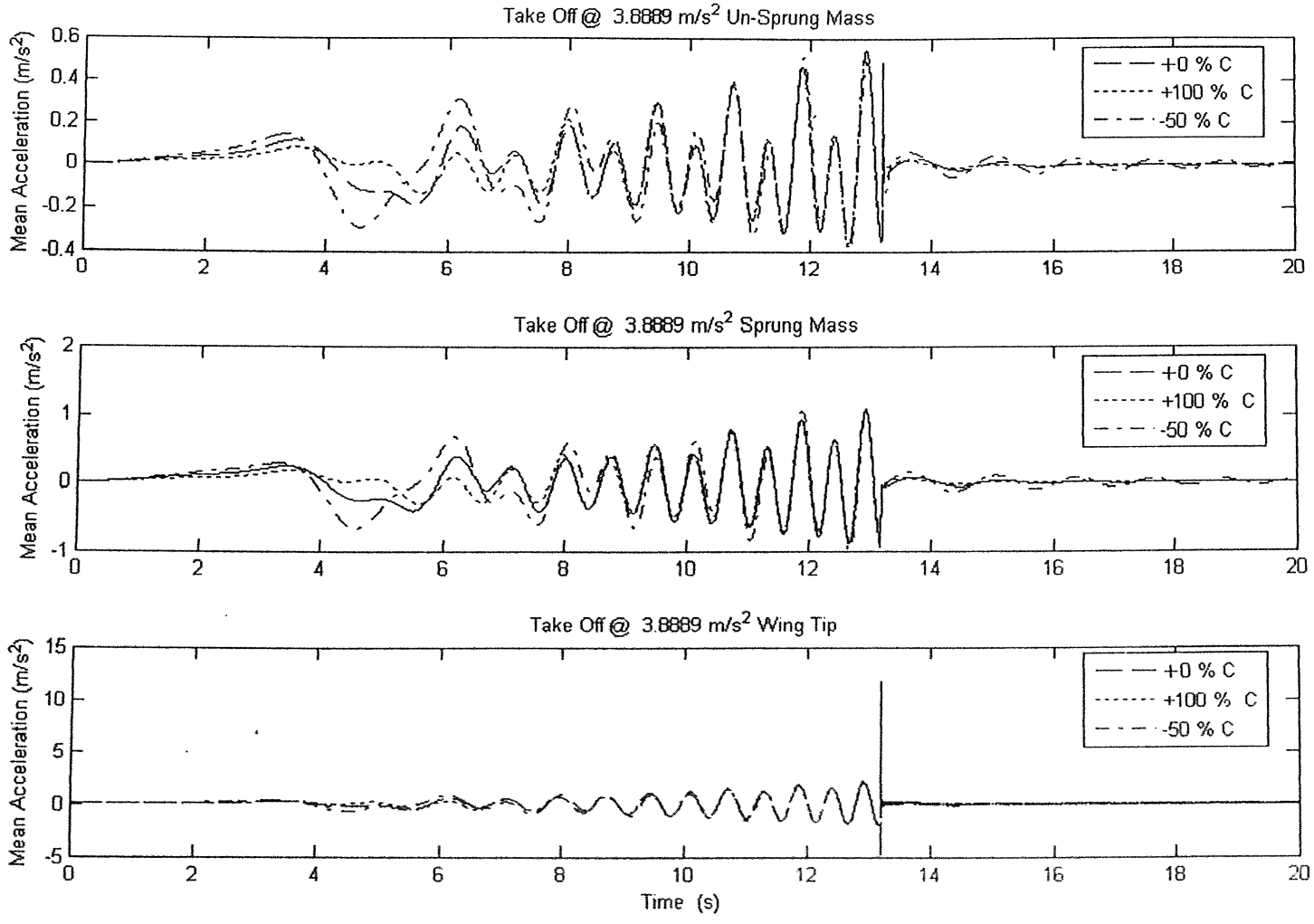

Fig 5.47 Mean acceleration during take off at 3.8889 m/s^2 (variation in damping coefficients)

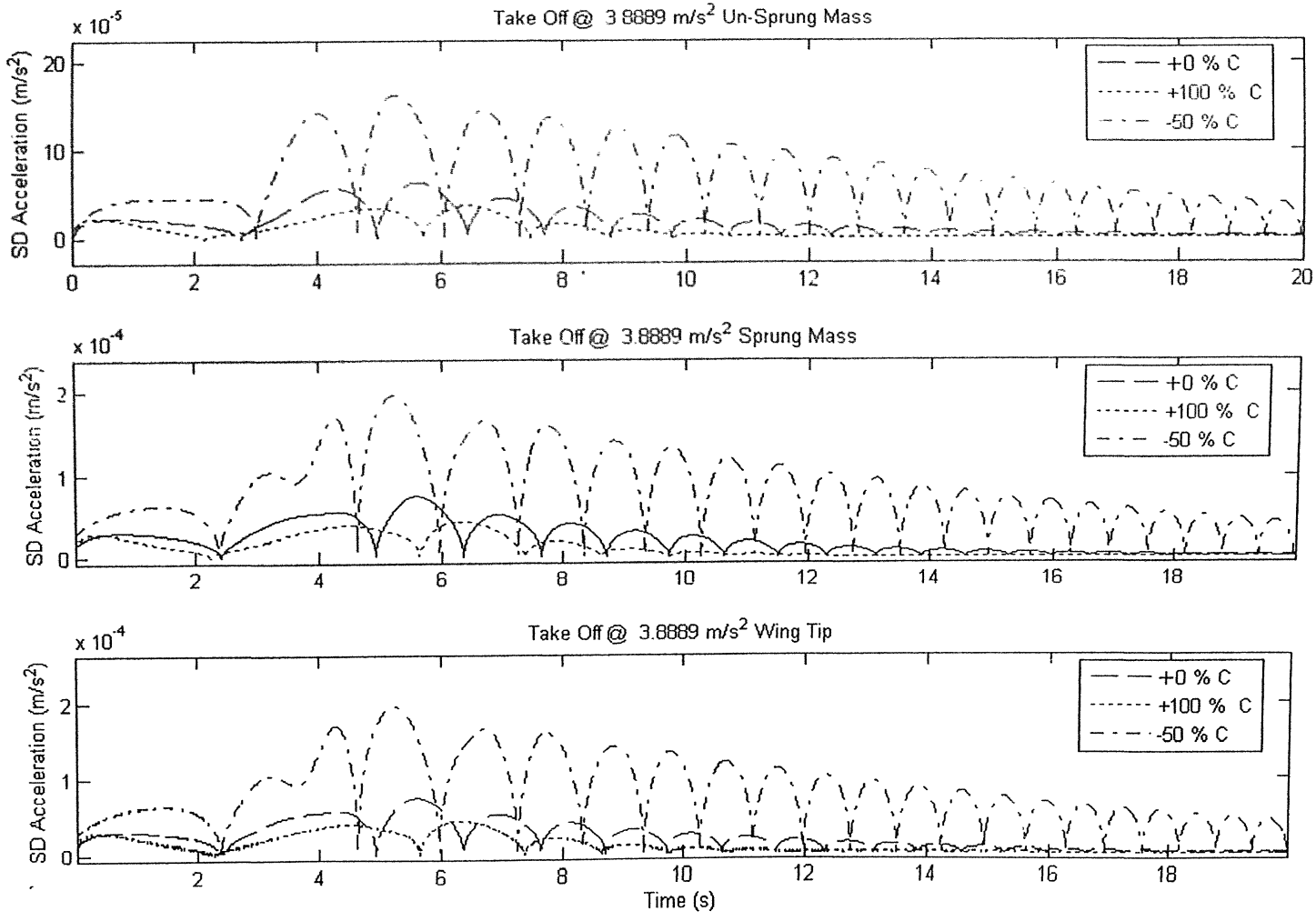

Fig 5.48 SD acceleration during take off at 3.8889 m/s^2 (variation in damping coefficients)

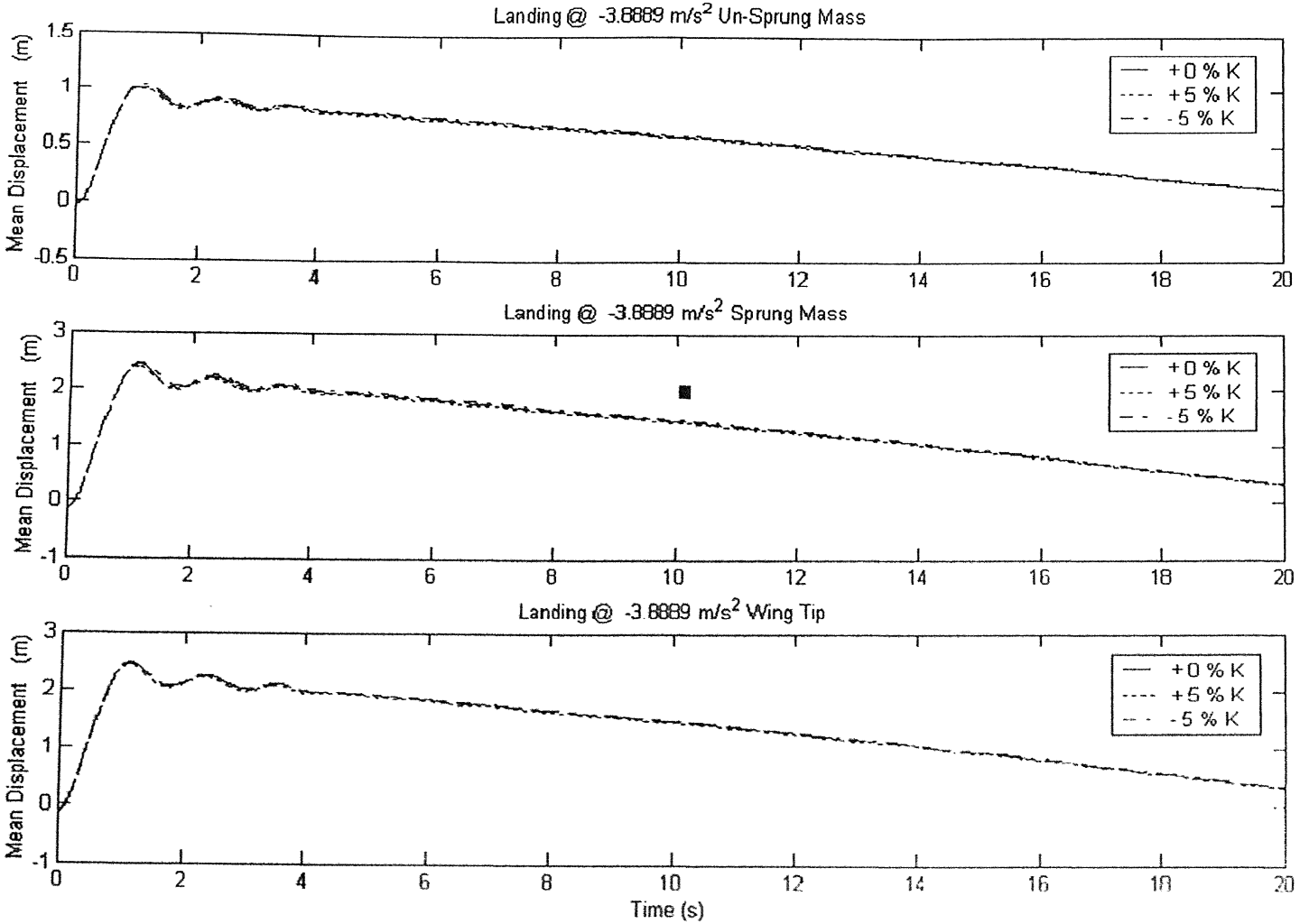

Fig 5 49 Mean displacement during landing at - 3 8889 m/s^2 (variation in nonlinear stiffness coefficients)

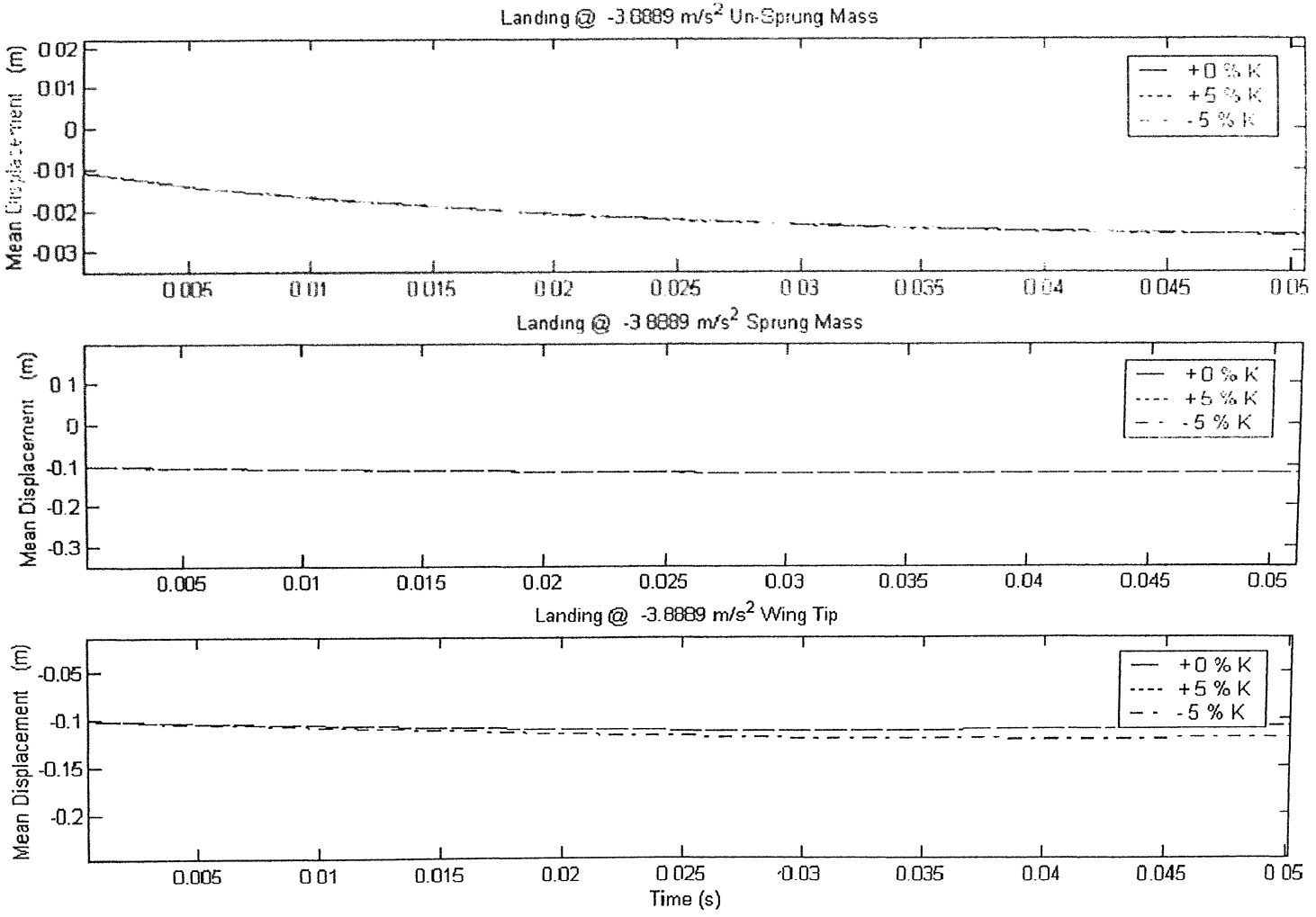

Fig 5.50 Mean displacement during landing at - 3.8889 m/s² (variation in nonlinear stiffness coefficients)

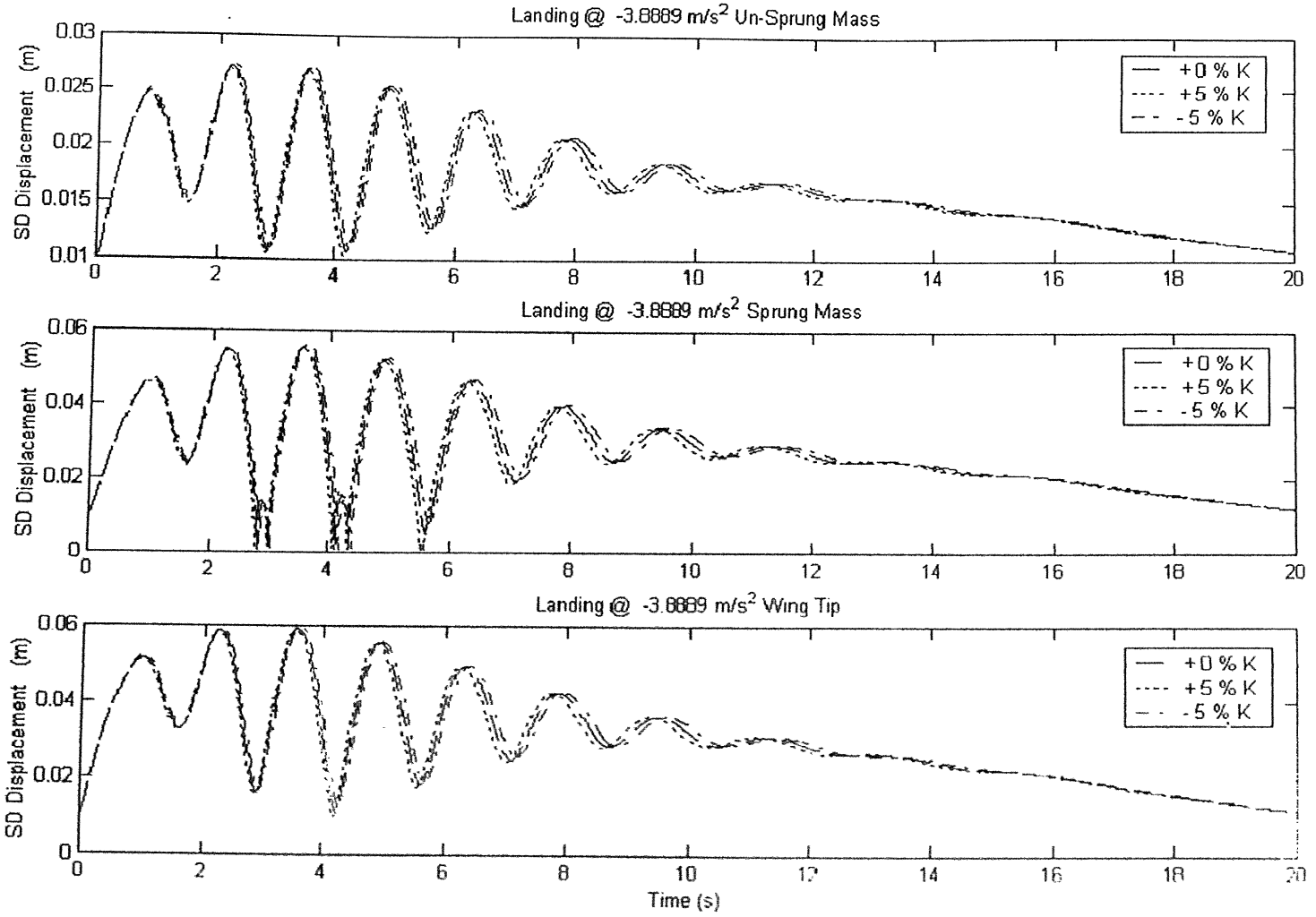

Fig 5.51 SD displacement during landing at - 3.8889 m/s^2 (variation in nonlinear stiffness coefficients)

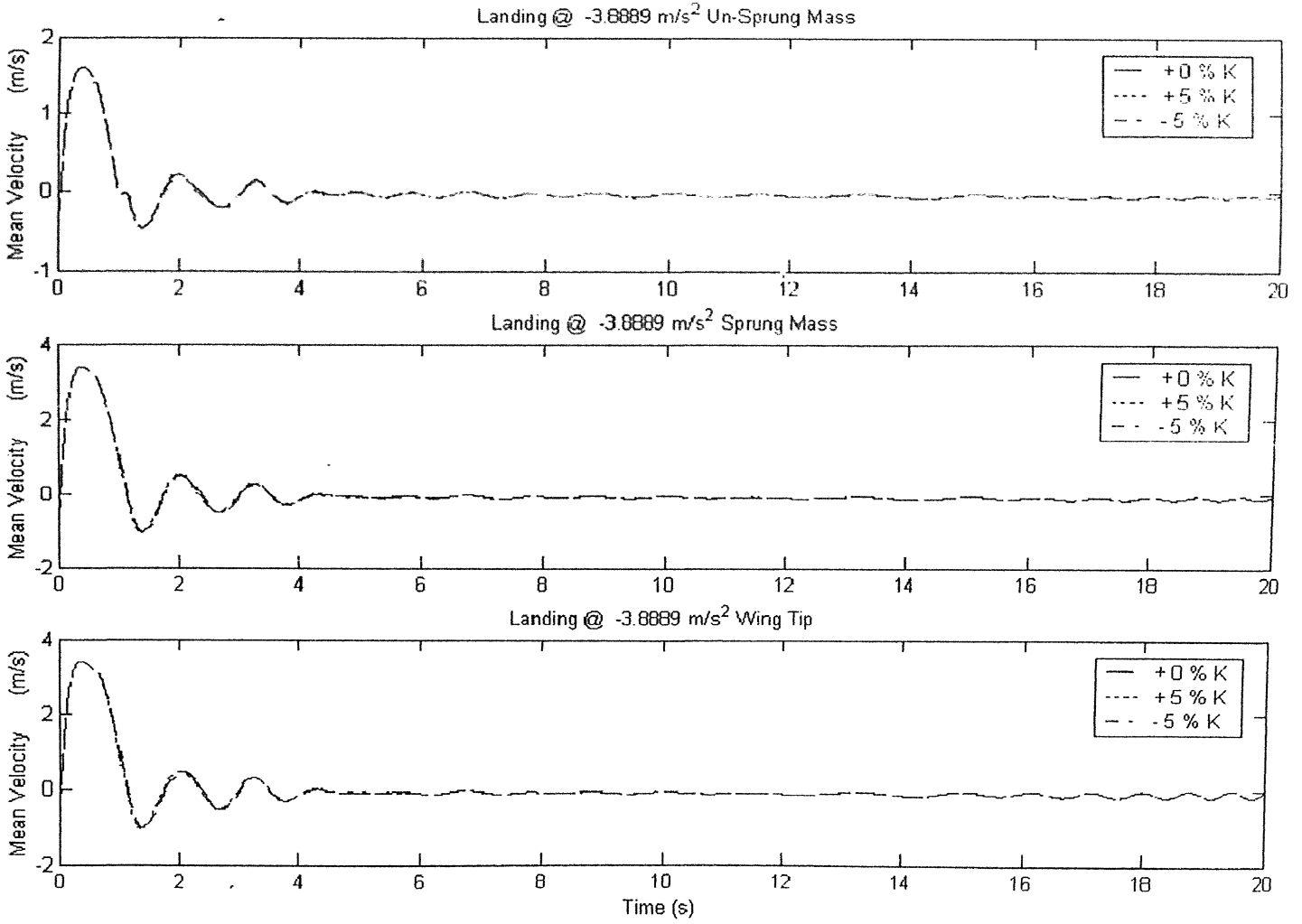

Fig 5.52 Mean Velocity during landing at - 3.8889 m/s² (variation in nonlinear stiffness coefficients)

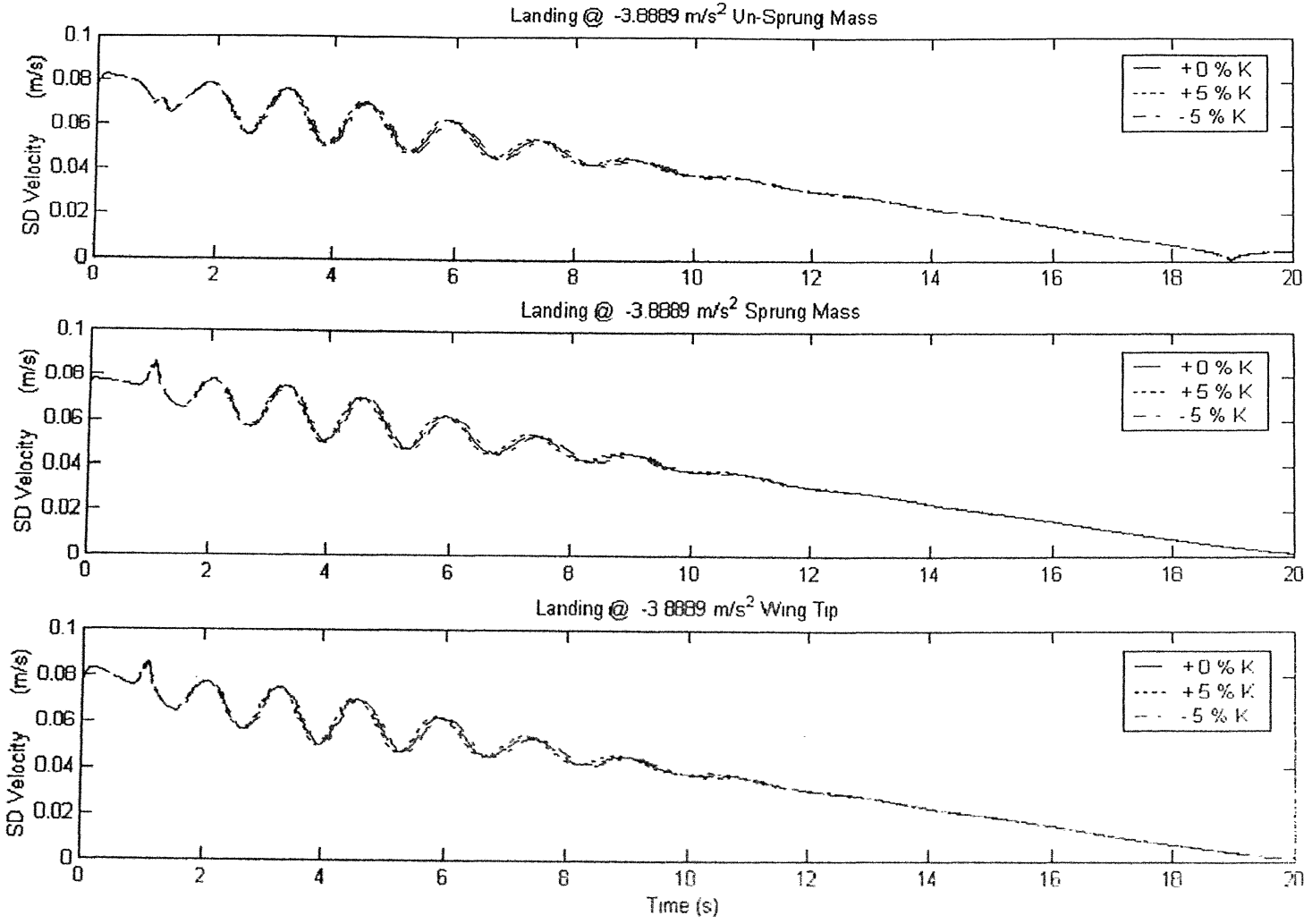

Fig 5 53 SD Velocity during landing at - 3.8889 m/s^2 (variation in nonlinear stiffness coefficients)

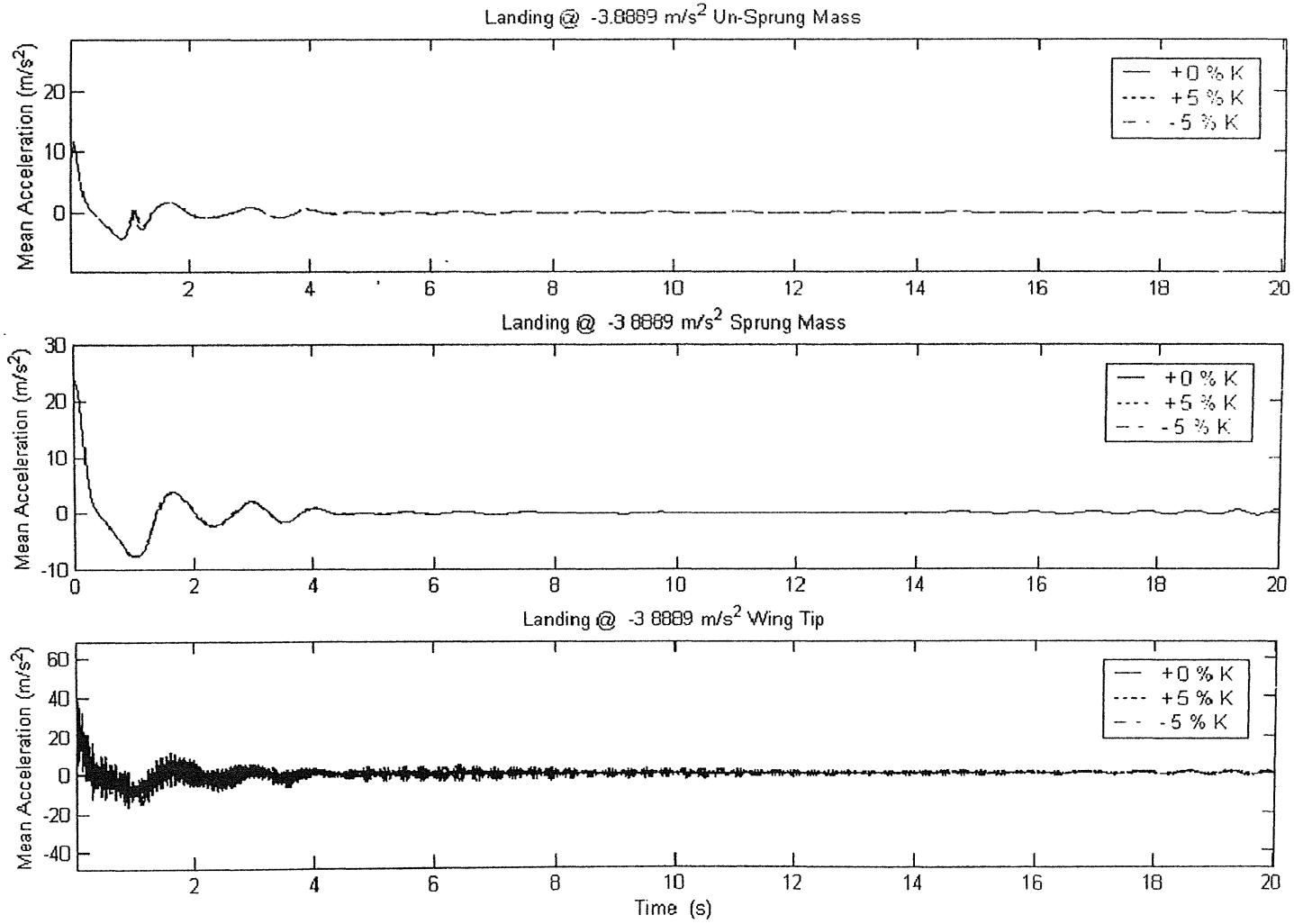

Fig 5.54 Mean acceleration during landing at - 3.8889 m/s^2 (variation in nonlinear stiffness coefficients)

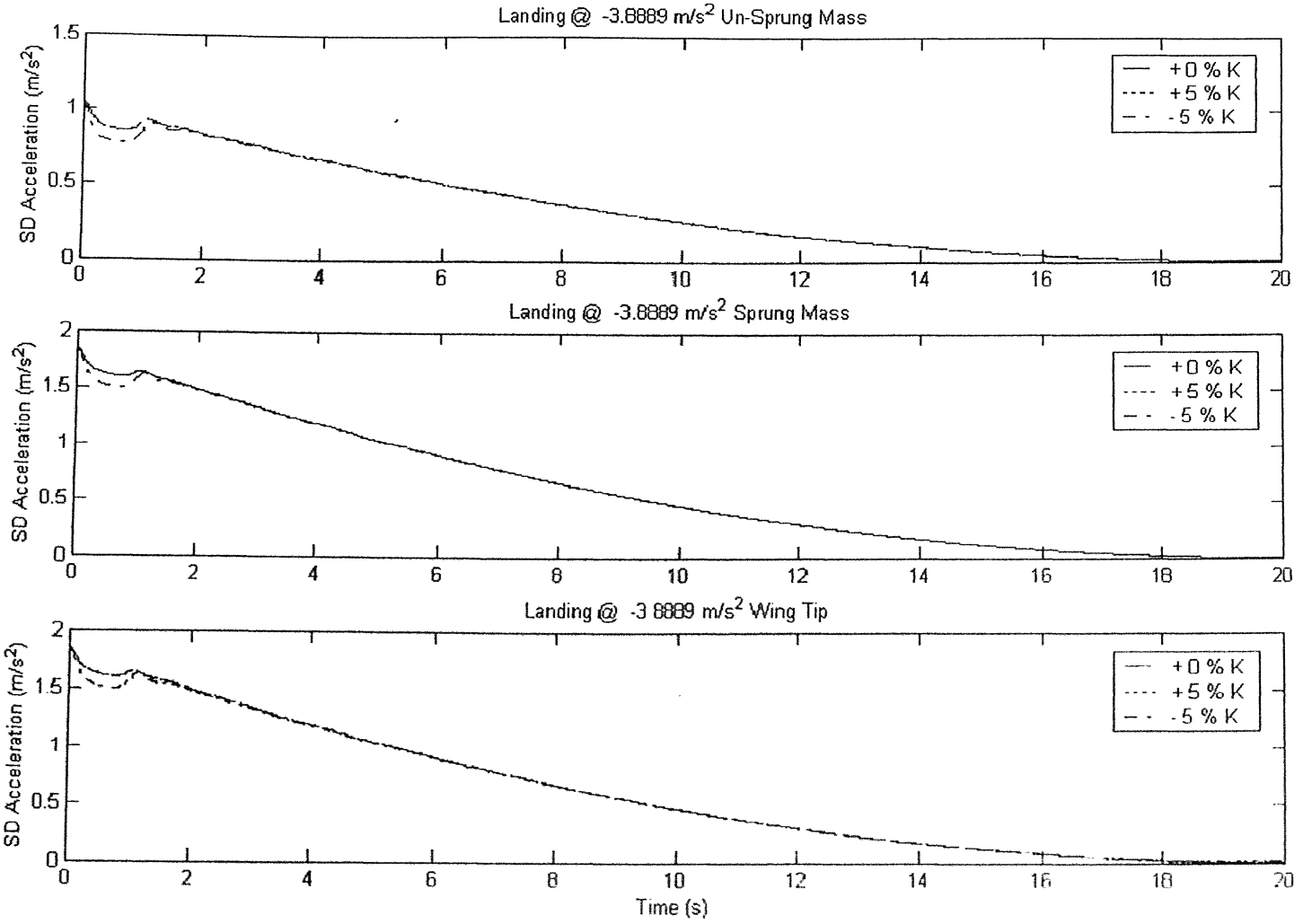

Fig 5.55 SD acceleration during landing at - 3.8889 m/s² (variation in nonlinear stiffness coefficients)

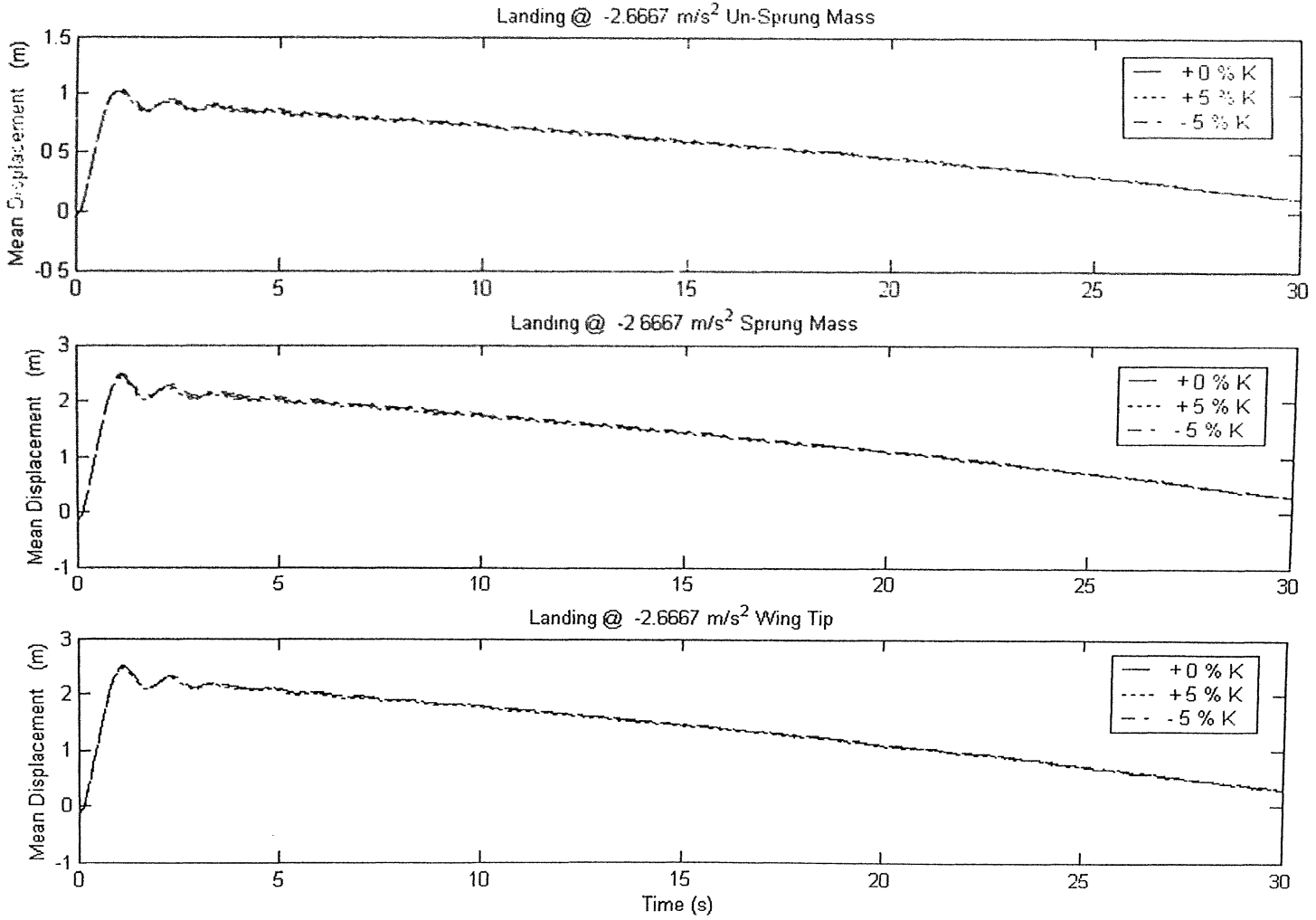

Fig 5.56 Mean displacement during landing at - 2.6667 m/s^2 (variation in nonlinear stiffness coefficients)

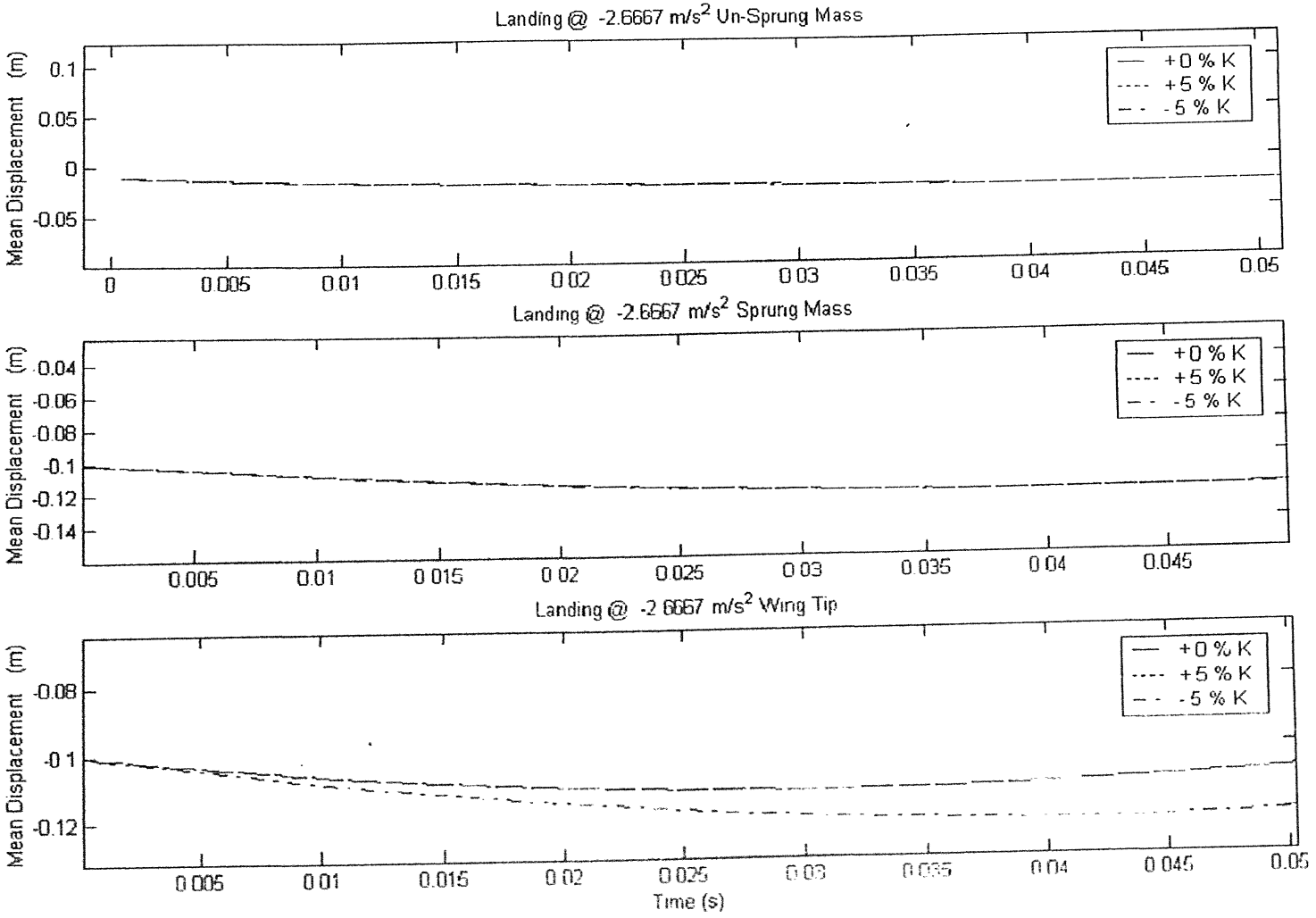

Fig 5.57 Mean displacement during landing at - 2.6667 m/s² (variation in nonlinear stiffness coefficients)

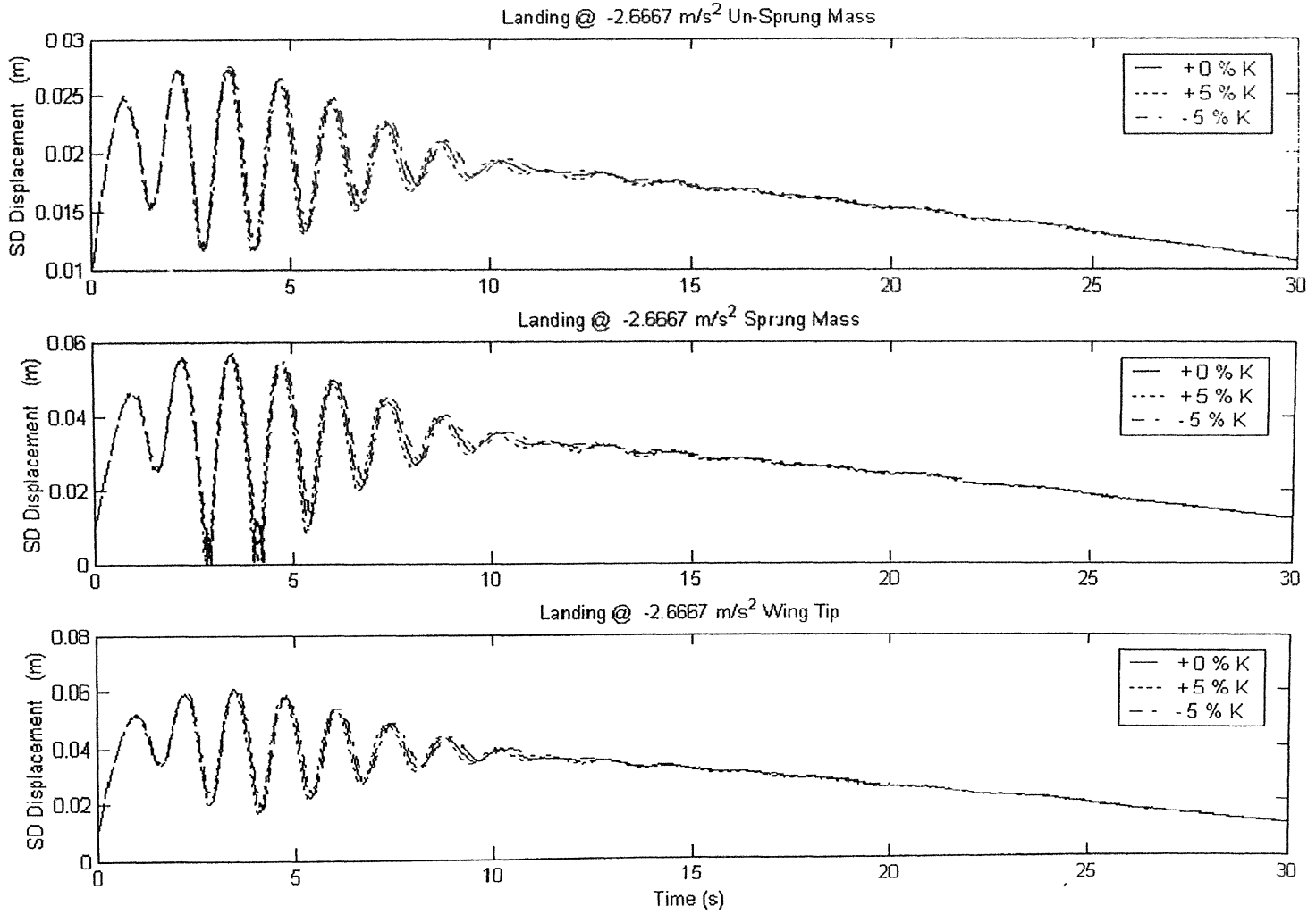

Fig 5.58 SD displacement during landing at - 2.6667 m/s^2 (variation in nonlinear stiffness coefficients)

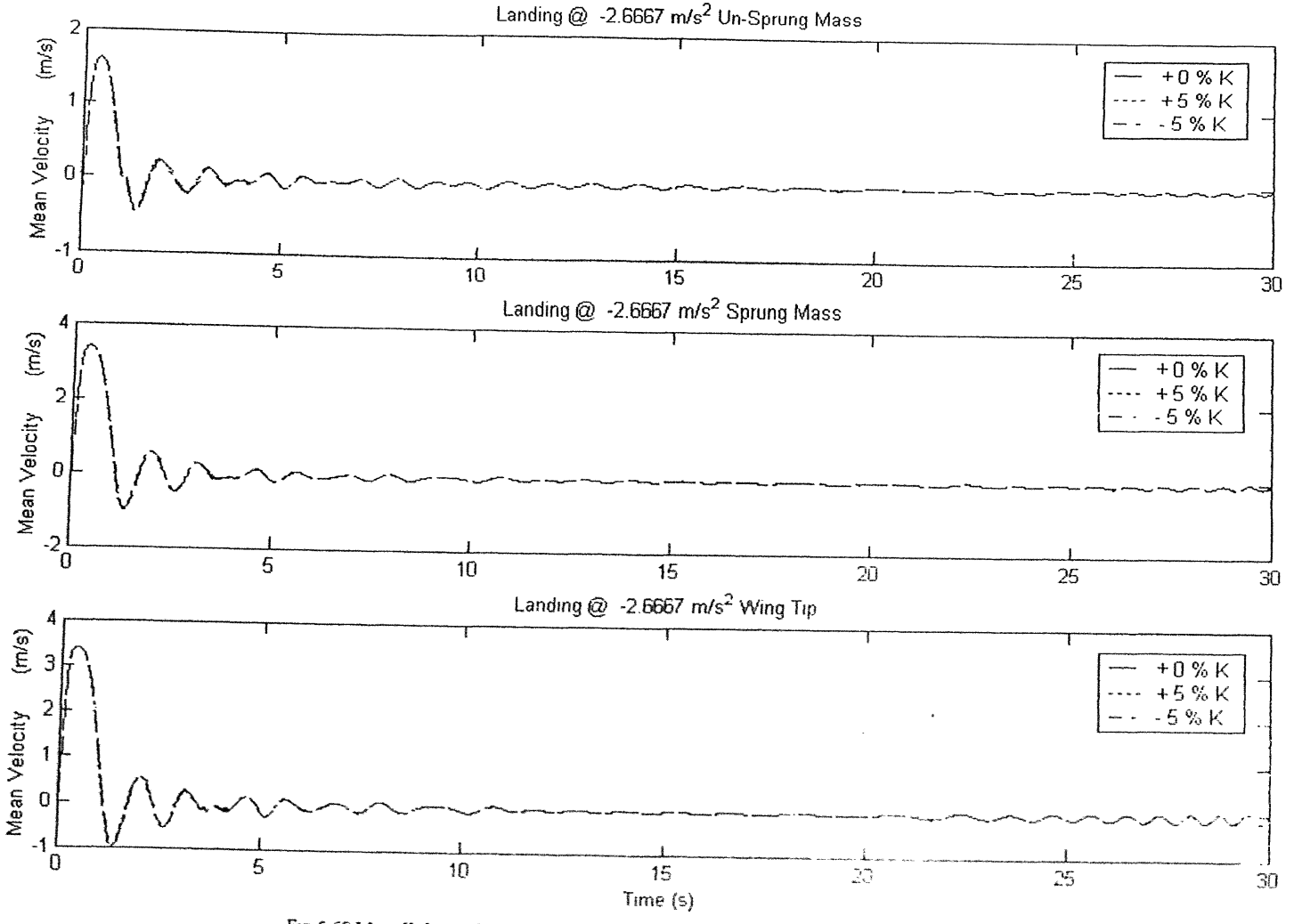

Fig 5.59 Mean Velocity during landing at - 2.6667 m/s² (variation in nonlinear stiffness coefficients)

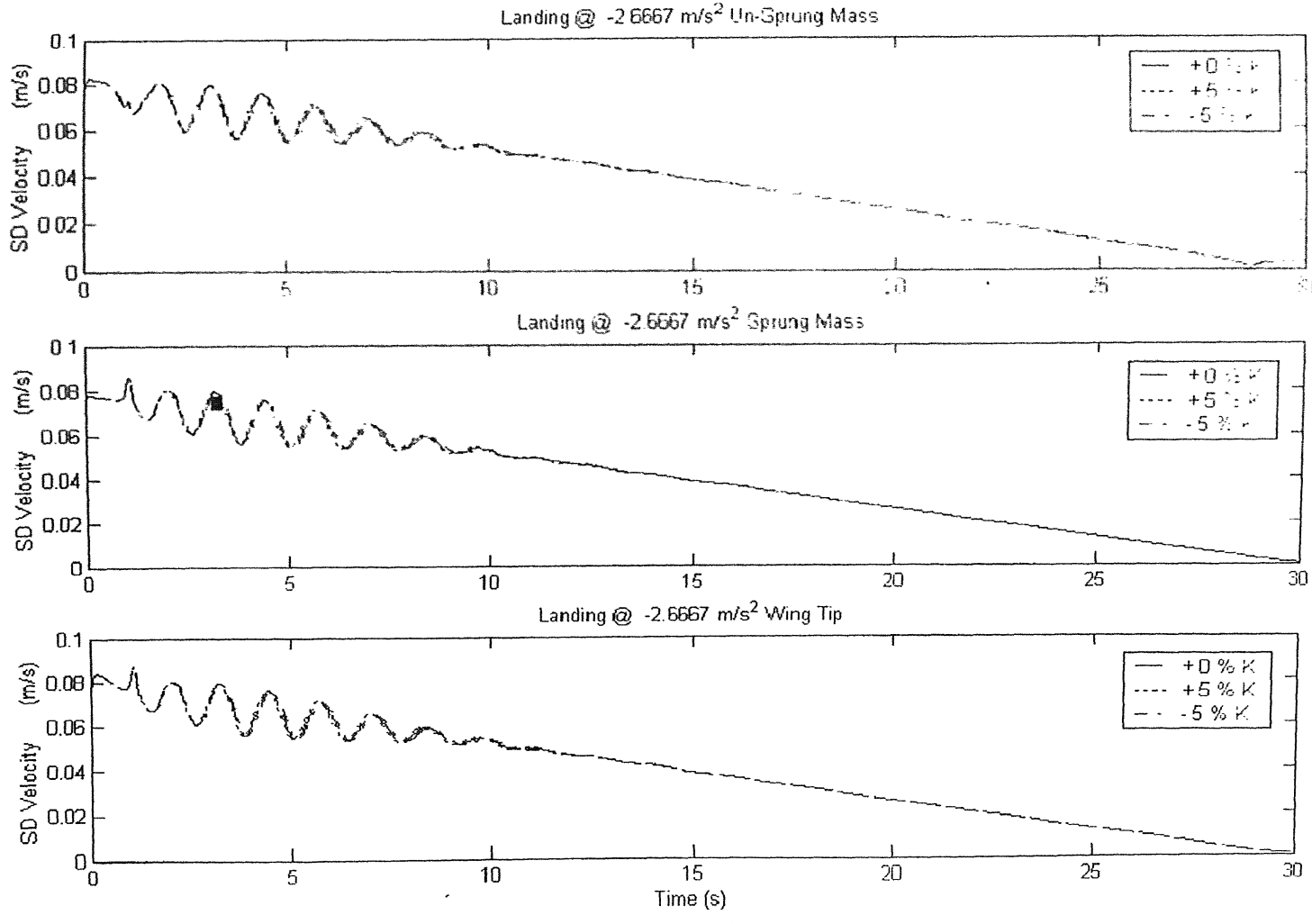

Fig 5.60 SD Velocity during landing at - 2.6667 m/s^2 (variation in nonlinear stiffness coefficients)

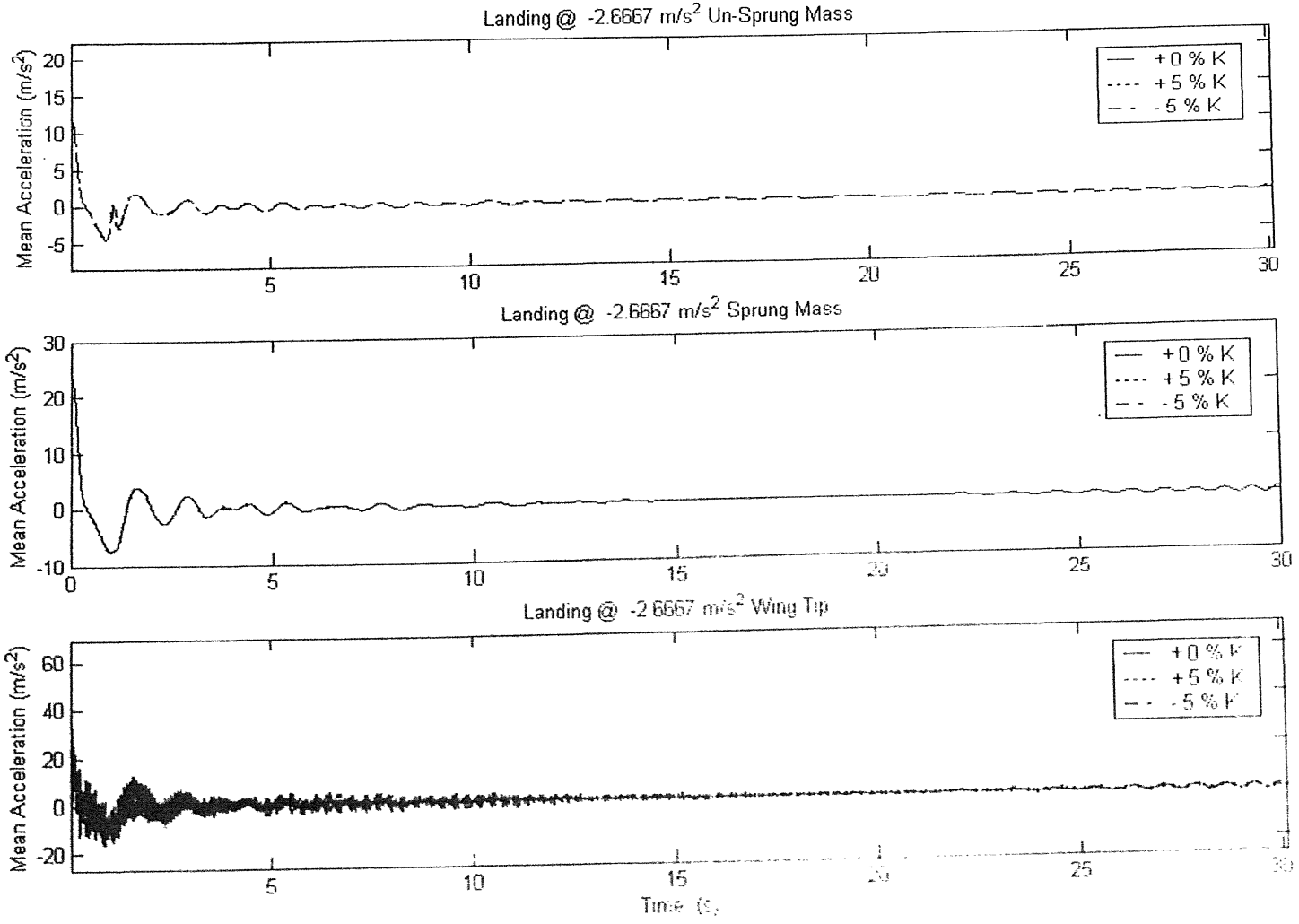

Fig 5.61 Mean acceleration during landing at - 2.6667 m/s² (variation in nonlinear stiffness coefficients)

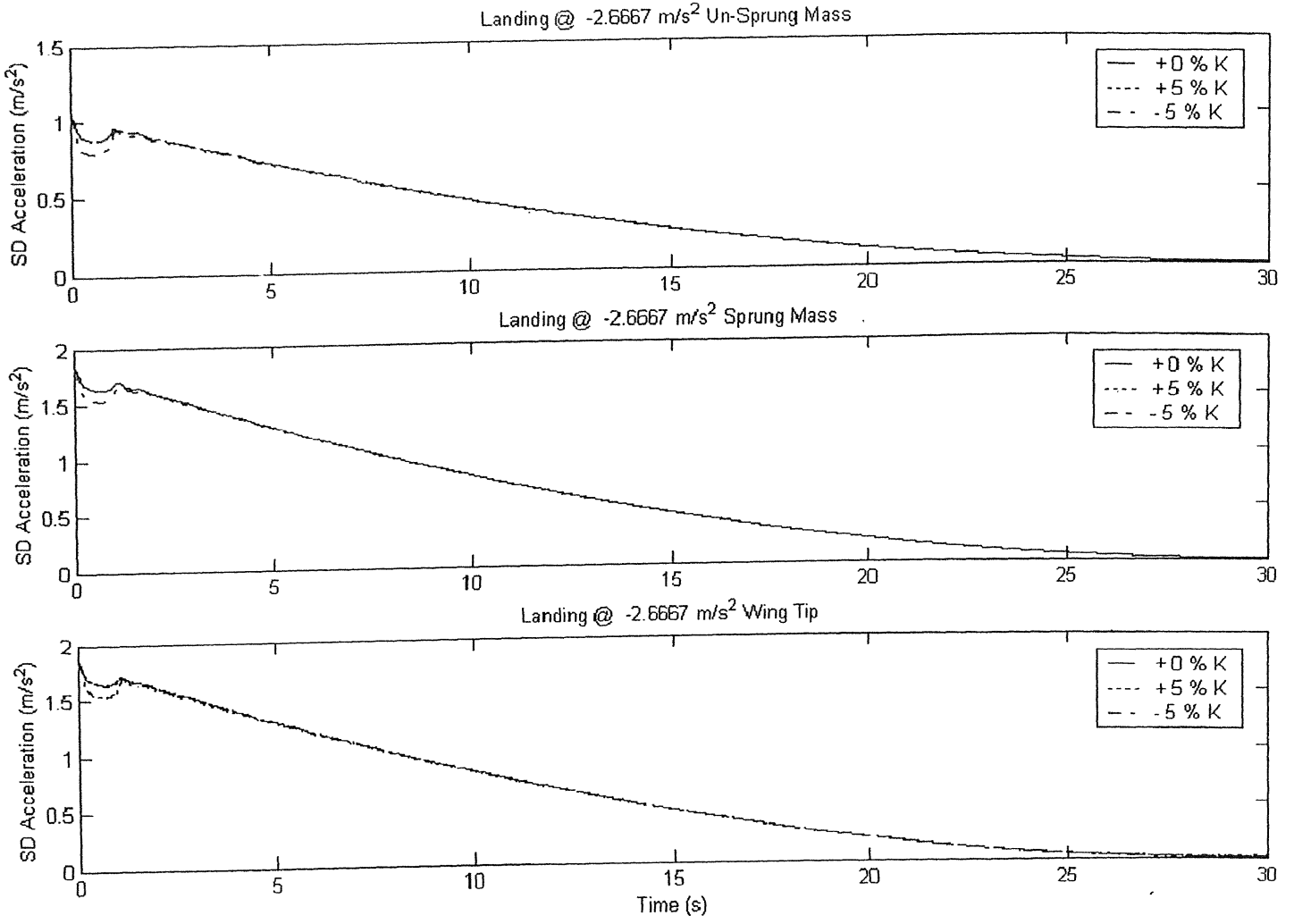

Fig 5 62 SD acceleration during landing at - 2.6667 m/s^2 (variation in nonlinear stiffness coefficients)

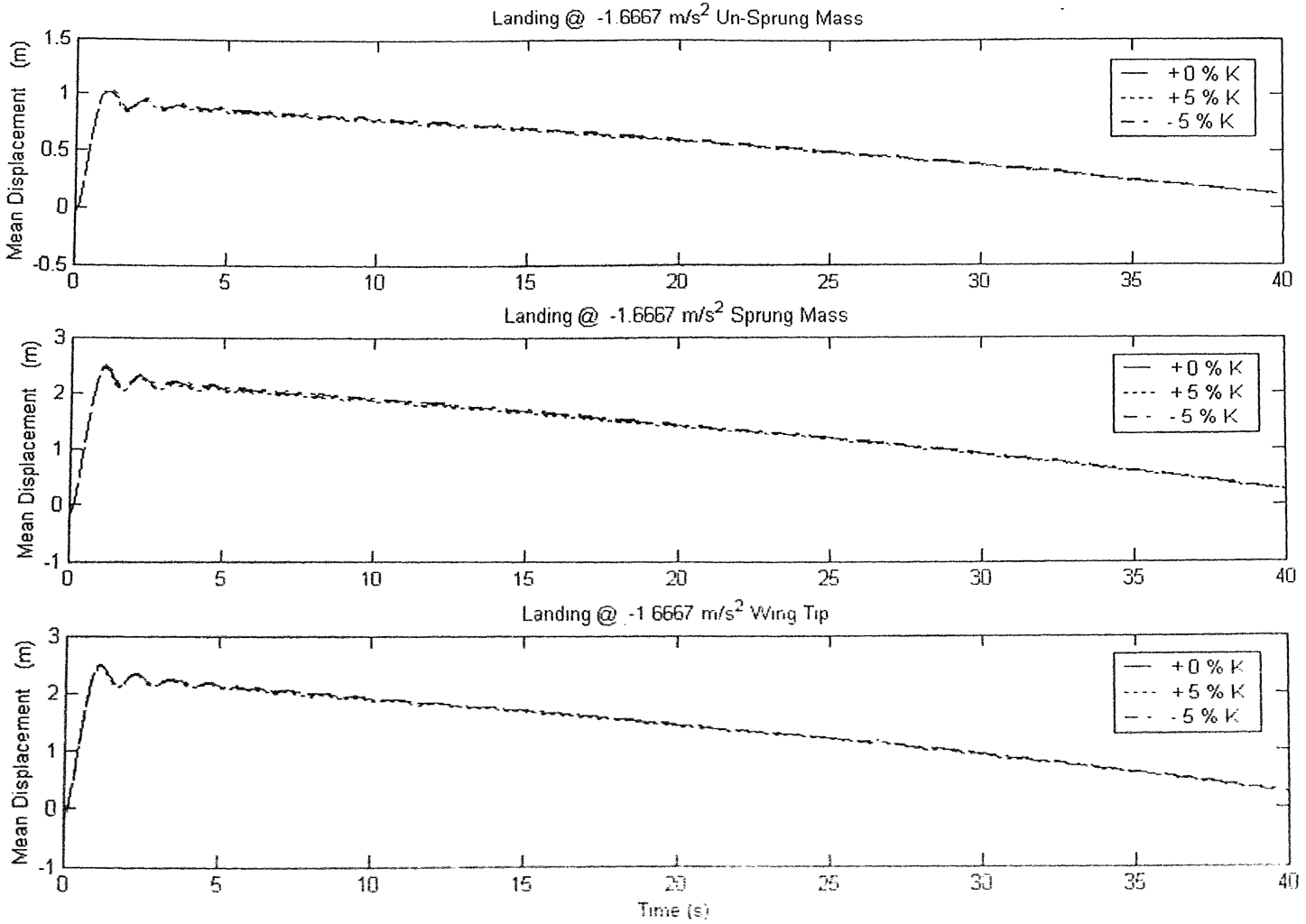

Fig 5.63 Mean displacement during landing at - 1.6667 m/s² (variation in nonlinear stiffness coefficients)

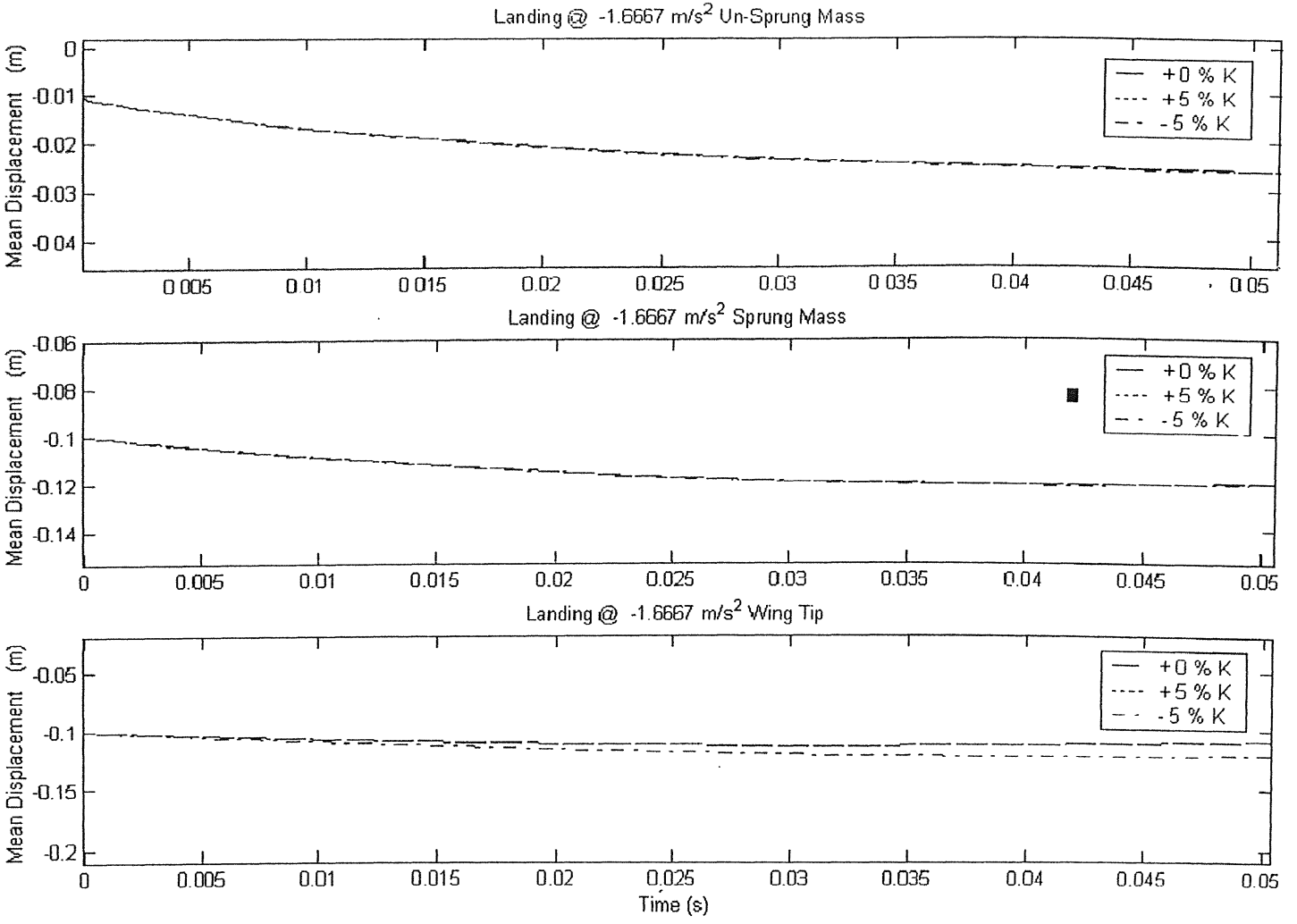

Fig 5.64 Mean displacement during landing at - 1.6667 m/s^2 (variation in nonlinear stiffness coefficients)

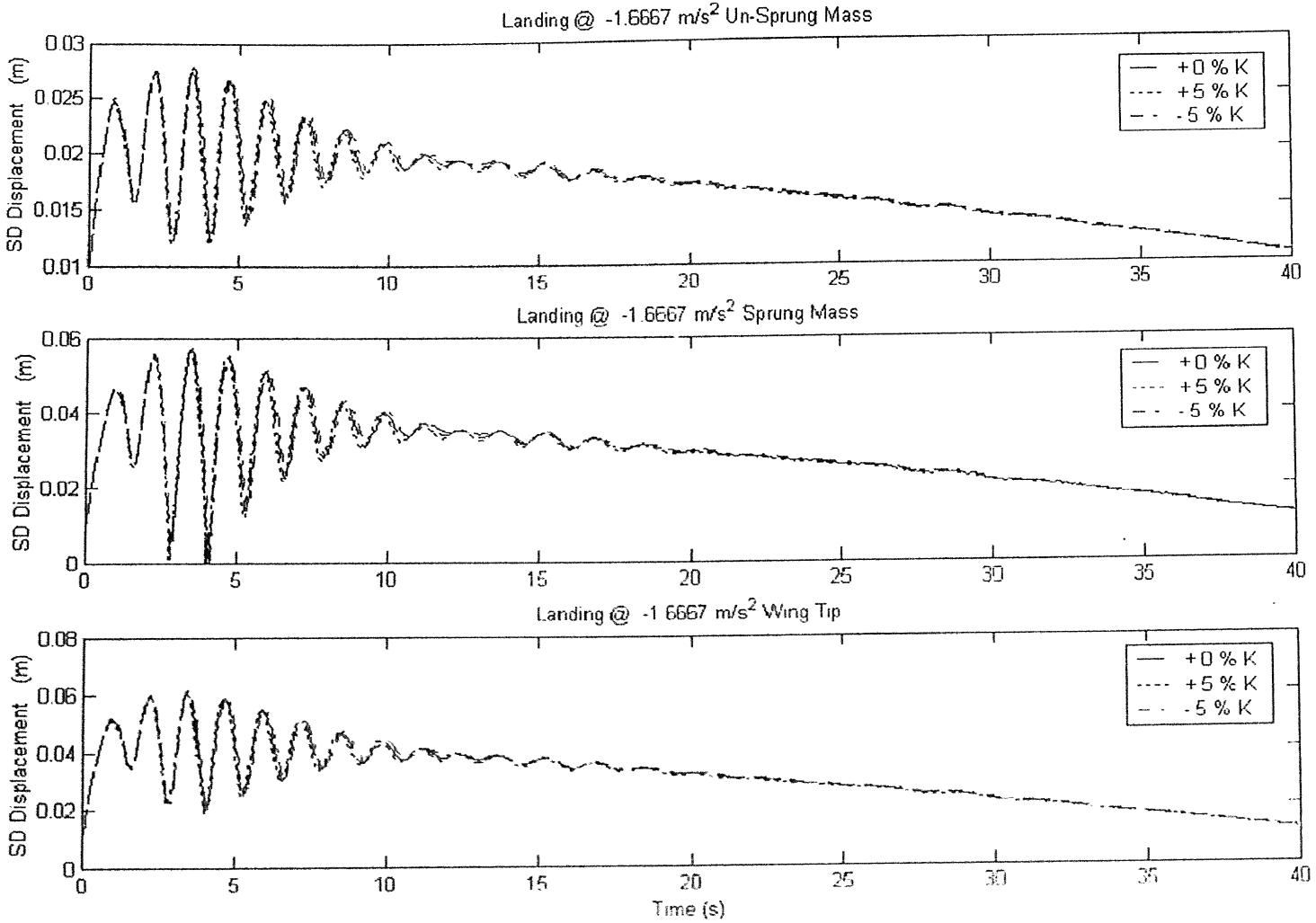

Fig 5.65 SD displacement during landing at - 1.6667 m/s² (variation in nonlinear stiffness coefficients)

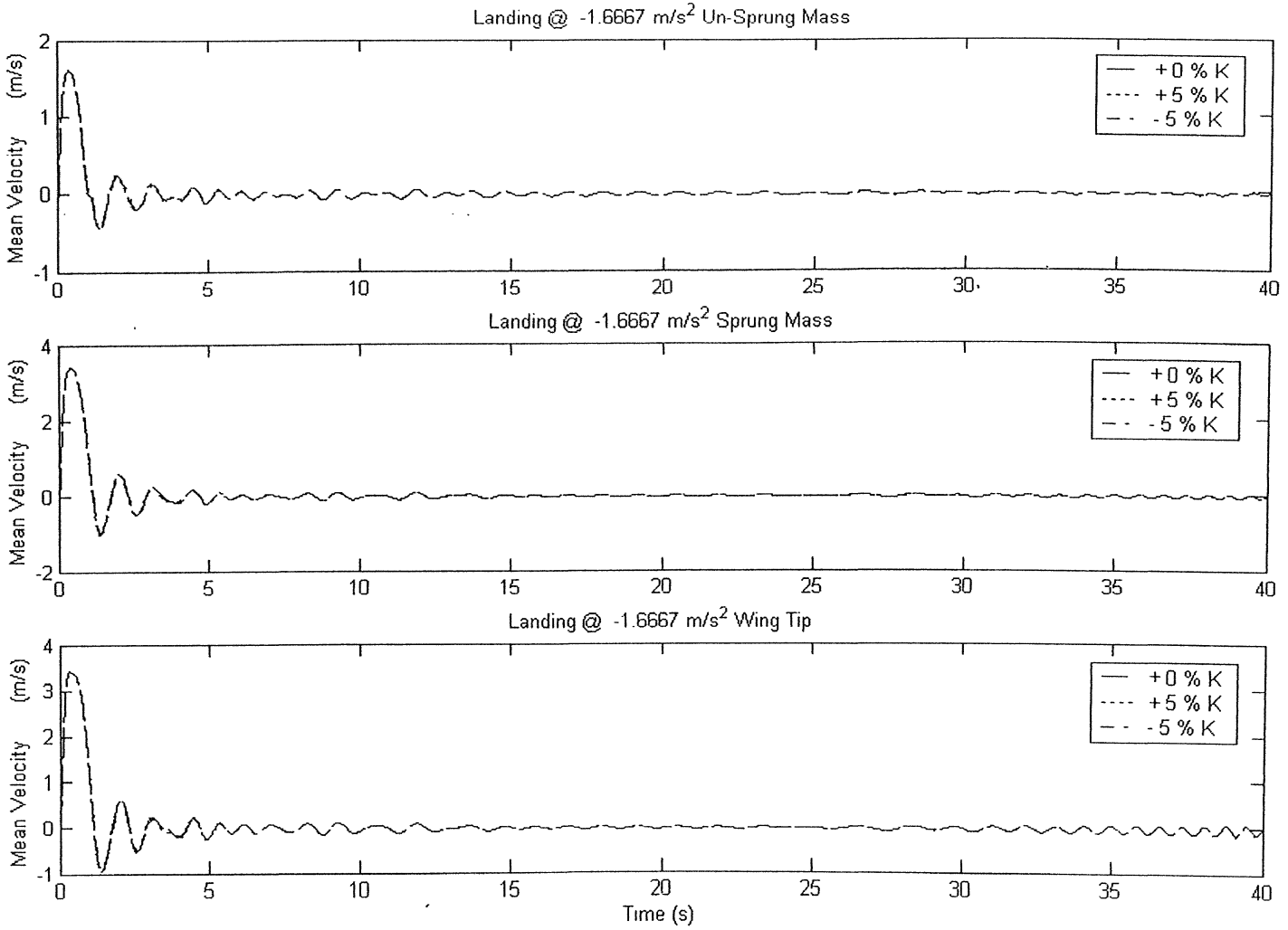

Fig 5.66 Mean Velocity during landing at - 1.6667 m/s^2 (variation in nonlinear stiffness coefficients)

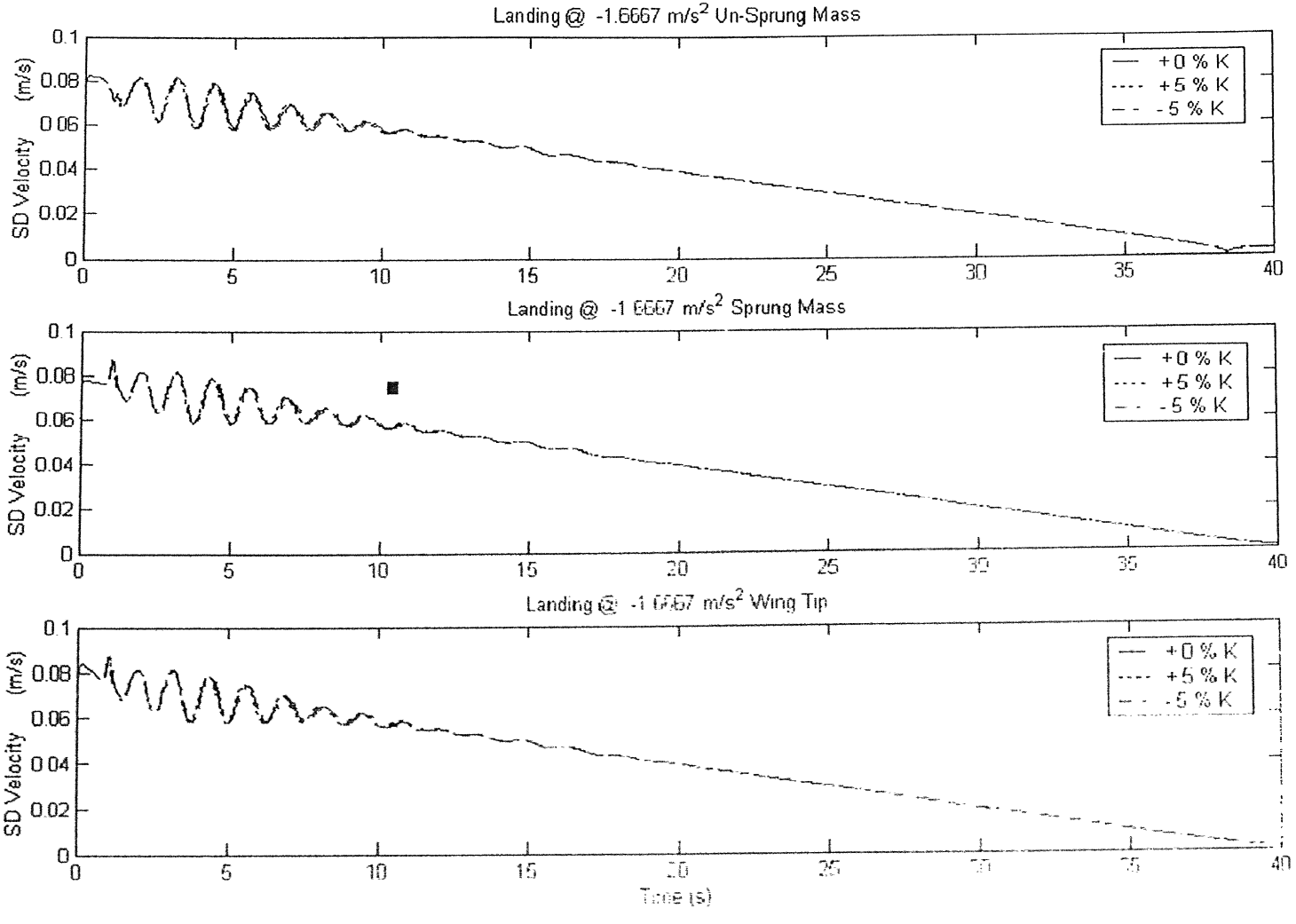

Fig 5.67 SD Velocity during landing at - 1.6667 m/s^2 (variation in nonlinear stiffness coefficients)

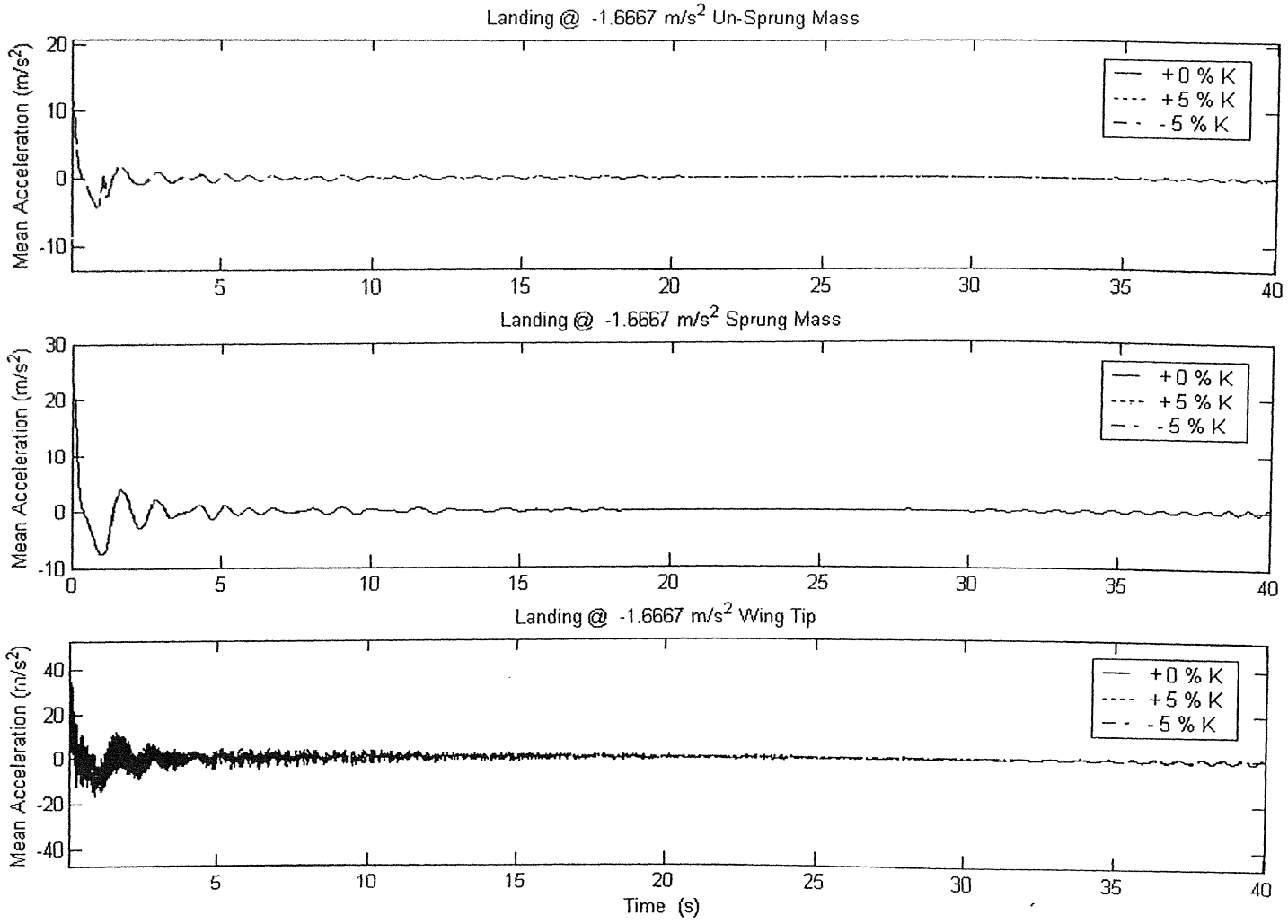

Fig 5.68 Mean acceleration during landing at - 1.6667 m/s^2 (variation in nonlinear stiffness coefficients)

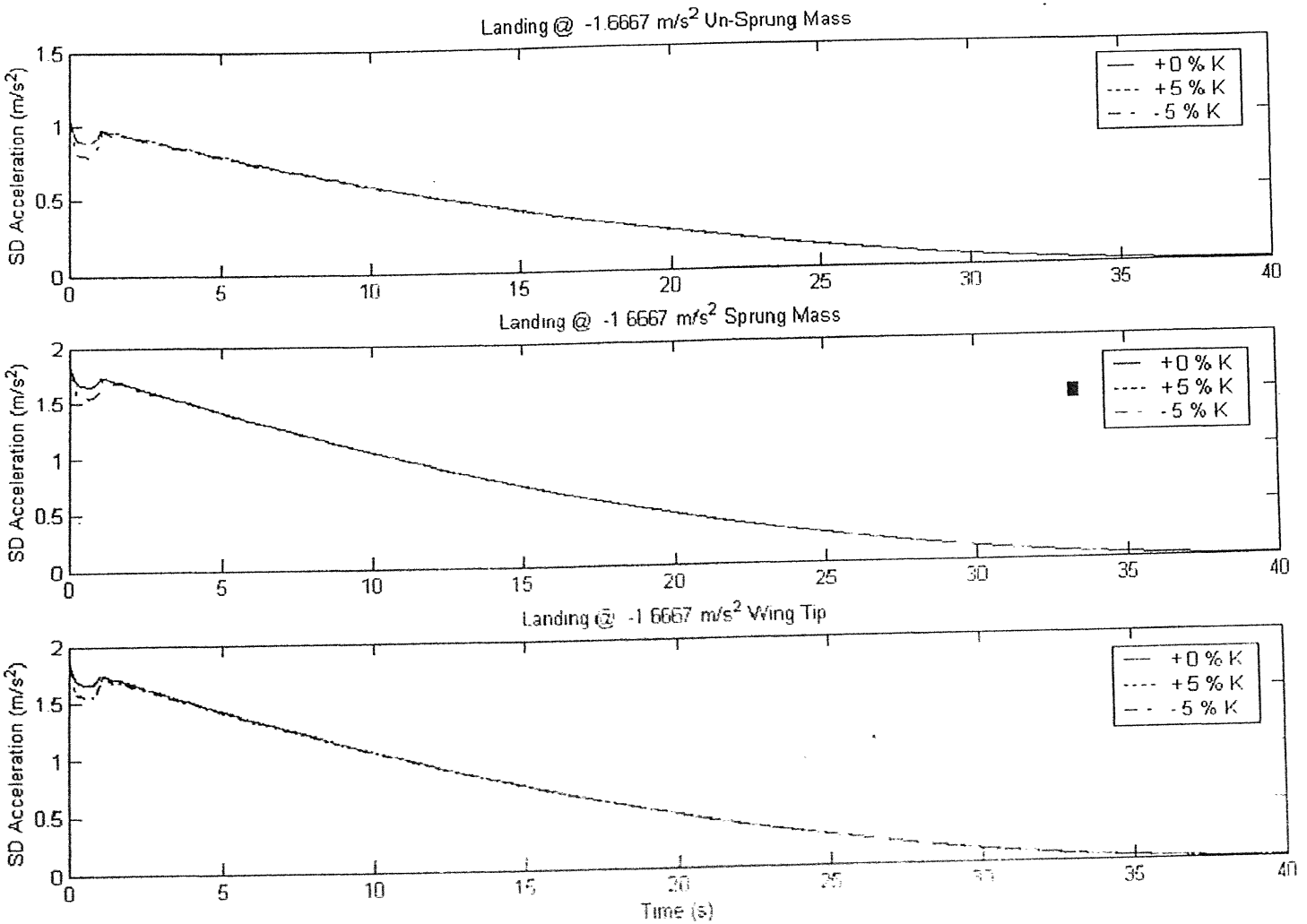

Fig 5.69 SD acceleration during landing at -1.6667 m/s^2 (variation in nonlinear stiffness coefficients)

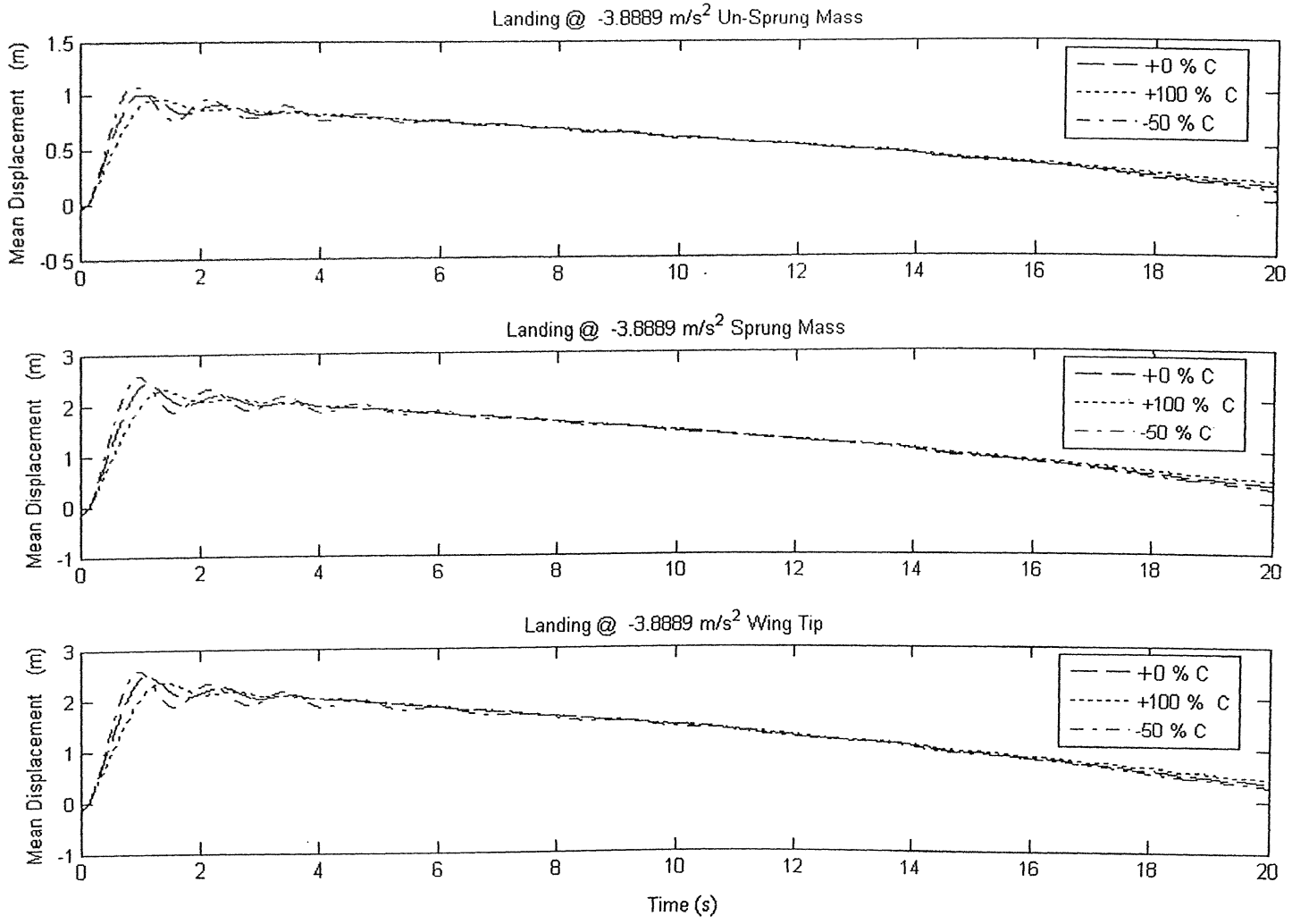

Fig 5.70 Mean displacement during landing at - 3.8889 m/s^2 (variation in damping coefficients)

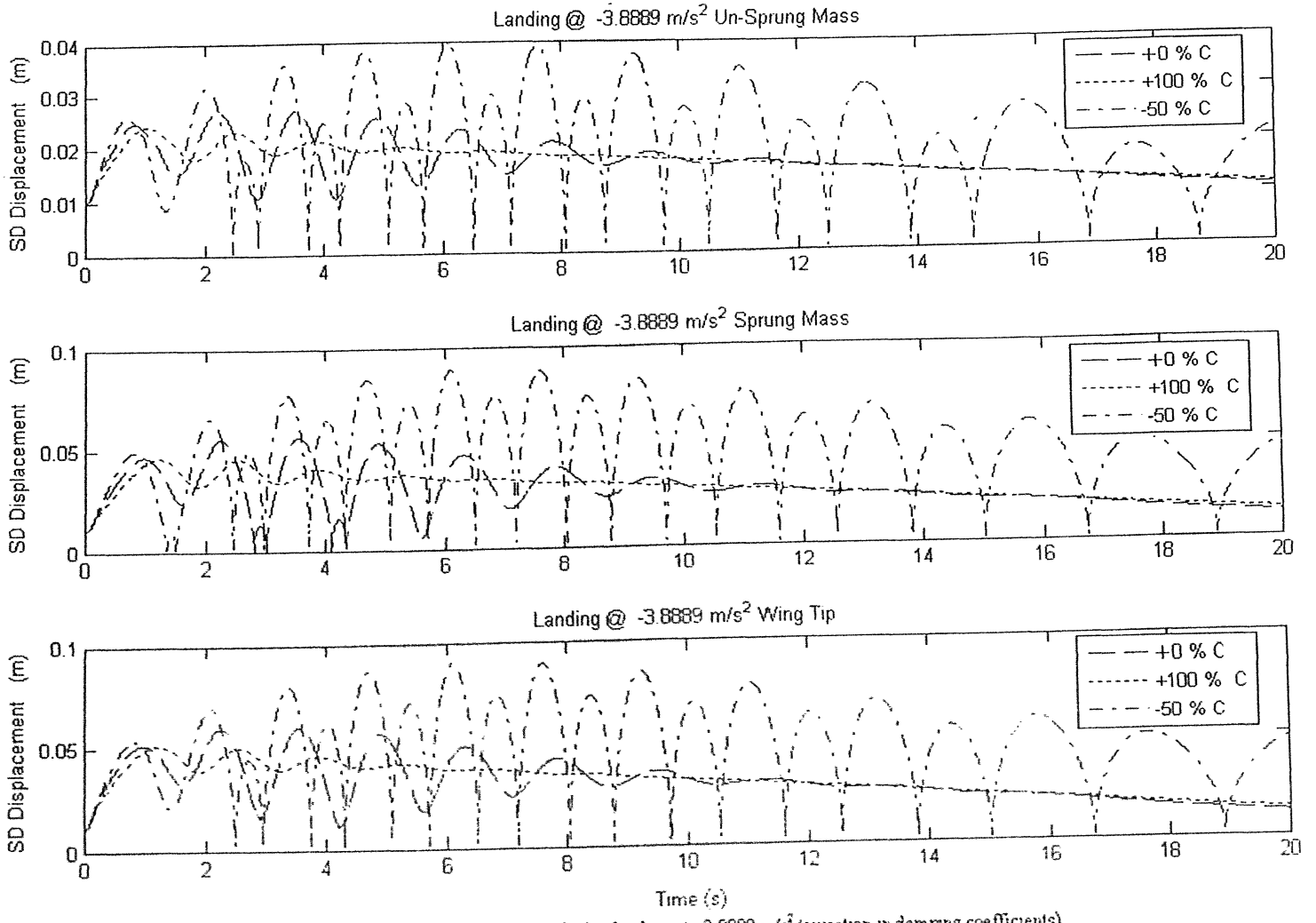

Fig 5.71 SD displacement during landing at - 3.8889 m/s^2 (variation in damping coefficients)

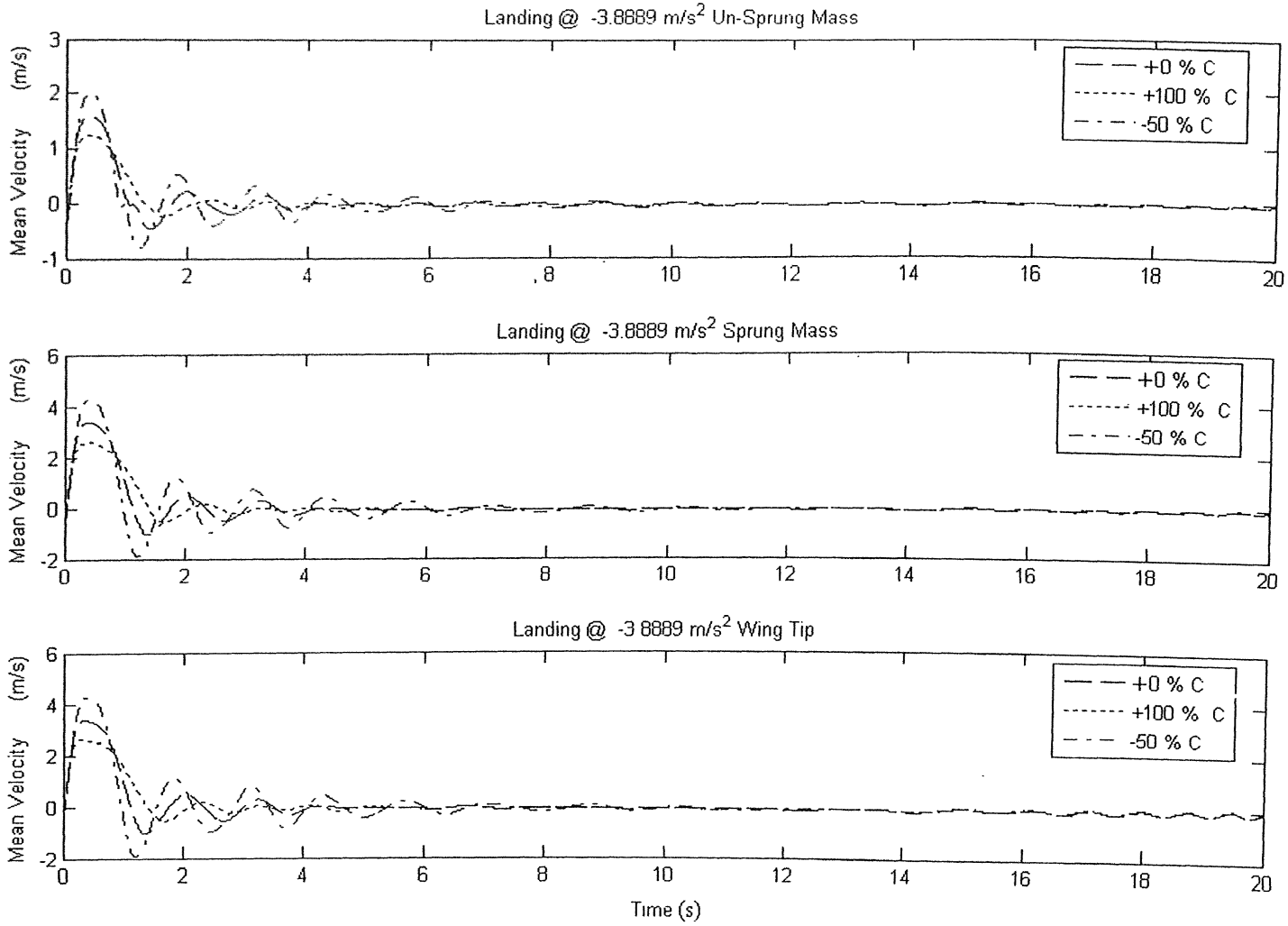

Fig 5.72 Mean Velocity during landing at - 3.8889 m/s^2 (variation in damping coefficients)

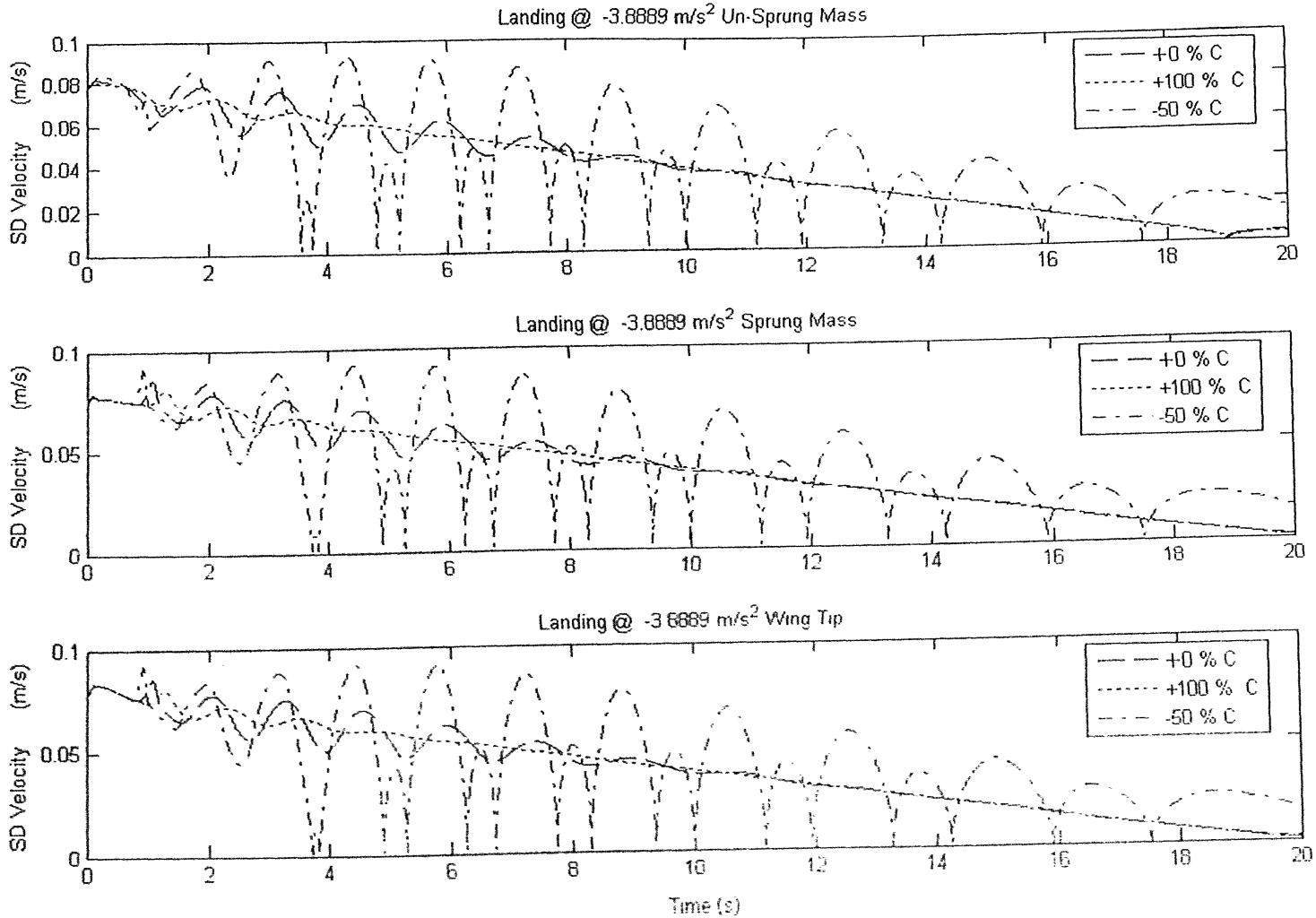

Fig 5.73 SD Velocity during landing at -3.8889 m/s² (variation in damping coefficients)

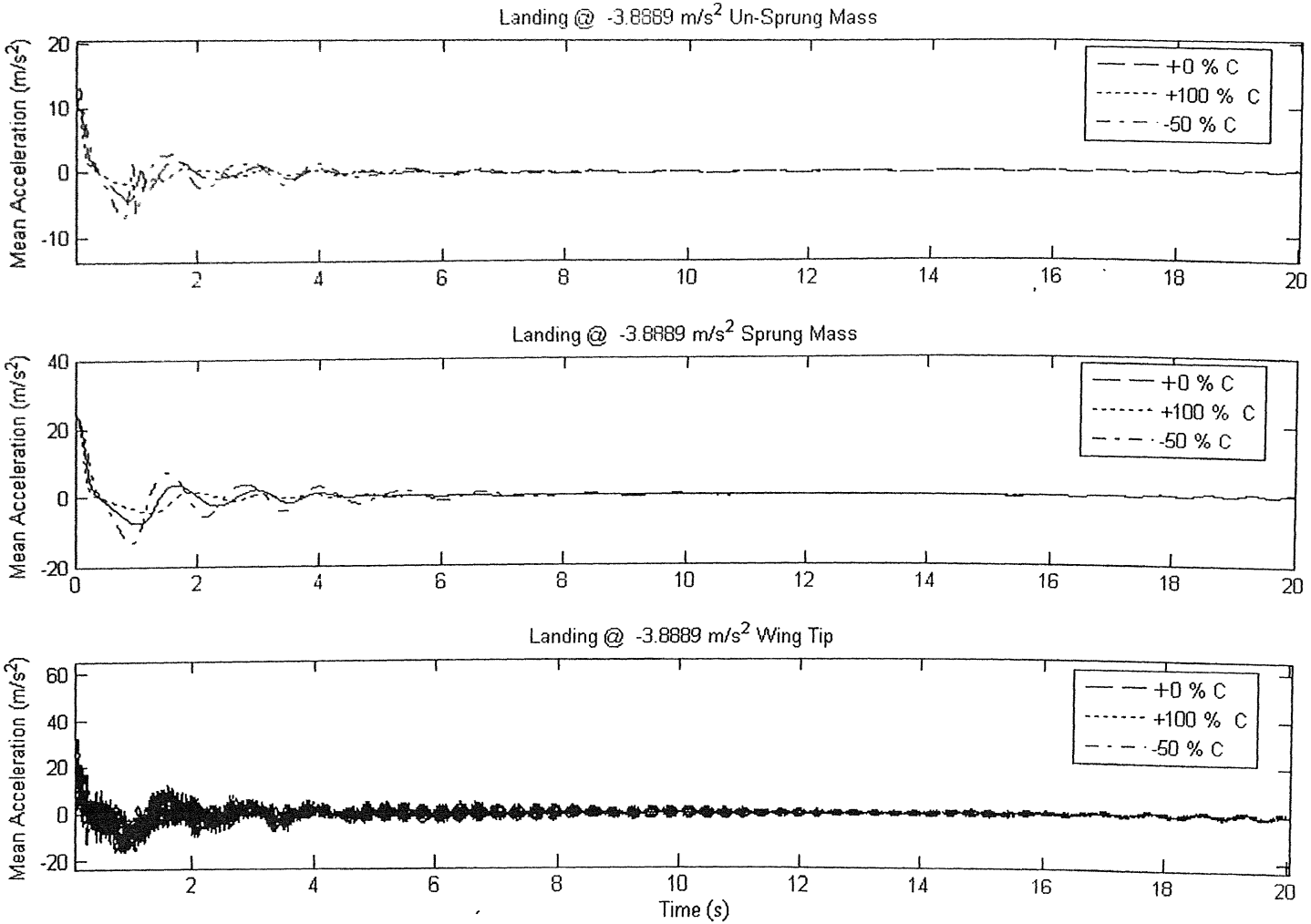

Fig 5.74 Mean acceleration during landing at - 3.8889 m/s^2 (variation in damping coefficients)

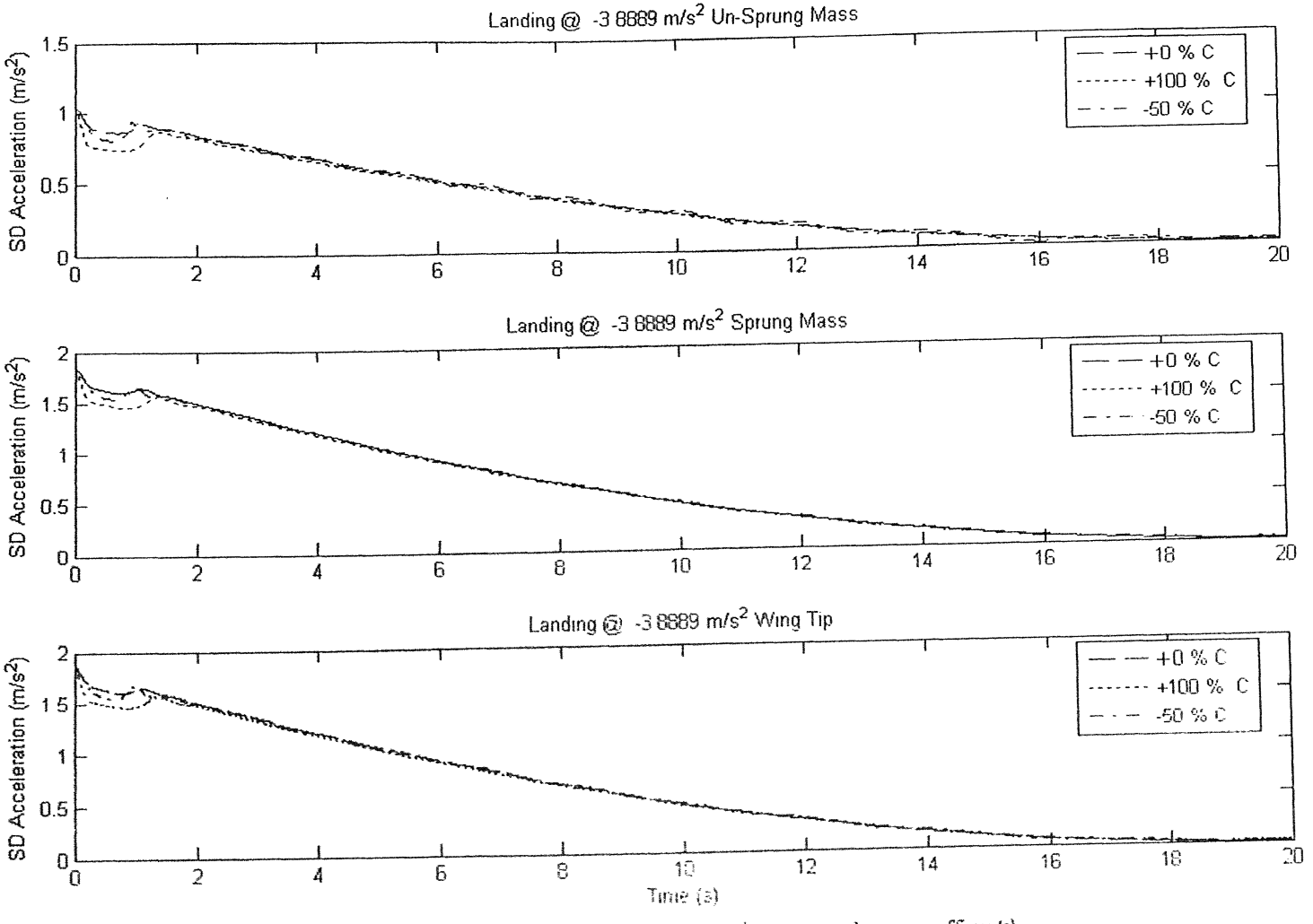

Fig 5.75 SD acceleration during landing at - 3 8889 m/s² (variation in damping coefficients)

Chapter 6

Conclusions

The present work is aimed for obtaining a method suitable for the nonlinear dynamic response of a flexible aircraft under random track induced excitations. It develops the response statistics of a single point contact, two degree of freedom heave model with two, one dimensional continuous members attached to it.

The work started with the study of different methods, which may be used for obtaining the response statistics of the vehicle's un-sprung mass, sprung mass and the wing tip. As stated earlier in chapter 2 (Solution Approaches), these methods have their own merits and demerits and hence were found not condusive for solving the system equations. The work has also shown that the method that is useful, powerful and fast is the combination of FEM (for discretization in space) and FDM (in time) for obtaining the response statistics of the flexible vehicle under random excitation. The effort required to obtain an analytical solution when the system is complex is tremendous (though not impossible) in comparison with the present methodology. This is because the usage of analytical methods for solving the nonlinear differential equations would give rise to a complex form of response and this call for the knowledge of the higher order statistics of the random track profile.

Based on the results obtained for a medium sized aircraft, the conclusions obtained for the three types of ground runs are presented below.

Conclusion: Taxi Run

1. The vehicle mean and SD of the response in the taxi runs have, as a dominant component, any periodicity in the track profile modified by the forward velocity. The sensitivity of the vehicle response to the track profile increases with the taxi velocity.

The sensitivity increases from the displacement to the velocity to the acceleration response.

2. After the initial rise, the transient response dampens quickly and there exists a steady state periodic motion, attributed to the mean track profile. The frequency of this oscillation is dependant on the vehicle's forward velocity and the wave number of the track.

3. The initial rise in the mean acceleration response increases as the vehicle's taxiing velocity increases

4. The range of variation of the nonlinear stiffness coefficients considered in the study has little effect on the response of the vehicle. The change in the nonlinear stiffness coefficient has no effect on the nature of the plot but has some effect in the magnitude of these plots.

5. The damping coefficients variation has strong effect on the vehicle response mean and SD. This is due to the fact that the variation taken in the damping coefficients are large.

6. The amplitude and the frequency of oscillation increase as the damping coefficients decreases.

Conclusion: Take off

1. Unlike the taxi run, the mean track profile periodicity is reflected only in the SD of the vehicle response. As the take off is an accelerating run, the input as well as the response frequency due to the track mean periodicity increases with time.

2. The mean displacement of the vehicle shows a constant increase in the height which can be attributed to the continued increase in the lift as the vehicle has an accelerating motion.

3. The mean velocity of the response shows an initial bump in the plot. This is attributed to the transient nature of the solution.

4. For the take off run, the effect of variation in the non-linear stiffness coefficients on the vehicle response is small. The effect of the variation in the damping coefficients has again large effect on the response of the vehicle. These observations are true for the range of variation selected for the study.

5. The low damping of the system indicates an initial higher response magnitude both in the mean and in the SD of the response.

Conclusion: Landing Run

1. The Mean response of the vehicle shows an initial dip in the response. This is attributed to the momentum gained due to the rebound effect.

2. The change in the nonlinear stiffness coefficient has little effect on the SD of the displacement of the vehicle response.

3. A distinct periodicity is observed in the mean velocity of the vehicle's response. There is a rapid decrease in the amplitude and the rate of this decrease depends on the damping coefficients.

4. A similar effect can be observed on the SD of the velocity response of the system due to change in the nonlinear stiffness coefficients. The effect of the change of the damping coefficients has a profound effect on the plots.

5. The mean acceleration plot can be interpreted as the plot of the force acting on the system. The plots shows heavy acceleration during the touch down of the vehicle and the magnitude of this acceleration decreases as time progresses.

6. The SD of the acceleration response shows a shallow dip. As stated before this is attributed to the reduction in the contact area of the tires with the ground because of the rebound effect after touch down of the aircraft.

The results obtained in the study can be used to design the suspension system of the aircraft. The aircraft experiences large reaction force during touch down while landing. This is the critical load condition for the vehicle system. The tires and the suspension system undergo large stresses during the landing run as seen from the acceleration plots of the vehicle response during landing. The damping has huge influence on the response of the vehicle.

Future work

The present study has presented a methodology for solving nonlinear vehicle models under random excitations. The following scope exists for its further work in the area.

1. The initial conditions may be treated as random variables. The stiffness and damping parameters can also be treated as random in nature.
2. The nonlinear dynamics of the flexible aircraft over a flexible runway, as an aircraft carrier deck, can also be studied. The runway may be assumed either as a linear model or as nonlinear model.
3. More sophisticated models like the two point contact heave-pitch model or the three point contact heave-pitch-roll model can also be studied and their response characteristics can be obtained with the same methodology used for the heave model.
4. These models may be further detailed to incorporate flexible fuselage under going coupled bending and torsion. The wings can also be assumed to undergo bending coupled with torsion.
5. Vibration control studies can be carried out with the proposed model and with the detailed models mentioned above.

6. A procedure for the fatigue life estimation can be developed for the undercarriage and flexible vehicle components.

7. The mean track profile can be altered to include more number of harmonic terms to describe a track in a more generalized way. The track model can also have step up and step down to simulate bumps, repair patches or pot holes on the track.

8. The tires can be modeled to incorporate the filtering effect of the flexible wheel when in contact with the non-uniform track.

9. The forward motion of the vehicle can be modified to incorporate different types of motions like the variable acceleration or the variable deceleration of the vehicle.

REFERENCES

[01] A. H. Nayfeh., Introduction to Perturbation Techniques, Wiley Publishers, 1981.

[02] A. H. Nayfeh., Perturbation Methods, John Wiley publishers, 1973.

[03] Yu. A. Mitropolskii and Nguyen Van Dao., Applied asymptotic methods in nonlinear oscillations, Kluwer academic publishers, Dordrecht, 1997.

[04] N. Kryloff and N. Bogoliuboff., Asymptotic Methods In The Theory Of Non-Linear Oscillations, Gordon and Breach science publishers, 1961.

[05] T. D. Burton and M. N. Hamadan, Analysis of non-linear autonomous conservative oscillators by a time transformation method, Journal of Sound and Vibration, Vol. 87, 1983, pages 543-551.

[06] T. D. Burton., A Perturbation method for certain non-linear oscillators, International Journal of Sound and Vibration, Vol.19, No.5, 1984, 397-407.

[07] Shijun Liao., Beyond Perturbation- Introduction to Homotopy Analysis Method, Chapman & Hall/CRC, CRC series: Modern mechanics and mathematics, 2004.

[08] S. J. Liao., A Second-Order Approximate analytical solution of a simple pendulum by the process analysis method, Transactions of the ASME, vol. 59, December 1992, pages 970-975.

[09] Shi-Jun Liao., An approximate solution technique not depending on small parameters: a special example, International Journal of Non-linear Mechanics, vol 30, No. 3, 1995, pages 371-380.

[10] Shijun Liao., On the homotopy analysis method for nonlinear problems, Applied Mathematics and computation, vol. 147, 2004, pages 499-513.

[11] Shi-Jun Liao., An analytic approximate technique for free oscillations of positively damped systems with algebraically decaying amplitude, International Journal of Non-linear Mechanics, Vol. 38, 2004, pages 1173-1183.

[12] Ji-Huan He., Homotopy Perturbation Technique, Computer Methods in Applied Mechanical Engineering, Vol. 178, 1999, pages 257-262.

[13] Ji-Huan He., Homotopy Perturbation Method: a new nonlinear analytical technique. Applied mathematics and computation, Vol. 135, 2003, pages 73-79.

[14] C. W. S. To., An Implicit Direct integrator for random response of multi-degree-of-freedom systems, Computers and Structures, Vol. 33, No. 1, 1989, pages 73-77.

[15] C. W. S. To., The stochastic central difference method in structural dynamics, Computers and Structures, Vol. 23, No. 6, 1986, pages 813-818.

[16] C. W. S. To., Recursive Expressions for random response of nonlinear systems, Computers and Structures, Vol. 29, No. 3, 1988, pages 451-457.

[17] D. Yadav., Vehicle response statistics to non-stationary track excitation - a direct formulation, Mechanics Research Communications, vol. 17, 1990, pages 65-74.

[18] Sudip Talukdar., Dynamic response of flexible aircraft in ground runs over non-homogenously profiled flexible runway, PhD dissertation, Department of Aerospace Engineering, IIT Kanpur, July 1997.

[19] Shevell, R. C., Fundamental of Flight, Prentice Hall, New Jersey, 1989.

[20] W. Q. Zhu, Z. L. Huang and Y. Suzuki., Response and stability of strongly non-linear oscillators under wide-band random excitation, International Journal of Non-linear Mechanics, Vol. 36, 2001, pages 1235-1250.

[21] H. W. Rong, G. Meng, X. D. Wang, W. Xu and T. Fang, Response of a strongly non-linear oscillator to narrowband random excitation, Journal of Sound and Vibration, Vol. 266, 2003, pages 875-887.

[22] Rong Hai Wu, Meng Guang, Wang Xiangdong, Xu Wei and Fang Tong, Response statistic of strongly non-linear oscillator to combined deterministic and random excitation, International Journal of Non-linear Mechanics, Vol. 39, 2004, pages 871-878.

[23] Tung. C. C., Penizien, J. and Horonjeff, R., The effect of runway unevenness to dynamic response of supersonic transports, NASA CR-119, 1964.

[24] Kirk, C. L and Perry, P. J., Analysis of taxiing induced vibration by power spectral density method, Aeronautical Journal, Royal Aeronautical Society 75, pages 182-193, 1971.

[25] Virchis, V. J. and Robson, J. D., Response of an accelerating vehicle to random road undulation, Journal of Sound and vibrations Vol. 18, pages 423 – 427, 1971.

[26] Soboczyk, K. and Macvean, D. B., Non Stationary random vibration of system traveling with variable velocity, Stochastic problems in dynamics, University of Southampton Ed, Clarkson, B. L pages 412-434, 1976.

[27] Yadav. D and Ramamoorthy, R. P., Nonlinear landing gear behavior at touch down, Journal of Dynamic systems, Measurement and Control ASME, Vol. 113, pages 677 – 683, 1991.

[28] Yadav. D and Singh, C. V. K. Landing response of aircraft with optimal anti skid braking, Journal of Sound and Vibration Vol. 181, pages 401 – 416, 1995.

[29] Hac, A., Stochastic optimal control of vehicles with elastic body and active suspension, Journal of dynamic systems, Measurement and Control ASME, Vol. 108, pages 106 – 110, 1986.

[30] Conway, H. D. and Dubil, H. H., Vibration frequencies of truncated cone and wedge beam, Journal of Applied Mechanics, ASME, Vol. 32, pages 932 – 935, 1965.

[31] Sanger, D. J., Transverse vibration of a class of non uniform beam, Journal of Mechanical Engineering science, Vol. 10, pages 111 – 120, 1968.

[32] Gorman, D. J., Free Vibration analysis of beams and shafts John Willey and Sons, 1975.

[33] To, C. W. S., Vibration of cantilever beam with base excitation and tip mass, Journal of Sound and Vibration, Vol. 83, pages 445 – 462, 1982.

[34] Sudip Talukdar, Dynamic Response of flexible aircraft in ground runs over non-homogenously profiled flexible runway, PhD Dissertation, Department of Aerospace engineering, Indian Institute of Technology, Kanpur, July 1997.

[35] Bathe, K. J., Finite Element Procedures, Prentice - Hall of India Pvt. Ltd. 1997.